

Winter 2008

Structural modeling and monitoring of the Rollins Road Bridge for condition assessment

Jesse D. Sipple

University of New Hampshire, Durham

Follow this and additional works at: <https://scholars.unh.edu/thesis>

Recommended Citation

Sipple, Jesse D., "Structural modeling and monitoring of the Rollins Road Bridge for condition assessment" (2008). *Master's Theses and Capstones*. 433.

<https://scholars.unh.edu/thesis/433>

This Thesis is brought to you for free and open access by the Student Scholarship at University of New Hampshire Scholars' Repository. It has been accepted for inclusion in Master's Theses and Capstones by an authorized administrator of University of New Hampshire Scholars' Repository. For more information, please contact nicole.hentz@unh.edu.

**STRUCTURAL MODELING AND MONITORING OF THE ROLLINS ROAD BRIDGE FOR
CONDITION ASSESSMENT**

BY

JESSE D. SIPPLE

BS, University of New Hampshire, 2007

THESIS

**Submitted to the University of New Hampshire
in Partial Fulfillment of
the Requirements for the Degree of**

Master of Science

in

Civil Engineering

December, 2008

UMI Number: 1463237

INFORMATION TO USERS

The quality of this reproduction is dependent upon the quality of the copy submitted. Broken or indistinct print, colored or poor quality illustrations and photographs, print bleed-through, substandard margins, and improper alignment can adversely affect reproduction.

In the unlikely event that the author did not send a complete manuscript and there are missing pages, these will be noted. Also, if unauthorized copyright material had to be removed, a note will indicate the deletion.

UMI[®]

UMI Microform 1463237

Copyright 2009 by ProQuest LLC.

All rights reserved. This microform edition is protected against unauthorized copying under Title 17, United States Code.

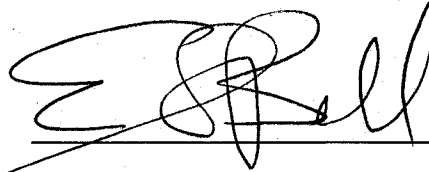
ProQuest LLC
789 E. Eisenhower Parkway
PO Box 1346
Ann Arbor, MI 48106-1346

ALL RIGHTS RESERVED

©2008

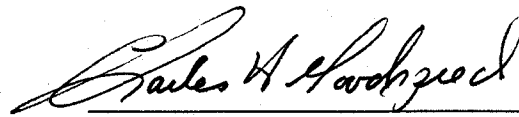
Jesse D. Sipple

This thesis has been examined and approved.



Thesis Director, Erin S. Bell

Assistant Professor of Civil Engineering



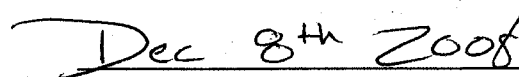
Charles H. Goodspeed

Associate Professor of Civil Engineering



Masoud Sanayei, Tufts University

Professor of Civil and Environmental Engineering



Date

Dedicated to:

Frank J. Feyder, Jr.

"This world always needs more good engineers"

ACKNOWLEDGMENTS

This research project was funded by the New Hampshire Department of Transportation Research Advisory Council. David Scott, Mark Richardson, and Steve Pieper from the NHDOT offered support, encouragement, and interest in the research project. Martha Bowman was a wealth of information and dedication to the project. All the participants of the load test made the process run smoothly and return great results. My advisor, Professor Erin S. Bell, gave me full support while still challenging me throughout this research project. Without your interest and dedication I would not have been able to finish so soon or with such a successful project, you even somehow convinced me to go for my doctorate. Professor Charles Goodspeed and Professor Masoud Sanayei were on my committee and offered terrific insight and contributions to the research project. Professor Raymond Cook was always there to bounce ideas off of and serve as a check to make sure I was still making engineering sense. My officemates kept things exciting over the past year and a half. Jack Welch and Chris Robert were great research partners, classmates, and friends making Kingsbury a fun place to work everyday. Last, but certainly not least, my family and friends who have completely supported me throughout this entire process, you all know who you are. Mom and Dad, I love you and thank you for supporting me and always being a constant source of encouragement. Matt Sipple, my brother, kept me in check and even provided me some help when I got a little too "researchy" for my own good. Thank you all for your support and guidance for you have made this a very exciting and enlightening time in my life.

TABLE OF CONTENTS

DEDICATION.....	iv
ACKNOWLEDGMENTS	v
LIST OF FIGURES	x
LIST OF TABLES	xiii
LIST OF EQUATIONS.....	xiii
ABSTRACT	xiv
CHAPTER I: INTRODUCTION.....	1
1.1 – Social Need	1
1.2 – Current State of Bridge Inspection	3
1.3 – Structural Health Monitoring	5
1.4 – State of the Art	7
1.5 – Case Studies.....	10
1.6 – Monitoring Model Creation.....	12
1.6.1 – Modeling.....	12
1.6.2 – Elastomeric Bearing Pads	13
1.6.3 – Carbon Fiber Reinforced Polymers.....	15
1.6.4 – New England Bulb Tee	16
1.6.5 – Temperature Effects	17
1.7 – Research Goals and Activities.....	18
CHAPTER II: INTRODUCTION OF ROLLINS ROAD BRIDGE.....	21
2.1 - Location	21
2.2 - History of the Rollins Road Bridge.....	22
2.3 – Rollins Road Bridge Specifics	25
2.3.1 – Bridge Deck.....	28
2.3.2 – Girders	28
2.3.3 – Bearing Pads	30
2.3.4 – Abutments	32
2.4 – Instrumentation Plan.....	32
2.5 - Previous Work at Rollins Road Bridge	39
CHAPTER III: FIELD TESTING PROTOCOL AND PROCEDURES.....	40
3.1 - Previous Load Tests	40

3.2 - April 2008 Load Test.....	41
3.2.1 – Truck Specifications.....	42
3.2.2 – Testing Plan.....	44
3.2.3 – Snapshot Quality Assessment.....	45
3.2.4 – Ambient Temperature Measurements.....	48
3.2.5 – Optical Displacement Measurements.....	49
3.2.6 – Global Displacement Measurements.....	50
CHAPTER IV: DATA QUALITY ASSURANCE AND DATA QUALITY CONTROL.....	53
4.1 - Data-to-data CFRP/Deck Analysis.....	53
4.1.1 – CFRP Reinforcement Data-to-Data Comparison.....	54
4.1.2 – Concrete Deck Data-to-Data Comparison.....	56
4.1.3 – Girder Data-to-Data Comparison.....	58
4.2 – Discussion of Data-to-Data Comparison.....	60
4.3 - Environmental Effects on Bridge Response.....	62
4.3.1 – Removal of Strain Caused by Environmental Factors.....	63
4.3.2 – Conventional Thermal Correction.....	66
4.3.3 – Empirical Thermal Correction.....	68
4.3.4 – Discussion of Thermal Correction Techniques.....	72
4.3.5 – Interpretation of Results.....	77
CHAPTER V: MODELING PROTOCOL FOR ROLLINS ROAD BRIDGE.....	79
5.1 - Program Selection.....	79
5.2 - Initial Modeling.....	82
5.3 - Modified Modeling Plan.....	83
5.3.1 – Modeling the CFRP Reinforce Concrete Deck.....	84
5.3.2 – Modeling the Prestressed/Precast/HPC NEBT Girders.....	86
5.3.3 – Modeling the Steel Reinforced Elastomeric Bearing Pad.....	88
5.3.4 – Modeling the Bridge Rail.....	91
5.4 - Special Topic Studies.....	91
5.4.1 – Hand Calculation Verification of SAP2000® Model.....	92
5.4.2 – Obtaining Strain from SAP2000® Model.....	93
5.4.3 – Stiffness Matrix Export.....	95
5.4.4 – Load Application.....	96
5.4.5 – Thermal Load Application.....	98

5.5 - Use of Rollins Road Bridge Load Test Data	99
5.6 – Three-Year Analysis of Rollins Road Bridge Load Test Data	100
5.7 – 2008 Analysis of Rollins Road Bridge Load Test Data	100
5.7.1 – Establishing a Running Benchmark for SAP2000® 2008 Model	101
5.7.2 – Established Model Loads	103
5.7.3 – Established Measured Response Values	103
5.8 – Load Test Data to SAP2000® Comparison	104
CHAPTER VI: MANUAL MODEL UPDATING	105
6.1 – Three Data/Model Comparisons	106
6.1.1 – Analysis of Modifying Bearing Pad Stiffness	107
6.1.2 – Analysis of Removing Specific Structural Elements	112
6.2 – Discussion of Manual Parameter Estimation Results	117
6.3 – Conclusions on Manual Parameter Estimating Results	118
6.4 – Variations in Data	120
6.5 - Optimal Conditions	121
CHAPTER VII: STRUCTURAL HEALTH MONITORING, PARAMETER ESTIMATION, AND MODEL UPDATING	123
7.1 - Parameter Estimation	123
7.2 - Central Artery Parameter Estimation	126
7.3 - Current Ongoing Research at UNH – MUSTANG	128
7.4 - Structural Health Monitoring Program	128
CHAPTER VIII: CONCLUSIONS, FUTURE WORK, AND RECOMMENDATIONS	131
8.1 – Key Observations	131
8.2 – Conclusions	132
8.3 – Future Work	134
8.4 – Recommendations	135
WORKS CITED	138
APPENDICES	142
APPENDIX A – CFRP REINFORCEMENT CALCULATIONS	143
APPENDIX B – LOAD CASES FOR ALL YEARS	144
APPENDIX C – CALCULATION OF REINFORCED ELASTOMERIC BEARING PAD STIFFNESS	148
APPENDIX D - CALCULATIONS FOR MODEL VERIFICATION	151

APPENDIX E – STRAIN CALCULATIONS 156

APPENDIX F – FIRST ANALYSIS OF ROLLINS ROAD BRIDGE LOAD TEST DATA FOR ALL
THREE YEARS 157

APPENDIX G – NONDESTRUCTIVE TESTING FOR DESIGN VERIFICATION OF BOSTON’S
CENTRAL ARTERY UNDERPINNING FRAMES AND CONNECTIONS (Santini-Bell, Sanayei,
Brenner, Sipple, & Blanchard, 2008) 176

LIST OF FIGURES

Figure 1: Steel reinforced elastomeric bearing pad at Rollins Road Bridge	14
Figure 2: Location of Rollins Road Bridge (Image Courtesy of Google Maps©)	22
Figure 3: Rollins Road Bridge prior to new bridge construction (Bowman M. M., 2002)	23
Figure 4: New Rollins Road Bridge, opened in 2000	25
Figure 5: Typical cross-section of Rollins Road Bridge (NHDOT Bureau of Bridge Design, 1999).....	27
Figure 6: NEBT Section at end and midspan, showing prestressing steel (NHDOT Bureau of Bridge Design, 1999).....	29
Figure 7: Elastomeric bearing pad details from Rollins Road Bridge Plans (NHDOT Bureau of Bridge Design, 1999).....	31
Figure 8: Conventional strain gauge attached to concrete	33
Figure 9: FISO EFO fiber optic strain gauge (FISO, 2008)	34
Figure 10: Deck temperature and concrete strain sensors (Adapted from (Bowman M. M., 2002))	34
Figure 11: Strain sensors embedded in NEFMAC grid (Adapted from (Bowman M. M., 2002)).....	35
Figure 12: Strain gauges in NEBT girder before prestressing (Adapted from (Bowman M. M., 2002)).....	36
Figure 13: Graphic of sensors used in Rollins Road Bridge analysis, (a) shows the sensors in section view and (b) shows the sensors in plan view	37
Figure 14: Load test researchers with DMI	39
Figure 15: NHDOT sand truck as load application during April 2008 load test.....	43
Figure 16: Trooper Huddleston (NH State Police) taking NHDOT wheel load measurements.....	43
Figure 17: April 2008 load test truck stop/analysis diagram.....	45
Figure 18: CFRP sensor recorded strain for two passes at same location, different time	46
Figure 19: Concrete deck sensor recorded strain for two passes at same location, different time	46
Figure 20: Girder sensor recorded strain for two passes at same location, different time	47
Figure 21: Load case 1 April 2008 load test.....	47
Figure 22: Load case 2 April 2008 load test.....	48
Figure 23: Load case 3 April 2008 load test.....	48
Figure 24: Load case 4 April 2008 load test.....	48
Figure 25: Rollins Road Bridge 2008 load test ambient temperature readings	49
Figure 26: Photo of load test while survey crew takes displacement reading	51
Figure 27: CFRP bottom grid station 2 above girder 5 strain readings for all three load tests	54

Figure 28: CFRP upper grid station 2 above girder 3 strain readings for all three load tests	55
Figure 29: CFRP upper grid station 2 above girder 4 strain readings for all three load tests	56
Figure 30: Bottom of concrete deck gauge station 2 above girder 4 strain readings for all three load tests	57
Figure 31: Top of concrete deck gauge station 1 above bay 3 strain readings for all three load tests.....	57
Figure 32: Bottom of concrete deck gauge station 1 above bay 3 strain readings for all three load tests.....	58
Figure 33: Girder 5 top gauge strain readings for all three load tests	59
Figure 34: Girder 4 top gauge strain readings for all three load tests	59
Figure 35: Girder 3 top gauge strain readings for all three load tests	60
Figure 36: Ambient temperature readings for all three load tests	61
Figure 37: Strain readings from girder 3 and girder 4 over the duration of the December 2000 load test to show difference between thermal effects and load application	62
Figure 38: Girder 3 top sensor raw data from April 2008 load test, with three zero-load data points and trend line included	64
Figure 39: Girder 4 top sensor raw data from April 2008 load test, with three zero-load data points and trend line included	65
Figure 40: Girder 3 top sensor raw and theoretical data from April 2008 load test, with three zero-load data points and trend lines included.....	67
Figure 41: Girder 4 top sensor raw and theoretical data from April 2008 load test, with three zero-load data points and trend lines included.....	68
Figure 42: Girder 3 top sensor raw, theoretical, and empirical data from April 2008 load test, with three zero-load data points and trend lines included.....	69
Figure 43: Girder 4 top sensor raw, theoretical, and empirical data from April 2008 load test, with three zero-load data points and trend lines included.....	70
Figure 44: Girder 3 top sensor empirical data with truck position from April 2008 load test.....	71
Figure 45: Girder 4 top sensor empirical data and truck position from April 2008 load test.....	71
Figure 46: Girder 3 raw and empirical data with manual model updating load cases .	73
Figure 47: Girder 4 raw and empirical data with manual model updating load cases .	74
Figure 48: Girder 5 top raw, theoretical and empirical Data from April 2008 load test, with three zero-load data points and trend lines included.....	75
Figure 49: Girder 5 middle raw, theoretical and empirical data from April 2008 load test, with three zero-load data points and trend lines included	75
Figure 50: Girder 5 top raw and empirical data with manual model updating load cases	76
Figure 51: Girder 5 middle raw and empirical data with manual model updating load cases	76

Figure 52: Truck run #3 snapshot for girder 3 with empirical data including traffic, modeled values at stop locations, and empirical values at stop locations..	77
Figure 53: SAP2000® Bridge Modeler (SAP2000, 2007).....	81
Figure 54: GT Strudl® bridge model (GT Strudl, 2007).....	83
Figure 55: Graphical representation of how CFRP is modeled as layered shell element	85
Figure 56: Layered shell properties for RRB deck (SAP2000, 2007).....	86
Figure 57: Preloaded NEBT section in SAP2000®	87
Figure 58: SAP2000® bridge tendon layout (SAP2000, 2007).....	88
Figure 59: Deformations of a laminated elastomeric bearing pad (Stanton, Roeder, Mackenzie-Helnwein, White, Kuester, & Craig, 2008).....	88
Figure 60: Stiffness parameters for modeled reinforced elastomeric bearing pad (SAP2000, 2007)	90
Figure 61: Section view of bridge rail connection to bridge deck (NHDOT Bureau of Bridge Design, 1999).....	91
Figure 62: Strain calculation diagram.....	95
Figure 63: Modeled cantilever beam with MATLAB® and SAP2000® stiffness matrix output.....	96
Figure 64: Truck load mesh to bridge deck graphic	98
Figure 65: Sample output from SAP2000® for temperature special study.....	99
Figure 66: Measured strain to strain due to applied truck load diagram	101
Figure 67: SAP2000® modeled strain data to strain due to applied truck load	102
Figure 68: Manual model updating using girder 3 top strain sensor	108
Figure 69: Manual model updating using girder 4 top strain sensor	109
Figure 70: Manual model updating using girder 5 top strain sensor	109
Figure 71: Manual model updating using girder 5 middle strain sensor	110
Figure 72: Manual model updating verification using girder 3 deflection measurements.....	111
Figure 73: Manual model updating verification using girder 4 deflection measurements.....	112
Figure 74: Manual model updating verification using girder 5 deflection measurements.....	112
Figure 75: Manual model updating using girder 3 top strain sensor	113
Figure 76: Manual model updating using girder 4 top strain sensor	114
Figure 77: Manual model updating using girder 5 top strain sensor	114
Figure 78: Manual model updating using girder 5 middle strain sensor	115
Figure 79: Manual model updating comparison using girder 3 deflection measurements.....	116
Figure 80: Manual model updating comparison using girder 4 deflection measurements.....	116
Figure 81: Manual model updating comparison using girder 5 deflection measurements.....	117
Figure 82: Quantification of bearing pad stiffness examples.....	119
Figure 83: Quantification of bearing pad stiffness results	119

Figure 84: Graphical representation of parameter estimation (Sipple, 2008)..... 125

LIST OF TABLES

Table 1: Structural health monitoring measurement comparison (Sanayei, Imbaro, McClain, & Brown, 1997) (Aktan, Farhey, Helmicki, Brown, Hunt, & Lee, 1997)	9
Table 2: Expert of the 2000 Rollins Road Bridge Inspection Report (NHDOT Bureau of Bridge Design, 2007)	23
Table 3: Excerpt from the 2007 Rollins Road Bridge Inspection Report (NHDOT Bureau of Bridge Design, 2007).....	25
Table 4: Deck concrete strength (Bowman M. M., 2002)	28
Table 5: Load test wheel weights for all three years.....	41
Table 6: December 2000 load test elevations (Bowman M. M., 2002)	51
Table 7: August 2001 load test elevations (Bowman M. M., 2002)	52
Table 8: April 2008 load test elevations.....	52
Table 9: Girder 3 and Girder 4 strain readings at point of zero-load	65
Table 10: Girder 3 and Girder 4 conventionally corrected strain readings at point of zero-load	68
Table 11: Girder 3 and Girder 4 empirically corrected strain readings at point of zero-load.....	70
Table 12: Hand calculations and SAP2000® model comparison for deflection and strain	93
Table 13: 2008 measured strain values corrected for environmental effects	104
Table 14: Manual model updating cases and corresponding bearing pad stiffness values for second analysis.....	108
Table 15: Manual model updating cases and corresponding bearing pad stiffness values for third analysis	113

LIST OF EQUATIONS

Equation 1: Axial strain caused by uniform change in temperature (Hibbler, 2005)	18
Equation 2: Conventional thermal change in length equation (Hibbler, 2005)	66
Equation 3: ROCTEST correction equation (Bowman M. M., 2002).....	66
Equation 4: Axial and rotational stiffness of one layer of elastomer (Stanton, Roeder, & Mackenzie-Helnwein, 2004).....	89

ABSTRACT

STRUCTURAL MODELING AND MONITORING OF THE ROLLINS ROAD BRIDGE FOR CONDITION ASSESSMENT

by

Jesse D. Sipple

University of New Hampshire, December, 2008

The health of the US infrastructure is on the minds of everyone following the August 1, 2007 collapse of the I-35W Bridge in Minneapolis, Minnesota. The safety of bridges nationwide should be a top priority for both our citizens and government since they are the backbone of this nation's economy, with 73% of all traffic and 90% of all truck traffic traveling over state-owned bridges. Performing nondestructive load tests, collecting structural response data, and structural modeling techniques allow bridge owners an objective insight into the health of a bridge. The art of reconciling the structural model to reflect collected field data also allows bridge owners to have an up-to-date analytical model of the bridge for condition assessment, decision-making, and asset management. The results from the Rollins Road Bridge load test accurately show that a model can be updated to match measured structural response from a nondestructive load test.

CHAPTER I

INTRODUCTION

1.1 – Social Need

Bridging the Gap, published by the American Association of State Highway and Transportation Officials (AASHTO) in July 2008, addressed the issues with our nation's aging infrastructure in response to the one year anniversary of the Interstate-35W Bridge collapse (Petroski, 2007). Five major problems of our nation's bridges are age and deterioration, congestion, soaring construction costs, maintaining bridge safety, and the need for new bridges. Five proposed solutions for our nation's bridges are investment, research and innovation, systematic maintenance, public awareness, and financial options (AASHTO, 2008). The collapse of the I-35W Bridge was a tragedy, however it did bring the safety of our aging infrastructure into the public eye. The *2006 Status of the Nation's Highways, Bridges, and Transit* report published by the U.S. Department of Transportation states that of the 594,101 bridges in the National Bridge Inventory, 13.1% are rated as structurally deficient and 13.6% are rated as functionally obsolete. The terms structurally deficient and functionally obsolete mean "deteriorated conditions of significant bridge elements and reduced load-carrying

capacity” and “function of the geometrics of the bridge not meeting the current design standards” respectively (U.S. Department of Transportation, 2006). In other words, structurally deficient means the bridge cannot properly support the design or required loading and functionally obsolete means the current configuration of the bridge cannot adequately handle traffic loads imposed the bridge.

With more than 3 trillion traveled bridge vehicle miles annually, 223 billion miles being truck traffic, traffic loading is one of the major factors in the deterioration of America’s bridges. The construction boom of Interstate Highway System in the mid-1950s to mid-1970s resulted in an unprecedented period of infrastructure construction. These 590,000 bridges are essential for the transportation of the nation’s commerce as well as carrying thousands of commuters to and from work every day (AASHTO, 2008). Bridges are essential for the economy of this country but are easily overlooked since they are traveled safely day in and day out.

The average bridge in the United States has an age of 43 years old and a design life of 50 years. Therefore, the need for another large infrastructure construction project to replace the aging infrastructure is imminent. Prioritization of red listed bridges will be required to achieve this daunting but necessary task in an efficient fashion (NHDOT, 2008). The decision to replace or repair, and how to repair each individual bridge structure, is a common and difficult management issue for bridge owners (Farhey, 2005).

The New Hampshire Section of the American Society of Civil Engineers (NHASCE) published the *2006 Report Card for New Hampshire’s Infrastructure*, which

states that out of the 2,113 state and 1,621 municipality owned bridges 145 and 363 bridges, respectively are on the red list. The red listed bridges have known deficiencies, load capacity reductions, or bridge configuration which require inspection more frequently than the standard 2 year inspection routine. Another 167 state and 226 municipal bridges are listed as either structurally deficient or functionally obsolete. These numbers are a 10% decrease in red listed bridges and a 2% increase in structurally deficient or functionally obsolete bridges from the *NHASCE 2002 Report Card*. New Hampshire has been successful in removing an average of 10 state and 16 municipal owned bridges from the red list per year for the last 10 years. The report states that there is a substantial need for investment to maintain this trend (NHASCE, 2006).

1.2 – Current State of Bridge Inspection

In response to all of the problems presented to bridge owners, visual inspection is the typical asset management solution. The typical protocol used for visual bridge inspection is the National Bridge Inspection Standards. Several state departments of transportation (DOTs) use the PONTIS (AASHTOWare, 2008) program distributed by AASHTO. PONTIS is a comprehensive tool used to store and manage bridge information collected during inspection, inspection data, and examine the needs of all bridge in the specific network (Hearn, 2007). The way to gather information put into PONTIS is through Federal Highway Association's (FHWA) National Bridge Inspection Program (NBIP). This program was developed in 1967 in response to the Silver Bridge collapse in Ohio (Phares, Rolander, Graybeal, & Washer,

2000). In 2000, Brent Phares polled state and county DOTs as well as inspection contractors and found the most common form of nondestructive evaluation is through visual inspection (Phares, Rolander, Graybeal, & Washer, 2000). Visual inspections are typically scheduled every 24 months. This interval can be shortened to closely monitor any problem areas until issues are resolved by repair or replacement. This is adequate for most bridges under normal conditions, but not if there is a damage-causing event such as impact or natural disaster between inspections.

Visual inspections are not always objective in categorizing damage and cannot quantify structural condition issues with bridges (Farhey, 2005). As seen in a recent request for proposal, NCHRP 12-82 [RFP], the idea of regularly scheduled bridge inspections is not an efficient way of resource management for already stretched DOTs (Beal, 2008).

The information bridge owners need to obtain through visual inspections is threefold; to find out if there was a change to the serviceability of the bridge or load capacity, what the reliability of the bridge is, and how long the structure will operate at its current capacity. Due to these needs and given that public safety and resource management are important issues to bridge owners. Having an inexpensive continuous bridge monitoring system that can provide useful information of the condition of the bridge, deterioration over time, damage indices, and early warning of unsafe conditions would be an invaluable tool. This continuous monitoring and the strategy and methodology of its implementation is the goal of structural health monitoring (Guan, Karbhari, & Sikorsky, 2007).

1.3 – Structural Health Monitoring

Visual inspections are performed by highly trained personnel that have honed the ability to spot possible areas of concern that could lead to potential problems or that need to be investigated further through training and experience. However, a more objective method of bridge assessment may be possible through the use of structural health monitoring (SHM) techniques. This method is more objective by obtaining numerical data which can be correlated to the health of the bridge. Data is collected from sensors via data acquisition systems, the data is analyzed to provide measurements of structural health which in turn will determine if a reduced bridge load rating or immediate attention is warranted. This technology could be easily integrated into new bridge construction and rehabilitation projects as well.

An analogy to describe the need for structural health monitoring is human health care. From the moment a person is born, they undergo tests to determine their health. By the time a person is 40 years old, it is possible that they have undergone a stress test to determine the health of their heart, x-rays to determine bone health, etc. A bridge is not a human, but when thinking about the amount of people bridges carry every day, their safety should be looked at closely. The presence of structural health monitoring tools, sensors, and cameras allow bridge owners invaluable tools in damage assessment and hazard and asset management.

The study and deployment of SHM techniques is a multidisciplinary research area which uses nondestructive testing (NDT) techniques and instrumentation plans in order to examine the global response or specific structural components. To date,

beneficial developments have been seen through instrumentation of short-span bridges as short-span bridges are easier to employ full-scale research tests on and have a more sensitive global response (Brownjohn, Moyo, Omenzetter, & Chakraborty, 2005). SHM systems include but are not limited to the use of strain gauges, temperature sensors, tilt meters, accelerometers, and data acquisition systems. SHM systems with post-processing protocol allow for real time evaluation of current bridge conditions, having the ability to provide early warning of deteriorating or unsafe conditions. SHM systems can also provide long term structural health information. This information can help bridge owners decide when and how to repair or replace bridges by optimizing maintenance budgets while improving the safety of the general public (Guan, Karbhari, & Sikorsky, 2007).

Technically and economically feasible, practical, and rapid solutions created through administrative and engineering solutions are necessary for modern bridge management programs (Farhey, 2005). The data collection from bridges is only one part of SHM. A major component of SHM is the art of reconciling the collected data with an analytical model. Another large part of SHM is identifying characteristics of the bridge and possible means of failure by using finite element modeling and analysis along with field tests to provide an accurate model of the structural behavior at the bridge (Farhey, 2007). Creating a structural model which aids in the design process is common practice for bridge designers. Modifying that design model into a monitoring based model to be used with the goal of performing parameter estimation and model updating makes the SHM process a very useful tool in bridge management (Bell,

Sanayei, Javdekar, & Slavsky, 2007). "The best 'model' of the bridge is the bridge itself," (Howell & Shenton III, 2006) which makes conducting a load test the best way to obtain information on the bridge behavior. Information obtained from the NDT can be correlated to the behavior seen in the bridge model. A SHM program that compares data to data without providing accountability and a predictive model, gives little quantification of the data, and is therefore of little use to bridge owners (Guan, Karbhari, & Sikorsky, 2007).

1.4 – State of the Art

Data can be collected on all types of structures in different ways, but what makes the information beneficial for decision making is how it is used to obtain value added information. Several SHM research projects have been performed using different SHM techniques. A popular method in SHM and damage detection is the use of vibration data and modal parameters (Brownjohn, Moyo, Omenzetter, & Chakraborty, 2005). This is popular because it does not require measuring displacement, strain, and rotations, which are subject to load application and environmental effects. Modal/vibration testing can be done fairly easily and often, using traffic as the excitation, to obtain results that aid in damage detection, parameter estimation, and model updating. Continuous monitoring with vibration testing allows observing seasonal changes, detecting damage, and observing gradual changes to the bridge. However, due to recent advancements in technology, static measurements such as strain, tilt, and displacement are easier to obtain and viewed as

being more reliable than in past generations (Robert-Nicoud, Raphael, Burdet, & Smith, 2005).

Static experimental data has been used in parameter estimation and model updating, and in certain situations has proven to be more economical than dynamic loading (Sanayei, Imbaro, McClain, & Brown, 1997). Adding the parameter estimation and model updating component of SHM provides a decision making and predictive aspect to the program. Static measurement data is more practical when compared to dynamic measurements, due to lower computational cost and better insight into actual parameters (Sanayei, Imbaro, McClain, & Brown, 1997). Parameter estimation techniques, through the use of a finite element model and model updating, allow direct variation of structural parameters such as area, moment of inertia, and modulus of elasticity. Table 1 shows the advantages and disadvantages to the three typical types of static measurements. Multiresponse, using strain, displacement, and rotation, parameter estimation has been shown as a robust method for flexibility-based parameter estimation and model updating using the University of Cincinnati Infrastructure Institute bridge deck laboratory model (Sanayei, Bell, Javdekar, Edelmann, & Slavsky, 2006).

Table 1: Structural health monitoring measurement comparison (Sanayei, Imbaro, McClain, & Brown, 1997) (Aktan, Farhey, Helmicki, Brown, Hunt, & Lee, 1997)

	Pros	Cons
<i>Displacement</i>	<ul style="list-style-type: none"> • Typical measured response • Easy to rapidly deploy • Global, overall measurement 	<ul style="list-style-type: none"> • Reference dependent • Difficult to measure
<i>Strain</i>	<ul style="list-style-type: none"> • Typical measured response • Not reference dependent • Direct structural behavior due to gauges being installed on surface of structural element 	<ul style="list-style-type: none"> • Need baseline reading • Expense associated with strain gauges and data collection
<i>Rotation</i>	<ul style="list-style-type: none"> • Typical measured response • Not reference dependent 	<ul style="list-style-type: none"> • Needs to settle out before readings

Parameter estimation on an in-service bridge was performed for calibrating a model for special permitting for an overloaded vehicle pass by Bridge Diagnostics, Inc. in 2000 (Grimson, Commander, & Ziehl, 2008). Three superloads were scheduled to cross the Bonnet Carré Bridge near Norco, Louisiana with the first weighing 2,460-kips and the second and third weighing 1,000-kips. The permitting and rating process for allowing the superloads to pass was done before any decision was made about integrating a load test into the process. The bridge was instrumented with quarter bridge electronic resistance strain gauges. A model was created based on material properties, containing elastic supports for boundary conditions, and initial observations from the bridge. The model was then calibrated using snoop truck weighing 66-kips passing along the length of the bridge. The calibration included modifying certain properties and boundary conditions and performing parameter estimation and model updating in order to match the results from the field test data. Calibration of the model involved 3,276 strain comparisons obtained from 28

locations, with 117 analysis load cases. The load cases and locations consisted of three truck paths with 39 truck positions along each pass.

Once the tedious calibration process was completed to an acceptable level of accuracy, the superloads were applied to the model. The results showed that the model was fairly accurate with modeled peak strains being within 10% of predicted peak strains. There was a discrepancy between model and measured data where the peak strains were experienced. That problem was fixed by adjusting the percentage of load carried by each dolly. A benefit from this process, as opposed to traditional load rating procedures, was the response of the entire structure was investigated as opposed to the conventional method of load distribution factors and beam analysis. Researchers found that the field-verified model process is identical to the typical process of load rating (Grimson, Commander, & Ziehl, 2008).

1.5 – Case Studies

The Rollins Road Bridge (RRB) Research Project is not the first to do SHM on an in-service bridge. In fact, there is an increasing popularity to integrate SHM into existing and new bridge projects as aging infrastructure becomes a top priority to the US traveling public.

One specific case, similar to the RRB project, was a successful test on the Morristown Bridge on Route 100 in Vermont, US. The bridge was instrumented with internal temperature and fiber optic strain gauges on the glass fiber reinforced polymers (GFRP) reinforcement and in the concrete deck. A theodolite was used to measure deflections on the girder and deck during the load tests. In this specific

application, the load test looked at the data and determined that the strain in the GFRP bars was significantly less than the ultimate and the tensile strain in the concrete was well below the cracking strain for concrete. Slab and deck deflections were significantly less than AASHTO limits (Benmokrane, El-Salakawy, El-Ragaby, & Lackey, 2006). The Morristown Bridge Project did not correlate the load test data to any model. They looked directly at the stresses experienced by the material in which the gauges were attached and compared that with known material properties; element behavior as opposed to overall system response. Another project was done on the Wotton Bridge in Wotton, Quebec with similar results, and, again, with no use of a comparative model, parameter estimation, or model updating (Benmokrane, El-Salakawy, El-Ragaby, & Lackey, 2006).

Previous research on the Rollins Road Bridge was performed and a data-to-data comparison was examined by Martha Bowman in 2002 (Bowman M. M., 2002) (Bowman, Yost, Steffen, & Goodspeed, 2003). Initial testing on the RRB showed that transverse strains in the carbon fiber reinforced polymers (CFRP) grid can be estimated using conventional ACI design methods and the CFRP properties. There was a variation between predicted and measured strains and the variation was attributed to temperature effects. The stress on the CFRP was less than 1% of the grid's ultimate tensile capacity and less than 2% of the grid's ultimate compressive capacity during the load test. Future work for this research project suggested that tests to determine deflections due to only temperature change would provide insight into how the bridge globally responds to those temperature changes (Bowman M. M., 2002).

Nationally, there are several projects focused on instrumentation and evaluation of in-service structures. Once the funding for those projects expires, the continuation of retrieval and analysis of this data is limited by availability of future funding and personnel, as was the case with RRB before this project began. SHM with parameter estimation can be performed with this data to create and continuously update a model that evolves as the bridge ages. This model may be able to capture loads applied and deterioration experienced. This process could aid in the tracking of the bridge as it ages and give objective information related to bridge asset management needs.

1.6 – Monitoring Model Creation

The goal of a monitoring based model is to capture accurate structural behavior. When creating a model for structural health monitoring, it needs to be different than models created for design purposes. Bridges are typically designed according to design codes which have a goal to produce a safe bridge design in a practical time frame. SHM modeling involves selecting of appropriate software where characteristics can be easily added such as the modeling of elastomeric bearing pads, carbon fiber reinforced polymers, prestressing, and bridge girder geometry.

1.6.1 – Modeling

With the current advancements in bridge modeling programs, such as SAP2000® (Computer & Structures Inc., Berkeley, CA) and GT Strudl® (Georgia Tech – CASE Center, Atlanta, GA), finite element modeling has often become part of the

bridge design process. The SAP2000® Bridge Information Modeler can be used to compute influence lines and bridge response due to applied vehicle loads, dynamic loads, moving vehicle loads, self weight, and several other load applications including thermal loads (Computer Structures, Inc., 2007). Programs like SAP2000® and other structural analysis and design programs are used mainly as an aid in the design process in conjunction with local codes.

The type of model used in a SHM program has different characteristics and areas of focus than a model used for design purposes. The SHM model must be accurate enough to capture the behavior of the bridge and be used in parameter estimation and model updating. Boundary conditions are an important and sensitive detail in modeling, such as those associated with accurately modeling elastomeric bearing pads. All loads applied to the bridge during a load test, whether they are vehicle, temperature, or wind must be included in the SHM model. All structural properties and components of the bridge during load testing such as elastomeric bearing pads, carbon fiber reinforcement polymers, the New England Bulb Tee girder, bridge rails, and temperature effects must also be included in the SHM model.

1.6.2 – Elastomeric Bearing Pads

Elastomeric bearings are recently the most common type of bearing used in bridge construction in the U.S. and have been used in bridge construction since the 1950s (Stanton, Roeder, Mackenzie-Helnwein, White, Kuester, & Craig, 2008). Figure 1 shows the steel reinforced elastomeric bearing pad used at Rollins Road Bridge. Elastomeric material is used in the bearing pad which can be thought of as thick (~5/8-

inch) layers of neoprene often separated by thin (~1/8-inch) plates of steel. This type of bearing is so popular because they resist typical bridge loads and allow for deformations without the need for machined or moving parts. This adds to the fact that they are economically feasible and are favorable when it comes to seismic codes. Simplicity of construction, economical feasibility, and favorability in seismic areas has made the elastomeric bearings the conventional type of bearing for bridges in the U.S. (Stanton, Roeder, Mackenzie-Helnwein, White, Kuester, & Craig, 2008).

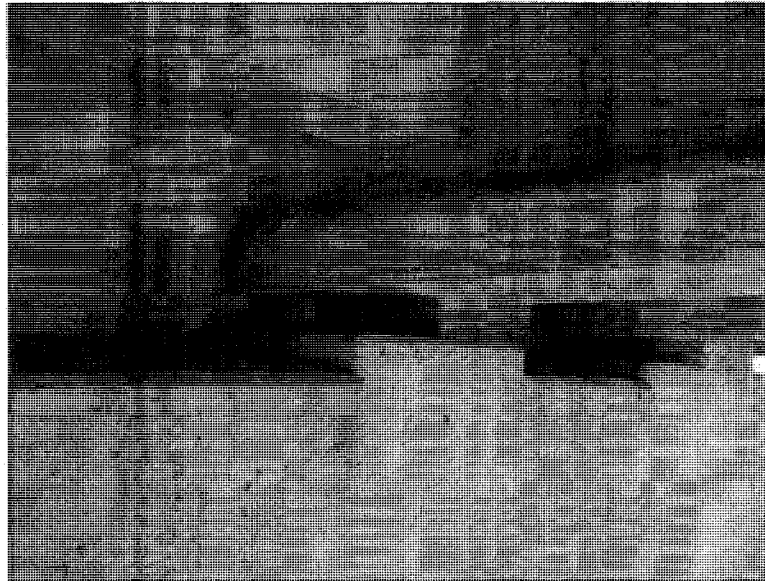


Figure 1: Steel reinforced elastomeric bearing pad at Rollins Road Bridge

One specific type of elastomeric bridge bearing pad is the steel-reinforced elastomeric bearing pad which is typically used for the highest loads. These steel-reinforced bearings contain layers of rubber and steel that are bonded together forming an alternating layered bearing. These bearing pads are stronger and stiffer in compression than non-reinforced pads while still allowing the same shear deformations. The current methods of handling steel-reinforced elastomeric bearing in the AASHTO code are based on limited research or theoretical results. Rotation of

the bearing pad was not considered a high-priority issue when the elastomeric design limits were developed, and the research done for tension limits used limited laboratory samples done almost 60 years ago. The design standards are viewed to be highly conservative and to not be verified experimentally (Stanton, Roeder, Mackenzie-Helnwein, White, Kuester, & Craig, 2008).

The difference between the requirements for design models and monitoring models can be seen with elastomeric bearing pads. The *NCHRP Report 596 – Rotation Limits for Elastomeric Bearings* goes into extensive detail on how to calculate the rotational and axial stiffness values from experimentally determined equations. Conservative bearing stiffness values are suitable for design since they work and do not cause the structure to be under-designed. In SHM models, the behavior must be accurately captured, so a conservative estimate could cause misleading results.

1.6.3 – Carbon Fiber Reinforced Polymers

Using carbon fiber reinforced polymers (CFRP) as the primary reinforcement in a concrete bridge deck is fairly new to civil engineering structures. The increased use of these products is due to advancements in technology making it feasible in today's construction market. Composite materials, such as CFRP, use the strength of the base material, carbon fibers, held together and given stability by a polymer resin. These materials have been widely used in other industries such as transportation, marine, and aircraft. Several advantages to using CFRP composites are it is lightweight, nonmagnetic, high strength to weight ratio, corrosion resistance, low maintenance, and weather resistance. CFRP is favorable for civil structures because it increases

service life, reduces maintenance costs due to corrosion resistance from deicing salts, reduces time in field installation due to less weight, and rapid construction time due to ease of installation.

One disadvantage for the use of CFRP is the high initial cost of the fiber and polymer resins. CFRP reinforced bridges are beginning to be viewed as financially viable due to the life-cycle advantages that CFRP offers (Nystrom, Watkins, Antonio, & Murray, 2003). However, the lack of a well established database for the use of fiber reinforced polymers in civil engineering structures causes designers to be reluctant to the material (Karbhari, et al., 2003).

The CFRP is modeled in SAP2000® by using the layered shell element type. This allows for the user to input different material types and thicknesses throughout the depth of the shell finite element type.

1.6.4 – New England Bulb Tee

The New England Bulb Tee (NEBT) girder was developed by the Precast/Prestressed Concrete Institute (PCI) New England Technical Committee for Bridges, which is a partnership between all six New England state highway departments, private consultants, and area precasters. This specific beam was developed because the use of the standard AASHTO I-girder was limited in New England. Local precasters did not own the forms to support deeper sections needed for long spans and structural steel was already competitive in the construction market. The goal of this committee was to establish a precast girder that would be competitive to steel in the New England (Bardow, Seraderian, & Culmo, 1997).

In order for the precast girder to survive in the New England markets, it had to be able to be used on long spans, while depth, weight, and shipping length were kept to a minimum. These limitations are necessary because most of the roads in the region were built for horse drawn vehicles, therefore when they are reconstructed, the vertical clearance under the bridges must be able to handle the vertical clearance of the taller modern railroad underneath the bridge while allowing for the higher truck loads on the deck of the bridge. Again, due to the original nature of the roads, turning radii is tight and the roads are very narrow, making the transportation of precast concrete beams difficult. A large component of using precast sections is getting those sections into place, which requires use of large cranes which also pose a problem in the New England region due to utility lines, private boundary limits, and small roads (Bardow, Seraderian, & Culmo, 1997).

The end results from the PCI New England Technical Committee for Bridges was a bulb tee shaped girder that would work for both pretensioning and post-tensioning by having a web width of 7-inches with five variable depths depending on the overall depth of the beam. The prestress tendon configuration consists of 10 draped 13-mm strands and 21 straight 13-mm strands in the base. The NEBT girder has been used in different projects in New England since its development in the early 1990s (Bardow, Seraderian, & Culmo, 1997).

1.6.5 – Temperature Effects

Few researchers have addressed the effects on bridges due to temperature changes (Sohn, Dzwonczyk, Straser, Kiremidjian, Law, & Meng, 1999) (Wipf, 1991).

Research has shown that temperature can have an effect on boundary conditions (Peeters & De Roeck, 2001). A large focus and impediment in the research of thermal movements is getting accurate bridge material temperatures from ambient air temperatures (Branco & Mendes, 1993).

AASHTO does take longitudinal thermal expansion of the bridge into account in their bridge code (Moorty & Roeder, 1992). These movements are typically accounted for by the installation of bearing pads and expansion joints in order to minimize the large forces that could develop if not properly accounted for. The equation that AASHTO suggests to use for these movements is seen in Equation 1. This equation raises an important question; what is used as the coefficient of thermal expansion of the entire bridge assembly? Secondly, as mentioned before bearing pads and bridge joints are typically used to account for thermal movements, but how can one be sure if they are working properly?

Equation 1: Axial strain caused by uniform change in temperature (Hibbler, 2005)

$$\varepsilon_T = \alpha * \Delta T$$

1.7 – Research Goals and Activities

The Rollins Road Bridge Project builds upon previous research in instrumentation done to expand the field of SHM and monitoring model creation as described above. The project began where the previous project terminated, after the completion of two successful load tests, and an analysis of the behavior of carbon fiber polymer reinforcement in the cast-in-place concrete deck. This project specifically addresses the durability of the CFRP in the RRB via data-to-data comparison as seen in Chapter IV: Data Quality Assurance and Data Quality Control and provide the NHDOT

with accessible and objective data to gage the performance of the CFRP for use in future projects. A load test was performed on April 2008, and the data from this test was used, in similar fashion, to determine the health of the bridge using data-to-data comparison as was done in the December 2000 and August 2001 load tests.

This research also goes a step further by creating an analytical model to compare the data in order to obtain a correlation between field measurements and an analytical model. A model has been created and updated to the most current conditions of the bridge, using information from an April 2008 load test and as shown in Chapter VI: Manual Model Updating; and will be turned over to the New Hampshire Department of Transportation (NHDOT) to be used for bridge management and to aid in developing their SHM program. This research project will also pass along information relating to how the NHDOT can use tools they currently possess to enhance their current bridge management program by adding SHM, instrumentation, and parameter estimation and model updating. These additions will provide a value-added aspect to their asset management and condition assessment programs.

These new methods will also be tied into the current NHDOT practice of visual inspection and bridge assessment of load rating and special permitting. For this project, the visual inspection report was used to develop the criteria for model creation and updating for RRB eight years since it has been in-service. The goal is that the model will utilize all information received through visual inspection and instrumentation to enhance that visual inspection report with objective data. Even though the instrumentation plan for RRB was not designed specifically for SHM and

parameter estimation, a goal of this research project is to determine the level of information relating to the health of the bridge can be drawn from the data available from the bridge.

A small parameter estimation study was done for this research project on a load test done in 2000 on the Central Artery/Tunnel Project in Boston, MA where underpinning frames were tested using NDT techniques, strain and displacement readings were measured, and a finite element model was used. Parameter estimation was successfully completed and determined rotational stiffness between columns and beams (Santini-Bell, Sanayei, Brenner, Sipple, & Blanchard, 2008). The Central Artery/Tunnel project will be discussed further in Chapter VII: Structural Health Monitoring, Parameter Estimation, and Model Updating.

CHAPTER II

INTRODUCTION OF ROLLINS ROAD BRIDGE

2.1 - Location

Rollins Road Bridge is located in Rollinsford, New Hampshire. Rollinsford is in southeastern New Hampshire about 12 miles from the Atlantic Ocean, see Figure 2. The bridge is not considered to be located in a coastal region, which would add considerations associated with being close to saltwater. The bridge serves as an overpass to carry Rollins Road over Main Street and an active B&M Railroad (NHDOT Bureau of Bridge Design, 1999). The weather in the area is typical of New England, with an annual snowfall of 60 inches, as recorded in Concord, NH about 35 miles west of the bridge (National Climatic Data Center). Such harsh winters mean a heavy use of deicing agents on the road surface throughout the winter months. The effects from the use of these harsh chemicals can be seen in the deck of the previous 70-year old RRB. The deck had to be replaced/repared several times due to deterioration accelerated by use of deicing agents (Bailey & Murphy, 2008).



Figure 2: Location of Rollins Road Bridge (Image Courtesy of Google Maps©)

2.2 - History of the Rollins Road Bridge

The original Rollins Road Bridge was a two lane bridge, steel stringer with concrete deck, four simple spans in series making a total length of 172-feet, and built in the 1930's, see Figure 3. The NHDOT decided that due to corrosion of both the steel reinforcement in the concrete deck and the steel stringers, the bridge needed immediate repair or replacement (Bowman, Yost, Steffen, & Goodspeed, 2003). The last inspection report of the old RRB was done during the construction of the new bridge, shown in Table 2. The report notes that there were several problems with the bridge, including a rating of 3 for serious deck condition.



Figure 3: Rollins Road Bridge prior to new bridge construction (Bowman M. M., 2002)

Table 2: Expert of the 2000 Rollins Road Bridge Inspection Report (NHDOT Bureau of Bridge Design, 2007)

26 October 2000 Bridge Inspection Report	
<i>Deck</i>	3 Serious
<i>Superstructure</i>	4 Poor
<i>Substructure</i>	6 Satisfactory

The NHDOT planned to remove the old Rollins Road Bridge and construct a new bridge in its place to open in the year 2000. The new Rollins Road Bridge was designed and constructed with funding from the Innovative Bridge Research and Construction (IBRC) program which is administered by the Federal Highway Administration (FHWA). The new Rollins Road Bridge, referred to from this point forward as Rollins Road Bridge, is the focus of this research project on SHM for the NHDOT. The purpose of the IBRC program is “to reduce congestion associated with bridge construction and maintenance projects, to increase productivity by lowering the life-cycle costs of

bridges, to keep Americans and America's commerce moving, and to enhance safety" (Office of Bridge Technology, 2008).

Two requirements of the IBRC program are the bridge is to be constructed with high performance and innovative materials and be instrumented. The focus of the IBRC program is using technology in the bridge to require less maintenance while keeping ease of construction a high priority in the design of the structure. The goal of the instrumentation in RRB is to follow the progress of the new materials used in the bridge, again not for SHM. However, even though the instrumentation plan was not specifically designed for SHM, this research project was able to successfully utilize some of the sensors, including strain and temperature, in the bridge to capture the behavior of the bridge during NDT load tests.

Rollins Road Bridge, opened in December 2000 and seen in Figure 4, is a simply supported single span of 110-feet with a concrete beam and concrete deck superstructure. The center pier was also not included in the new bridge design for safety purposes. The bridge has a rating of 99-tons (Fu, Feng, & Dekelbab, 2003) and is in very good condition, as seen in the most recent inspection report shown in Table 3.



Figure 4: New Rollins Road Bridge, opened in 2000

Table 3: Excerpt from the 2007 Rollins Road Bridge Inspection Report (NHDOT Bureau of Bridge Design, 2007)

09 July 2007 Bridge Inspection Report	
Deck	9 Excellent
Superstructure	9 Excellent
Substructure	9 Excellent

2.3 – Rollins Road Bridge Specifics

A large part of the SHM protocol is the development of an accurate bridge model in order to capture the behavior of the bridge in a useful manner. In order to create that model, the structural properties of the bridge must be known with high level of confidence and modeled accurately. Details of the bridge are presented in the Master of Science Thesis of Martha Bowman, entitled *Load Testing of the Carbon FRP Bridge Reinforce Concrete Bridge Deck on the Rollins Road Bridge, Rollinsford, New Hampshire* (Bowman M. M., 2002). Researchers at the University of New Hampshire (UNH) were actively involved in the design and even construction of RRB. Researchers

were present at stressing and pouring of the girders, the pouring of the concrete bridge deck, and several other times during the construction of the bridge. Due to this presence of researchers, and excellent support from the NHDOT designers and construction personnel during the entire process, much care was taken to ensure the bridge was constructed to specification and instrumentation installed properly.

As previously mentioned, in order to obtain funding from the IBRC, the bridge needed to contain high performance and innovative materials which ended up being carbon fiber reinforcement polymers (CFRP) in the deck and high performance concrete (HPC) in the girders. The bridge also needed to be instrumented, so fiber optic strain sensors in the CFRP, deck, and girder as well as temperature sensors were included in the design. The cross section of the bridge can be seen in and will be described in detail below.

Several bridge components were specifically looked at for inclusion in the bridge model. These components include the CFRP reinforced bridge deck, New England Bulb Tee girders, steel-reinforced elastomeric bearing pads, the bridge rail, and the instrumentation plan, see Figure 5. Modeling these components accurately plays an important role in creating a monitoring based analytical model.

2.3.1 – Bridge Deck

The bridge deck is an 8-inch cast-in-place (CIP) concrete deck with 0.5-inch saw cuts, making an effective depth of 7.5-inches. The concrete deck strength can be seen in Table 4. There are also three CIP diaphragms, one at each end and one in the midspan. A typical bridge deck is reinforced with steel rebar, however due to the location of the bridge and high use of deicing salts, carbon fiber reinforced polymers, commercially known as NEFMAC, was used instead of steel. The CFRP has a tensile strength, f_{tu} , of 190-ksi and an elastic modulus, E_f , of 10,400-ksi. Some advantages of the CFRP include its high tensile strength, reduced unit weight, non-corrosiveness in salt environment, attractive life cycle performance, and ease of installation. Some disadvantages are the higher initial cost and lack of contractor familiarity with the material. After speaking with NHDOT construction personnel about the use of the material, the construction workers were happy using the material since they could pick up a section by themselves and easily install it on the bridge, using zip-ties as connectors.

Table 4: Deck concrete strength (Bowman M. M., 2002)

<i>Days</i>	<i>f_c</i>
28	5.67
56	6.44
365	6.99

2.3.2 – Girders

The girders that the CFRP deck sits on are New England Bulb Tee prestressed, precast, steel reinforced girders, constructed with high performance concrete. Composite action between the deck and girders is achieved via 13-inch portions of the

CFRP grid used a shear transfer devices. The prestressing strand pattern is a draped strand pattern and a cross section of the girder, can be seen in Figure 6.

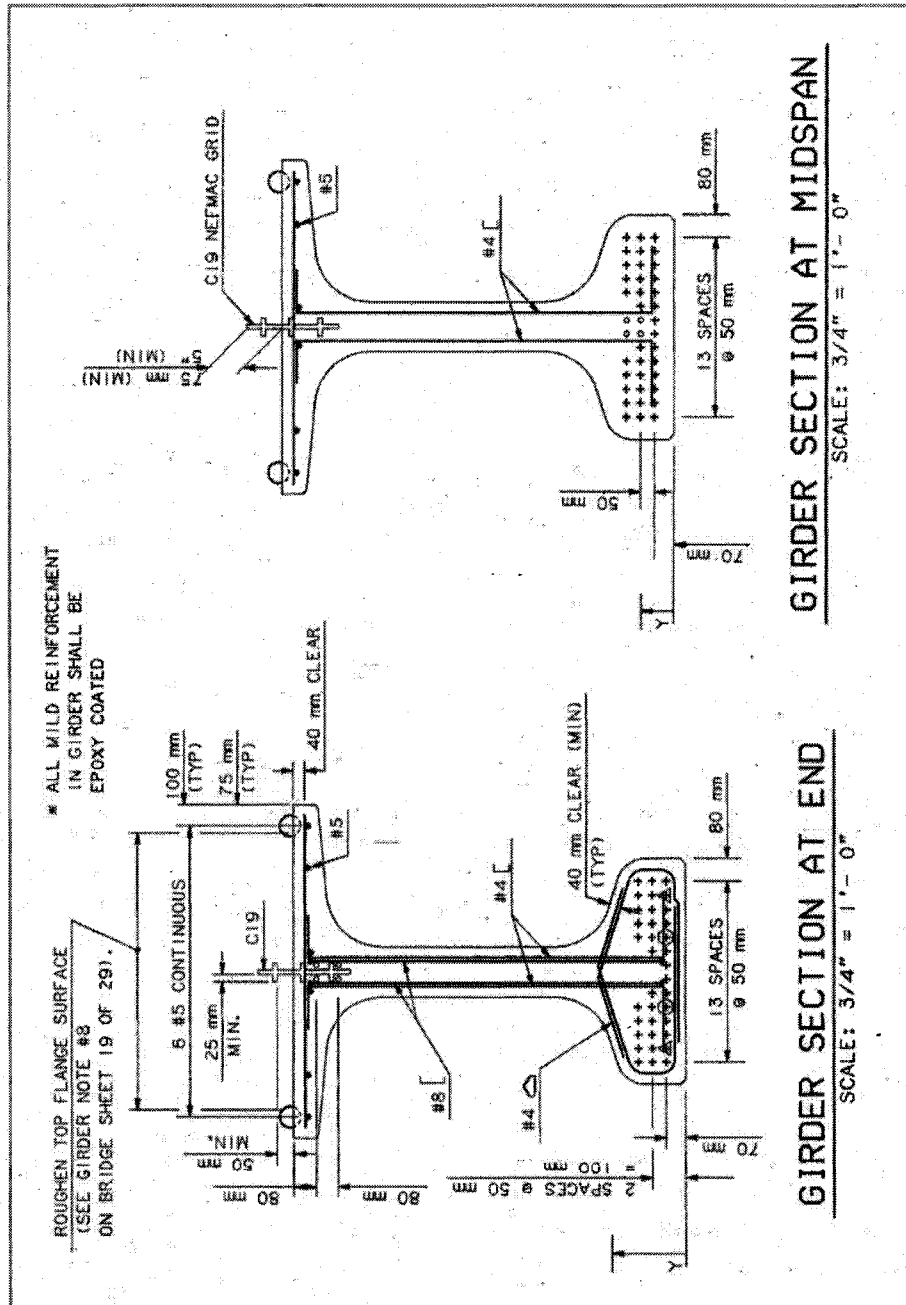


Figure 6: NEBT Section at end and midspan, showing prestressing steel (NHDOT Bureau of Bridge Design, 1999)

2.3.3 – Bearing Pads

Each NEBT girder sits on two, cylindrical, 16-inch diameter, steel reinforced, elastomeric bearing pad located at each end of the girder. The bearing pads were manufactured by The D.S. Brown Company (The D.S. Brown Company, 2008) and are commercially known as Versiflex Elastomeric Bearings. They have a total thickness of 5-and-1/8-inches, contain seven 1/8-inch steel reinforcing plates, have 60-durometer neoprene as the base material, and can be seen in plan and section in Figure 7. According to the AASHTO LRFD Bridge Design Specification Third Edition 2004, the elastomeric bearing pads are used to resist lateral movement due to temperature changes and load application (AASHTO, 2004). The bearing pads are important as they influence the boundary conditions for the model and obtaining the actual stiffness value of the bearing pads was important to the global behavior of the bridge model.

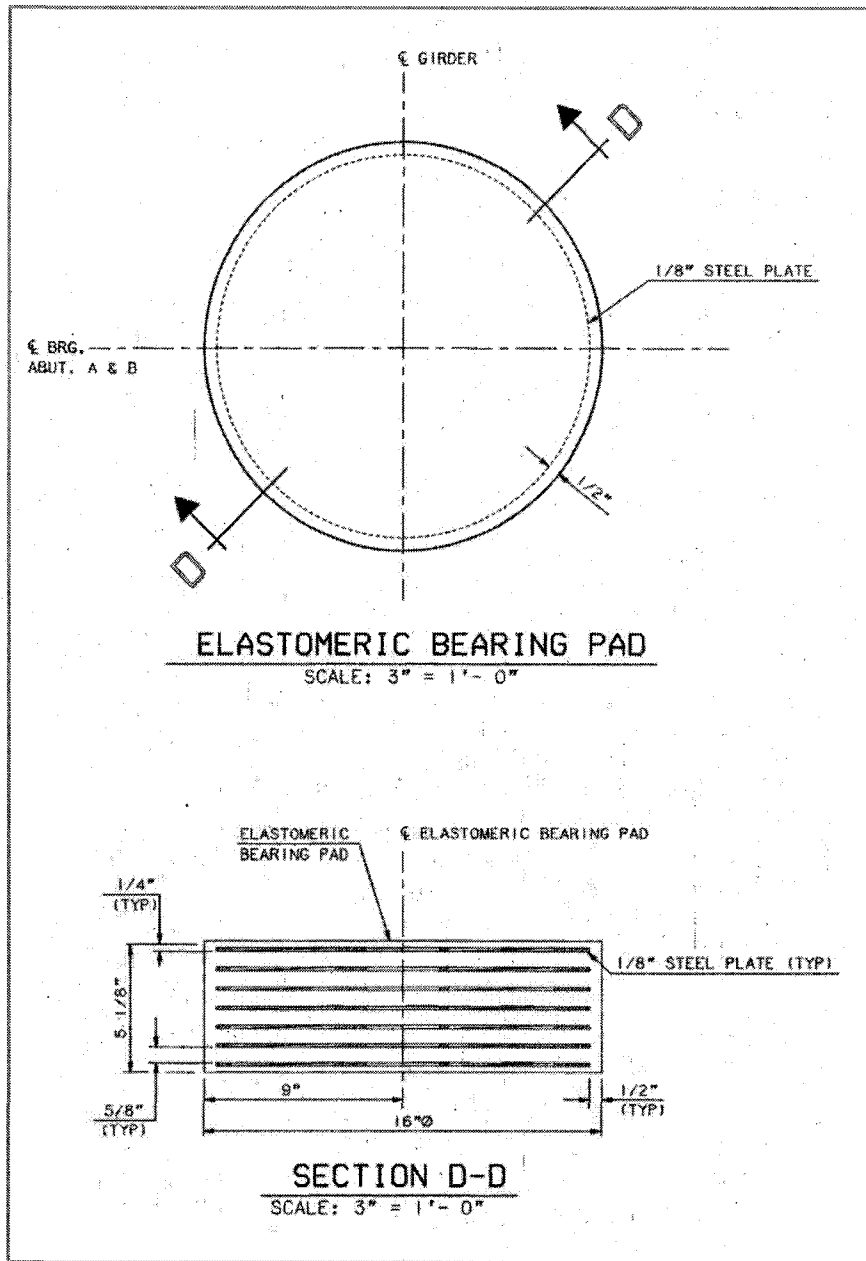


Figure 7: Elastomeric bearing pad details from Rollins Road Bridge Plans (NHDOT Bureau of Bridge Design, 1999)

2.3.4 – Abutments

The types of abutments used at RRB are classified as a heavy abutment (Taly, 1998). Visual inspections prior to load test noted no change to the abutment that would require modeling to capture changes in bridge behavior.

2.4 – Instrumentation Plan

As part of the IBRC, RRB was instrumented in order to capture the behavior of the CFRP and the bridge deck which contained an innovative material. All of the sensors in the deck are oriented in the lateral direction, perpendicular to the flow of traffic. This was done in order to understand the behavior of the deck as it bends over the girder when a load is applied. The only gauges oriented in the longitudinal direction, with the flow of traffic, were gauges in the precast, prestressed, high performance concrete NEBT girders. The purpose of these gauges was for researchers from the University of Nebraska at Lincoln to quantify the loss of prestress in the high performance concrete girders. These longitudinally oriented gauges proved to be most beneficial for the SHM program since they capture the global bending behavior of the bridge. The instrumentation plan was not designed for SHM, however full advantage was taken of the gauges for research in SHM.

The fiber optic concrete strain sensors used in this project are Fabry-Perot strain gauges for embedment in concrete (EFO). The actual Fabry-Perot strain sensor is mounted inside a stainless steel envelope with two end flanges to ensure durability and protection of the sensor for long term monitoring projects, such as RRB. The two end flanges also ensure proper adherence to the concrete. The fiber optic sensors are

also small in size, lightweight, non-conductive, resistant to corrosion, and immune to electromagnetic noise and radio frequencies eliminating need for shielding and lightning protection (Choquet, Juneau, & Bessette, 2000). The robustness of these fiber optic strain gauges make the extra cost of the gauge worthwhile since they are still working correctly after being in service for eight years.

Conventional strain gauges, seen in Figure 8, measure the time it takes for an electrical current to pass over a known distance. If there is a change in the time it takes to get from point A to point B, the change in time is correlated to a change in distance, therefore strain. A similar idea is used for fiber optic strain gauges; however light is used instead of an electrical current. Two mirrors are separated by a known length, and the change in time it takes light to travel between the mirrors is correlated to strain. A photo of the fiber optic strain gauges can be seen in Figure 9.

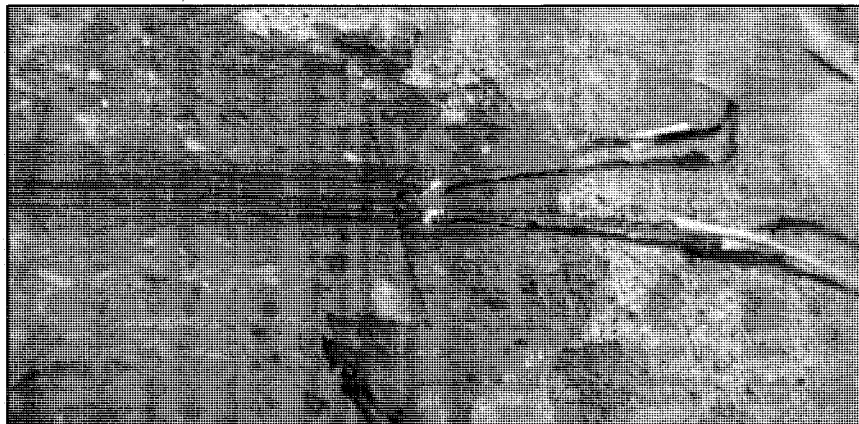


Figure 8: Conventional strain gauge attached to concrete

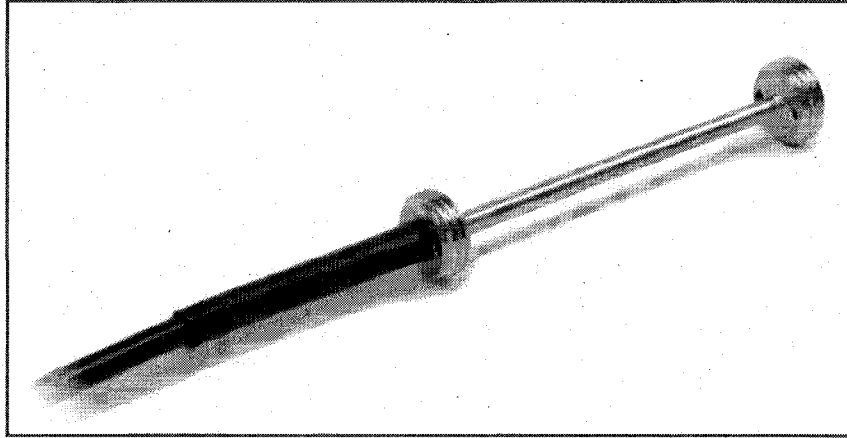


Figure 9: FISO EFO fiber optic strain gauge (FISO, 2008)

The deck gauges, Figure 10, were installed by researchers before the concrete deck was poured. Due to this presence of researchers during the installation and the deck placement could be a contributing factor to the success of the entire instrumentation plan. The gauges were connected to fiberglass studs, arranged in a planned depth throughout the deck. In RRB, all of these strain gauges are concentrated between girders 3 and 4, near the longitudinal midspan. Temperature sensors were also installed in the deck to obtain internal concrete temperatures.

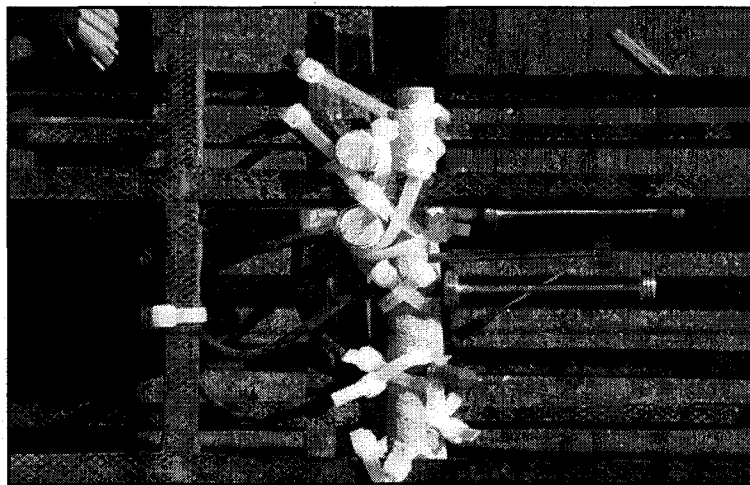


Figure 10: Deck temperature and concrete strain sensors (Adapted from (Bowman M. M., 2002))

Fiber optic strain gauges were embedded into the CFRP grid. Figure 11 shows the strain gauge being inserted between the carbon layers during the manufacturing process. A Kevlar reinforced polyurethane jacket was used around the fiber optic cable for protection. The process of embedding gauges into the CFRP allows for a unique strain reading, being inside the CFRP as opposed to a strain gauge being installed to the outside of a reinforcement bar.

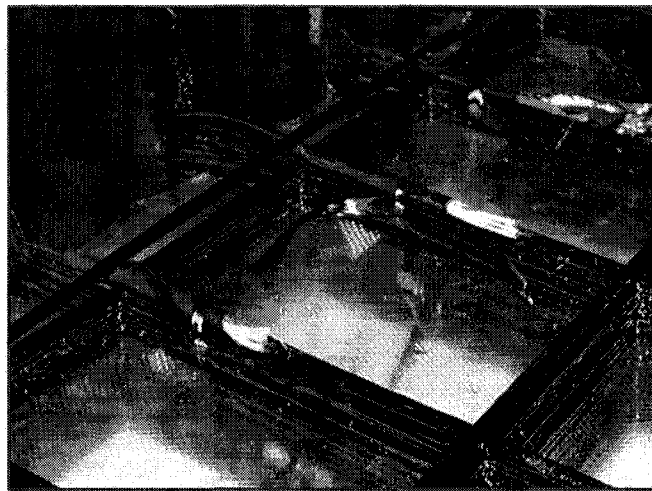


Figure 11: Strain sensors embedded in NEFMAC grid (Adapted from (Bowman M. M., 2002))

The girder sensors are the main focus of instrumentation for this research project. As mentioned before, they are the only sensors in the longitudinal direction allowing bending and axial stresses experienced by the bridge due to traffic to be observed. Longitudinally oriented gauges are best suited for SHM and parameter estimation program. The sensors in the girders are identical to the sensors in the deck. The purpose of these sensors was originally to instrument and observe the prestress loss in the high performance concrete girders. The results from this research, which also examined several other bridges, was used in creating the model and is located in *NCHRP Report 496* (Tadros & Al-Omaishi, 2003). Girders 3, 4, and 5 have strain sensors

installed at the longitudinal midspan of the bridge and at three different depths throughout the girder. These sensors were placed after tendon prestressing but before concrete placement, as seen in Figure 12. Figure 13 shows which gauges were used for analysis in this project. Only four out of the nine girder gauges were used because they were the four that had readings from all load tests and were still working in 2008.

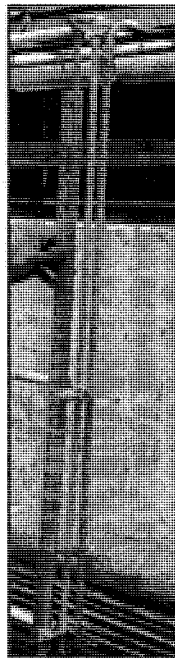
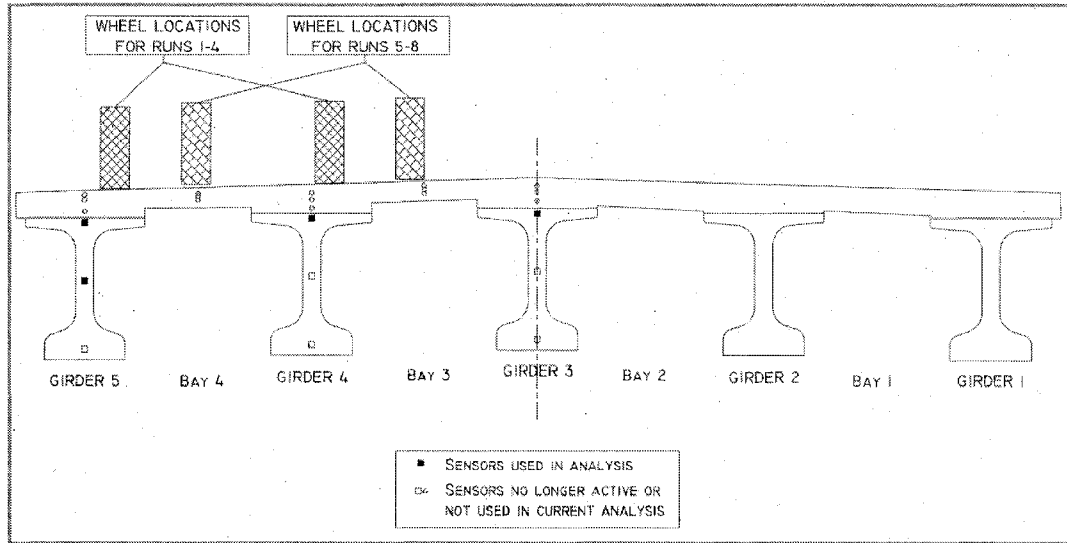
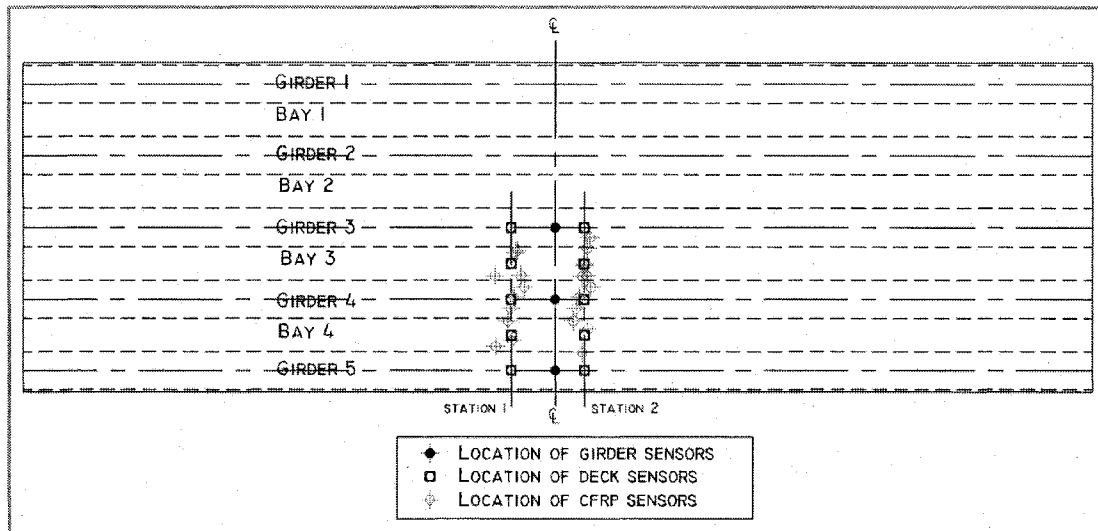


Figure 12: Strain gauges in NEBT girder before prestressing (Adapted from (Bowman M. M., 2002))



(a)



(b)

Figure 13: Graphic of sensors used in Rollins Road Bridge analysis, (a) shows the sensors in section view and (b) shows the sensors in plan view

The data management instrument (DMI) is located on-site and is in good working condition. The DMI is a 32-channel fiber optic data acquisition system provided by FISO Technologies, Inc. This particular DMI model has the ability to record continuous data or be calibrated for a controlled static load test. Since the start of the research project, continuous temperature and strain data has been downloaded from the bridge for use by future researchers to investigate the long term thermal

performance of the CFRP and concrete deck through trends and examining material properties. For the continuous, long term temperature and strain data the DMI is configured to take 60 readings over the period of an hour and average those values to produce one data point for that hour. This allows for two weeks of data to be collected at once without filling the memory capacity of the device. The DMI is also attached to a modem, allowing researchers to remotely call the bridge to download data or see current conditions. One downfall of collecting this continuous data is there is no traffic camera or weigh-in-motion sensor at the bridge to determine amount of traffic during the recording time.

The on-site DMI has a 32-channel capability and for the RRB Research Project Load Test, a second 32-channel DMI was rented from FISO Technologies, Inc. to be able to take full advantage of all working sensors. Out of the 81 sensors originally installed in the bridge, 53 were operational in April 2008. The 64-channels between the two DMIs allowed all 53 sensors to be recorded. The DMI was configured to record data as fast as possible, which ended up being every 4.8 seconds. Figure 14 shows two UNH researchers setting up the DMI on the morning of the load test.



Figure 14: Load test researchers with DMI

2.5 - Previous Work at Rollins Road Bridge

Two previous load tests were performed at RRB, one in December 2000 and the other in August 2001 (Bowman, Yost, Steffen, & Goodspeed, 2003). Bowman's (2002) research investigated the performance of the CFRP and concrete deck. Small, single beam models were used to get transverse forces and moments over the beams. Mostly data-to-data comparison was used in her research. Up to this point, no model of the entire bridge has been created. Data from the previous research did not give "initial" strain gauge readings, as this was not needed at the time. This proved to be an issue when trying to compare the data to a predictive model. As future work, it was also noted that the effects of temperature on the response bridge should be examined (Bowman M. M., 2002).

CHAPTER III

FIELD TESTING PROTOCL AND PROCEDURES

An important part of SHM, with parameter estimation and model updating, is performing nondestructive load tests at the bridge to capture structural behavior. Nondestructive testing techniques apply a load to the bridge while keeping the response in the linear elastic range in order to not damage the structure or cause accelerated deterioration. While loads are being applied, measurements of structural response are recorded. These measurements are taken in a variety of different methods included strain, displacement, rotation, and acceleration.

3.1 - Previous Load Tests

Two load tests have been conducted at RRB as part of previous research (Bowman M. M., 2002). One load test was conducted 56 days after pouring the concrete in December 2000 to establish a comparative baseline for the analysis of the CFRP and deck behavior. Another load test was performed in August 2001 to observe the progress of the CFRP in the deck. Both tests were conducted by UNH with cooperation of the NHDOT. Since the tests were performed to observe CFRP and deck performance, the sensors in those locations became the focus of the load tests. Girder

gauge data was also captured for future use and prestress loss research. The type of analysis done on the measured response was data-to-data comparison without comparing to a predictive model.

The truck used in the December 2000 load test had a gross weight of 75.6-kips (37.8-tons) while the August 2001 load test truck had a gross weight of 76.9-kips (38.45-tons). Actual wheel distributions can be seen in Table 5. Both of these trucks had three-axels, with each of the two rear axles containing four wheels. It was noted by the New Hampshire State Police personnel that weight of these trucks would have been over the legal limit for their configuration if they were not NHDOT trucks and not being used for a load test.

Table 5: Load test wheel weights for all three years

	2000		2001		2008	
	Driver Side	Passenger Side	Driver Side	Passenger Side	Driver Side	Passenger Side
Front Tires <i>kips</i>	11.20	11.80	10.45	10.10	5.25	5.25
Front Duals <i>kips</i>	13.50	12.90	13.55	14.60	N/A	N/A
Rear Duals <i>kips</i>	13.40	12.80	15.10	13.10	12.93	13.95

3.2 - April 2008 Load Test

The load test for the Rollins Road Bridge Research Project was conducted on 18 April 2008. The purpose of this load test was to collect data in a similar fashion to the previous load tests, while also collected data to be used for SHM. The biggest change between the 2000/2001 and the 2008 load test programs was the spacing between stop locations on the bridge. The 2000/2001 stop locations had to be close to the

CFRP and deck gauges to get accurate readings, while the 2008 load test was not as concerned with those local measurements and wanted to capture the global response. The difference between the two load test programs ended up being the removal of only a few stop locations. When researchers went to paint markings on the bridge for the 2008 load test, the old stop markings were still visible and a majority of the 2008 load test markings correlated to previous markings. Rollinsford Police Department was used for traffic control on the bridge during the load test. No traffic was allowed to pass while strain readings were being taken, and traffic was allowed to pass when the truck was being moved. Three zero-load readings were also taken during the duration of the load test, which proved to be crucial in relating measured response to the monitoring model. The NHDOT Survey Crew used differential leveling to obtain displacement readings during the load test.

3.2.1 – Truck Specifications

This load test, like the previous two load tests was done in conjunction with the NHDOT. A two axle NHDOT Sand Truck, as seen in Figure 15 and Figure 16, was used for load application to the bridge. The wheel weights of the truck were taken in similar fashion to the previous load tests by the New Hampshire State Police Mobile Weigh Station, seen in Figure 16. The gross weight of the truck was 37.4-kips (18.69-tons). This truck weighed less than requested weight of 35-tons; however the quality of the recorded data was acceptable.



Figure 15: NHDOT sand truck as load application during April 2008 load test



Figure 16: Trooper Huddleston (NH State Police) taking NHDOT wheel load measurements

The distribution of wheel loads can be seen in Table 5. Trooper Huddleston, the representative from the State Police, noted this truck would have been sighted as overloaded due to its current configuration, but was exempt because it is a NHDOT truck and part of a research project load test. Even though the truck was overloaded, it was still within the linear elastic range of behavior for RRB. Trooper Huddleston has

noted that the Haenni Scales, model #WL 101 (Haenni, 2008), have a variance of less than 1% and are tested and certified by the NH State Police.

The dimensions for the truck were 14-feet 9-inches between the center of the front and rear wheel. The rear dual had a thickness of 1-foot 8-and-½-inches. The rear axel, center of dual to center of dual, length was 6-feet 2-inches. The front wheel had a thickness of 8-inches and the length of the front axle from center of wheel to center of wheel was 7-feet.

3.2.2 – Testing Plan

The truck ran in the north-west direction and south-east direction a total of eight times, four in each direction. Two separate marking groups were laid out on the bridge. One group had a wheel directly on the girder and the other had the wheels straddling over a girder. Each group of markings was traveled two times per direction, two directions, equaling four times per marking group, two marking groups, a grand total of eight passes. Initial measurements for the markings were done using an estimated truck size, and the actual truck that was used for the load test was similar to those estimations. In runs one through four, the trucks wheels were on girders five and four. For runs five through eight, the trucks wheels straddled girder 4. All of the stop locations for the April 2008 load test can be seen in Figure 17.

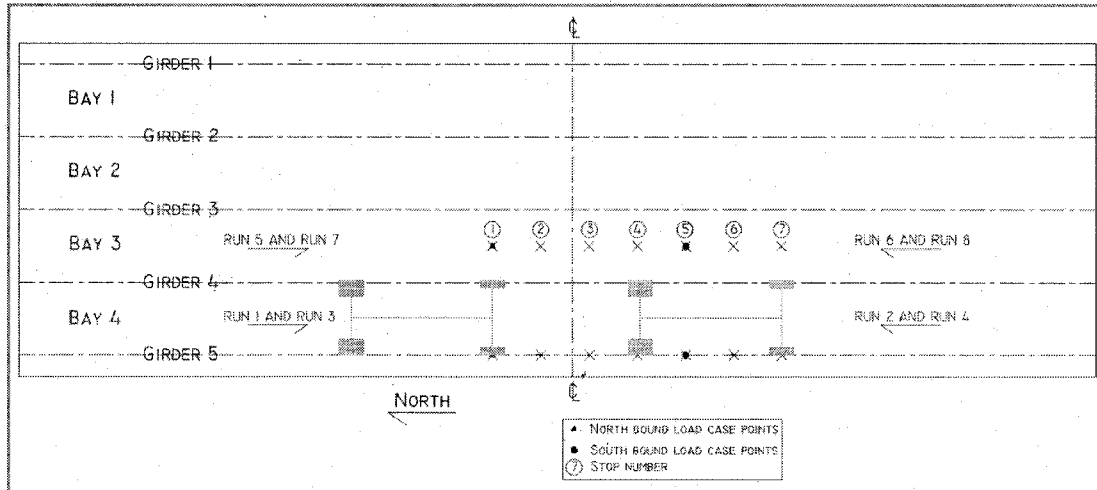


Figure 17: April 2008 load test truck stop/analysis diagram

3.2.3 – Snapshot Quality Assessment

The reason for having two passes in one direction on one group of markings was originally for statistical purposes. However, this was the first time that researchers realized something was effecting the strain readings on the bridge instead of just the direction and size of load application. This was later determined to be temperature. Figure 18, Figure 19, and Figure 20 show CFRP, deck, and girder gauge strain values respectively for passes over the same grouping in the same direction. The CFRP and deck readings show there is a difference of 10-microstrain and 5-microstrain in the girder gauge. If temperature was not an issue, and under original assumptions, these lines would have fallen right on top of each other. The effects on strain caused by temperature will be discussed in Chapter IV: Data Quality Assurance and Data Quality Control.

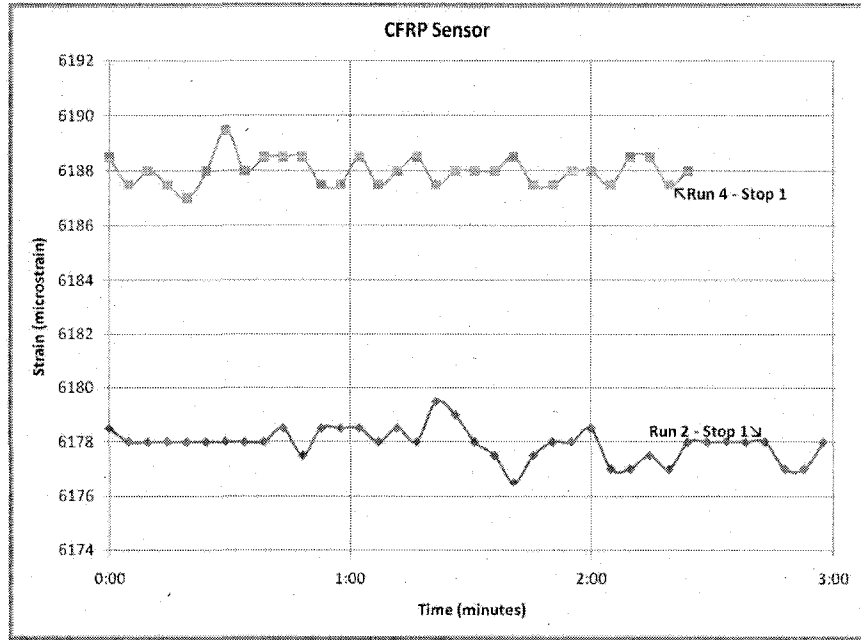


Figure 18: CFRP sensor recorded strain for two passes at same location, different time

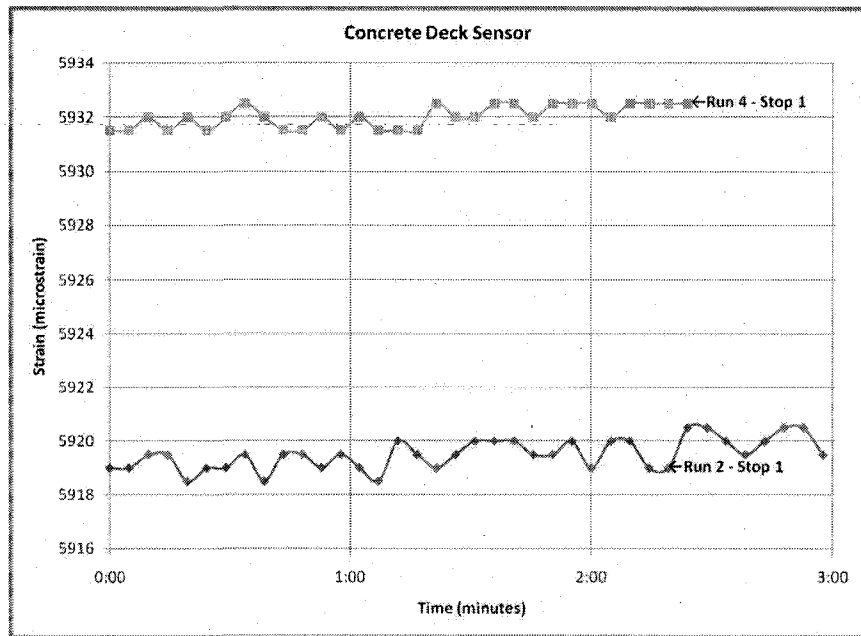


Figure 19: Concrete deck sensor recorded strain for two passes at same location, different time

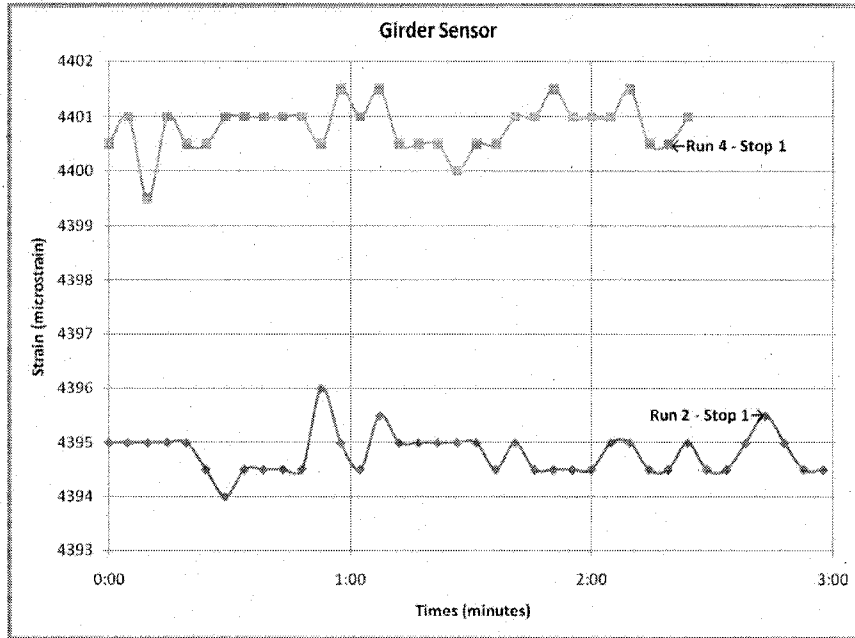


Figure 20: Girder sensor recorded strain for two passes at same location, different time

Out of the 56 stop points during the April 2008 load test, four points were used as the four modeled load cases. These stop points correlate to times there was temperature, strain, and deflection readings. The resulting load cases for the April 2008 load test can be seen below in Figure 21, Figure 22, Figure 23, and Figure 24. Similar methodology was done to make four load cases for both the December 2000 and August 2001 load tests, which all can be seen in Appendix B – Load Cases for All Years.

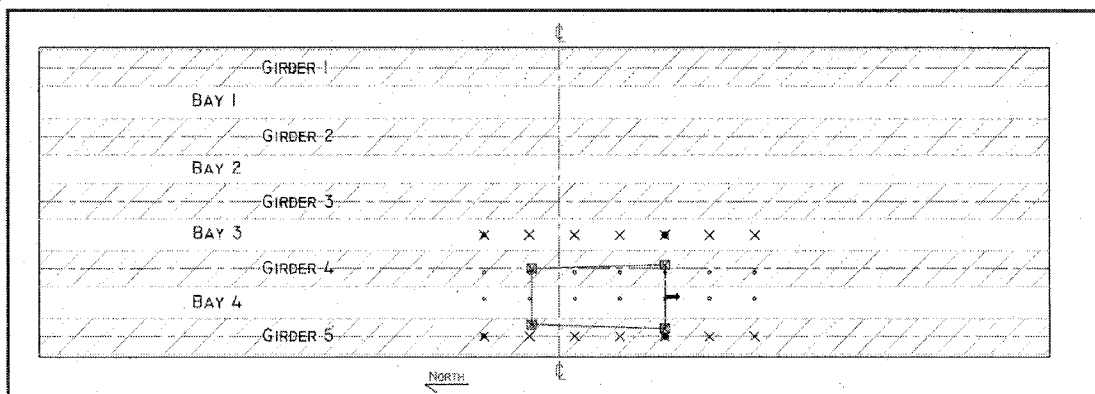


Figure 21: Load case 1 April 2008 load test

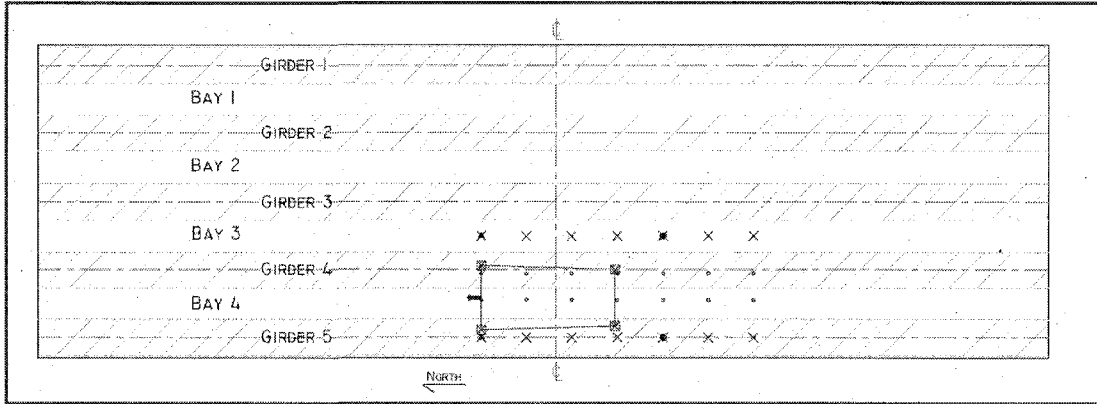


Figure 22: Load case 2 April 2008 load test

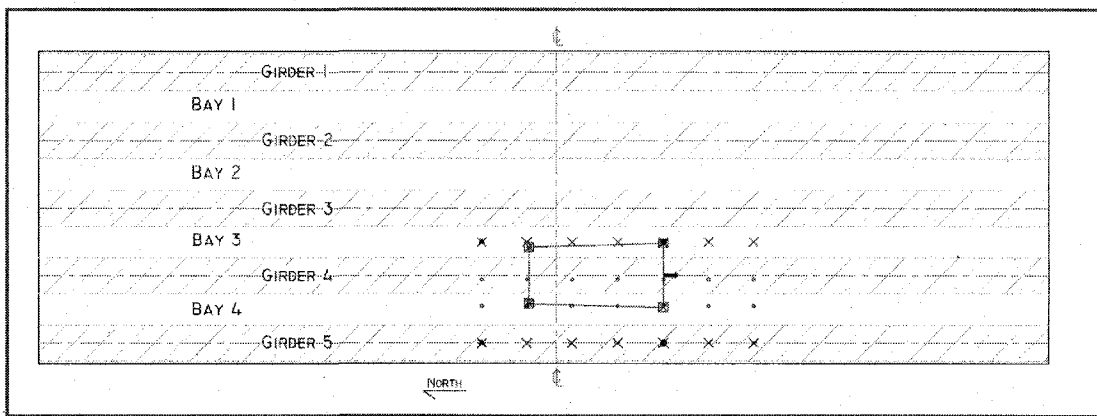


Figure 23: Load case 3 April 2008 load test

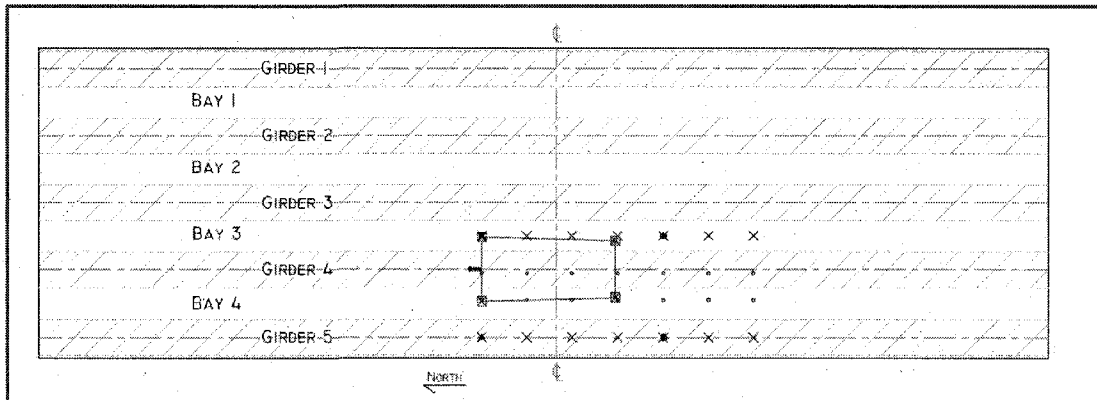


Figure 24: Load case 4 April 2008 load test

3.2.4 – Ambient Temperature Measurements

Ambient air temperature and deck surface temperatures were taken during the duration of the load test. Ambient temperature measurements were included when creating the load test program in case, and as proved to be, temperature played an

important role in the structural response of the bridge. Deck surface, ambient air above, and below the deck temperatures were taken at the same interval, every 15-minutes. Figure 25 shows the ambient temperature readings during the duration of the April 2008 load test. At the end of the load test there was about a 25°F temperature difference between above and below the bridge deck.

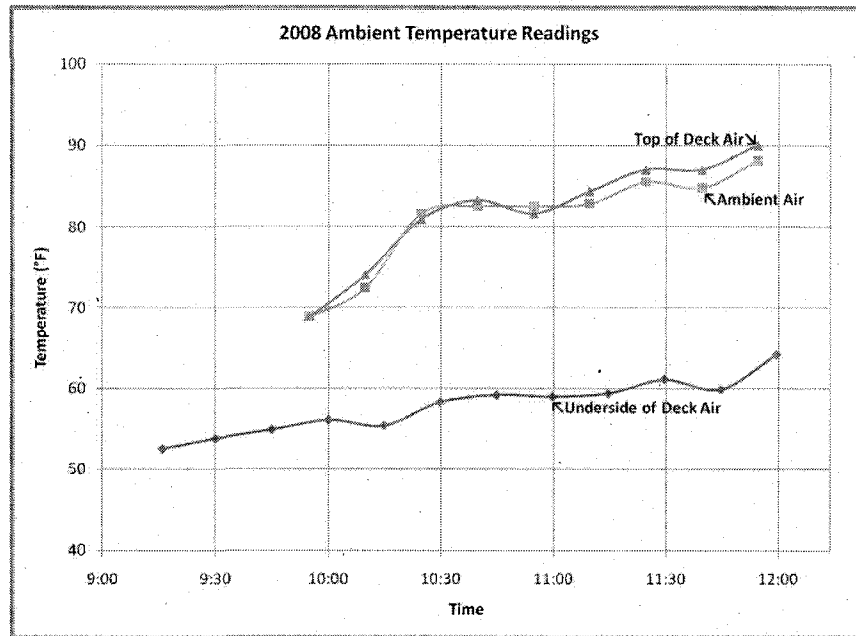


Figure 25: Rollins Road Bridge 2008 load test ambient temperature readings

3.2.5 – Optical Displacement Measurements

Optical displacement techniques were implemented during the load test. Several researchers from industry as well as two undergraduate researchers performed optical displacement field measurements. The two undergraduate researchers, Pat Nearing and Peter Krauklin, used this opportunity as a field test for their senior project. Rick Farad from River City Software in Exeter, NH and Ron Gamache of Transtech Systems, Inc., from Schenectady, NY were the industry researchers. The information obtained from these groups was not included in this

research; however these teams will use the survey displacement measurements to correlate back to the displacement obtained from the photographs. The goal of the optical displacement research is to find a financially viable and accurate way to take pictures of targets installed on the bridge during the load test, and after post-processing the images obtain accurate displacement measurements.

The undergraduate researchers from UNH had success in the laboratory and some difficulty with the field measurements. This difficulty could be due to field variables such as heat shimmer, settlement, and train vibrations. The optical displacement research will continue in conjunction with SHM projects at UNH. The results from the industry research partners have yet to be shared with the research group.

3.2.6 – Global Displacement Measurements

The Rollins Road Bridge has bolts installed to the underside of the girder and deck for purposes of taking displacement measurements. When planning the load test, researchers determined when the center of mass of the truck would be closest to the midspan of the bridge, therefore having the largest deflections on the single span structure. Displacement measurements were taken at five locations at the midspan of the bridge, on girder 5, bay 4, girder 4, bay 3, and girder 3. The NHDOT Survey Crew used a digital leveling rod to take the measurements. A NHDOT bucket truck was used to get a survey crew member up to the underside of the bridge, as seen in Figure 26.

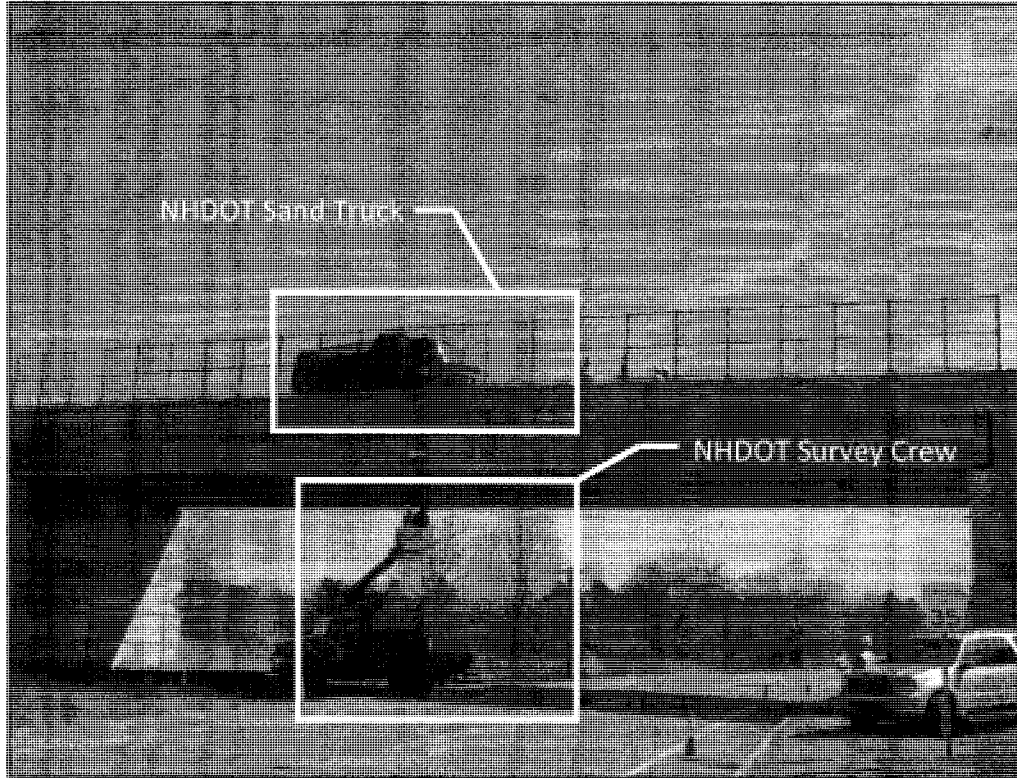


Figure 26: Photo of load test while survey crew takes displacement reading

Displacement readings are typically not used in SHM since they are highly reference dependent measurements. Strain and rotation are typically used to obtain structural response because they are not reference dependent. The repeatability of the deflection readings is limited due to factors including load truck vibration, wind, adjacent train, and measuring bucket stability. The deflection data can be seen below in Table 6, Table 7, and Table 8 and will be used for verification of the manually updated model as seen in Chapter VI: Manual Model Updating.

Table 6: December 2000 load test elevations (Bowman M. M., 2002)

	December 2000 Elevation (feet)								
	No Load	Girder 5 Front Wheel	Girder 5 Rear Wheel	Bay 4 Rear Wheel	Girder 4 Rear Wheel	Bay 3 Front Wheel	Bay 3 Rear Wheel	Girder 3 Front Wheel	Girder 3 Rear Wheel
Girder 3	151.7338	151.7254	151.7254	151.7235	151.7419	151.7365	151.7274	151.7311	151.7242
Bay 3	156.6243	156.6326	156.6233	156.6205	156.6635	156.6225	156.6246	156.6252	156.6234
Girder 4	151.6632	151.6518	151.6417	151.6448	151.6485	151.6474	151.6427	151.6443	151.6643
Bay 4	156.4805	156.4725	156.4591	156.4589	156.4662	156.4704	156.4678	156.4767	156.4660
Girder 5	151.5077	151.4863	151.4944	151.4925	151.5043	151.4986	151.4866	151.5274	151.5058

Table 7: August 2001 load test elevations (Bowman M. M., 2002)

August 2001 Elevation (feet)									
	No Load	Girder 5		Bay 4		Bay 3		Girder 3	
		Front Wheel	Rear Wheel	Front Wheel	Front Wheel	Front Wheel	Rear Wheel	South Direction	Rear Wheel
Girder 3	151.6776	151.6692	-----	151.6684	151.6705	151.6704	-----	151.6736	151.6749
Bay 3	156.5754	156.5573	-----	156.5634	156.5620	156.5732	-----	156.5597	156.5635
Girder 4	151.6090	151.5902	-----	151.5889	151.5914	151.6034	-----	151.5924	151.5976
Bay 4	156.4220	156.3997	-----	156.4112	156.4087	156.4117	-----	156.4033	156.4112
Girder 5	151.4622	151.4328	-----	151.4352	151.4402	151.4436	-----	151.4461	151.4489

Table 8: April 2008 load test elevations

April 2008 Elevation (feet)									
Run #	No Load	1	2	3	4	5	7	No Load	8
Girder 3	151.6552	151.6471	151.6553	151.6540	151.6490	151.6713	151.6480	151.6574	151.6537
Bay 3	156.5472	156.5521	156.5347	156.5350	156.5347	156.5436	156.5682	156.5485	156.5481
Girder 4	151.5794	151.5798	151.5862	151.5828	151.5868	151.5835	151.5871	151.6003	151.5761
Bay 4	156.3835	156.3952	156.3970	156.4063	156.4018	156.3856	156.4060	156.4209	156.3954
Girder 5	151.4224	151.4125	151.4169	151.4184	151.4191	151.4219	151.4112	151.4404	151.4231

CHAPTER IV

DATA QUALITY ASSURANCE AND DATA QUALITY CONTROL

Almost 2,000 data points per channel were collected on two DMIs recording 32 channels of data, resulting in approximately 120,000 data points recorded over the duration of a three hour load test. This is a sea of data for any researcher, however the load test was organized in such a fashion that this sea of data was easily managed. There were two goals for the data collected from this field test. The first goal was to perform a data-to-data comparison, following work of previous researchers and checking the performance of the CFRP. The second goal was to process the data so that it could be used for manual parameter estimation in this research project as well as the first runs in the MUSTANG Research Project.

4.1 - Data-to-data CFRP/Deck Analysis

The data-to-data comparison was done to check the health of the CFRP, deck, and girder. This method was used by Martha Bowman and was used for this research project as requested by the NHDOT to ensure the visual inspection report matches the structural response for RRB. Strain data was graphed with respect to time and can be

seen in the following pages. Three gauges from each the CFRP, deck, and girder were chosen at random, while trying to get a variety of locations, to get a representative sample of the bridge.

4.1.1 – CFRP Reinforcement Data-to-Data Comparison

Figure 27, Figure 28, and Figure 29 show the data-to-data comparison of the strain sensors in the CFRP. For sensor the CFRP bottom grid station 2 above girder 5 strain sensors data is below both the 2000 and 2001 test data, indicating no damage caused to the bottom grid, at station 2 above, girder 5 that would cause excessive strain.

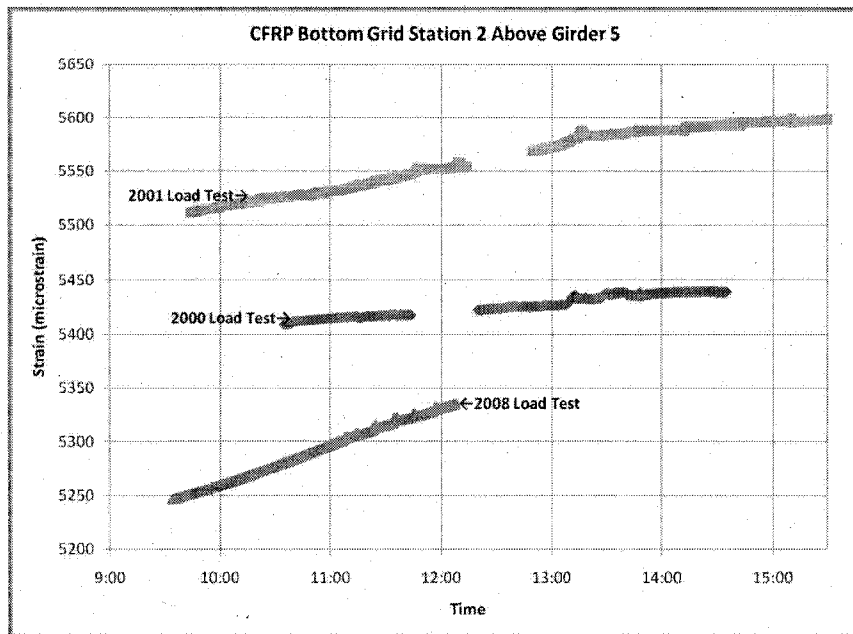


Figure 27: CFRP bottom grid station 2 above girder 5 strain readings for all three load tests

The sensor CFRP upper grid station 2 above girder 3 strain sensors shows the data starts below the December 2000 load test and then goes above that data. The data is still significantly lower than the August 2001 data, indicating no change to the upper

CFRP grid, at station 2, above girder 3. The slope of each line in this graph, and the following graphs, can be associated with the 6°F temperature change for December 2000, 16°F temperature change for August 2001, and the 19°F temperature change for April 2008. The difference in ambient temperature during the load tests correspond to the 2008 line having the greatest slope, followed by the 2001 line, and the 2000 line with the smallest slope. These graphs are at such a scale that the effects from the truck loads are hard to distinguish, however the overall trend of the line can be seen.

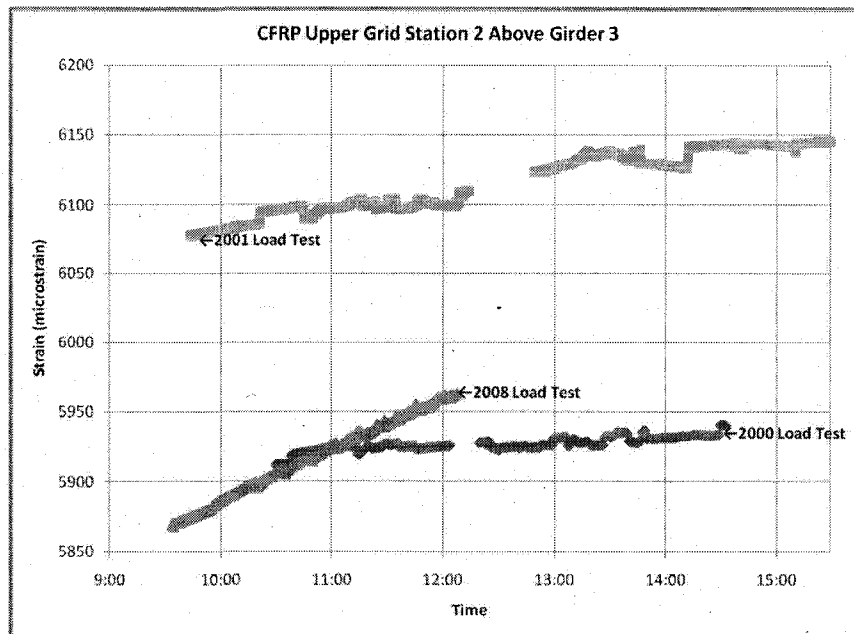


Figure 28: CFRP upper grid station 2 above girder 3 strain readings for all three load tests

The CFRP upper grid station 2 above girder 4 strain sensors shows the data is bounded by the December 2000 and August 2001 data, again indicating that the CFRP reinforcement in the upper grid, at station 2, above girder 4 has not experienced significant changes.

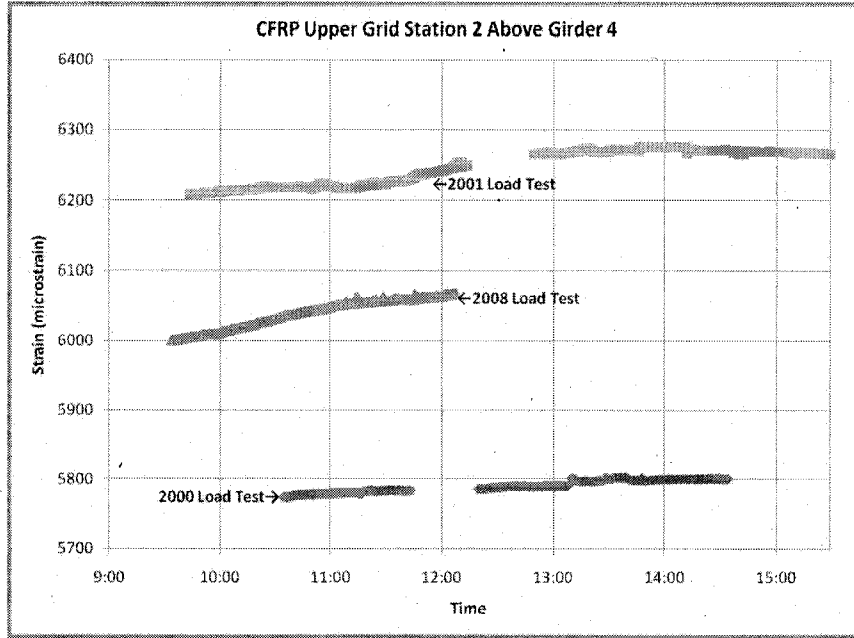


Figure 29: CFRP upper grid station 2 above girder 4 strain readings for all three load tests

4.1.2 – Concrete Deck Data-to-Data Comparison

Figure 30, Figure 31, and Figure 32 show the data-to-data comparison for strain gauges embedded in the concrete deck. The bottom of concrete deck station 2 above girder 4 strain gauge shows the strain values for the April 2008 test fall directly above the December 2000 load test values, and significantly below the August 2001 data. This demonstrates that the concrete at station 2, above girder 4 has not changed significantly.

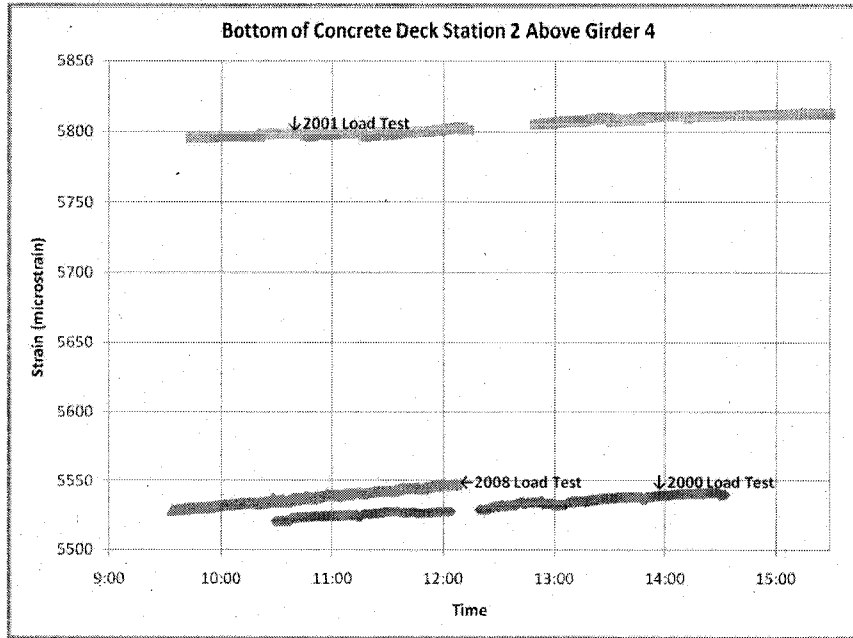


Figure 30: Bottom of concrete deck gauge station 2 above girder 4 strain readings for all three load tests

The top of concrete deck station 1 above bay 3 strain gauge shows that the April 2008 strain values fall below the strain values from both the 2000 and 2001 load tests, suggesting the concrete at station 1 above bay 3 has not experienced excessive deterioration.

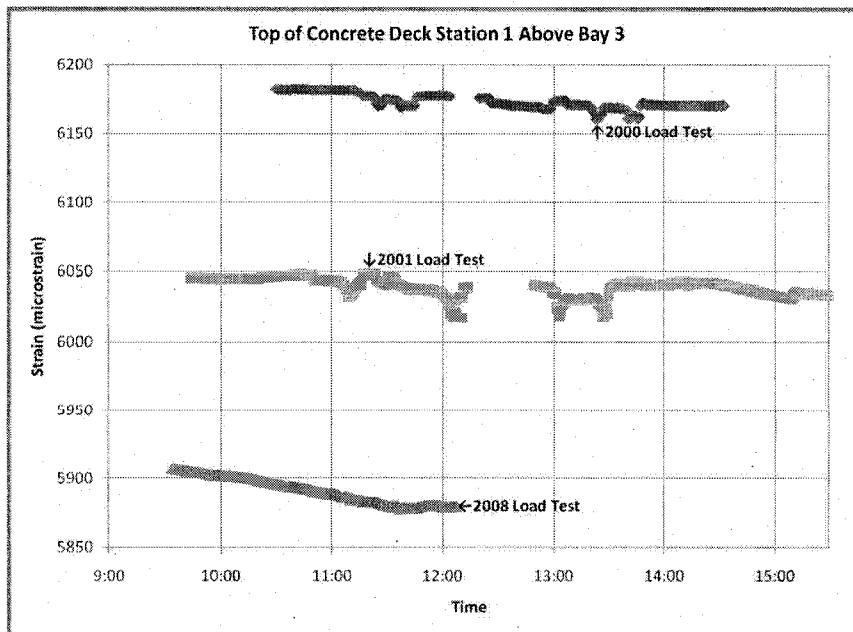


Figure 31: Top of concrete deck gauge station 1 above bay 3 strain readings for all three load tests

The bottom of concrete deck station 1 above bay 3 strain gauge shows again that the April 2008 data falls below the 2000 and 2001 load tests, inferring the concrete at station 1, above bay 3 has not experience damage.

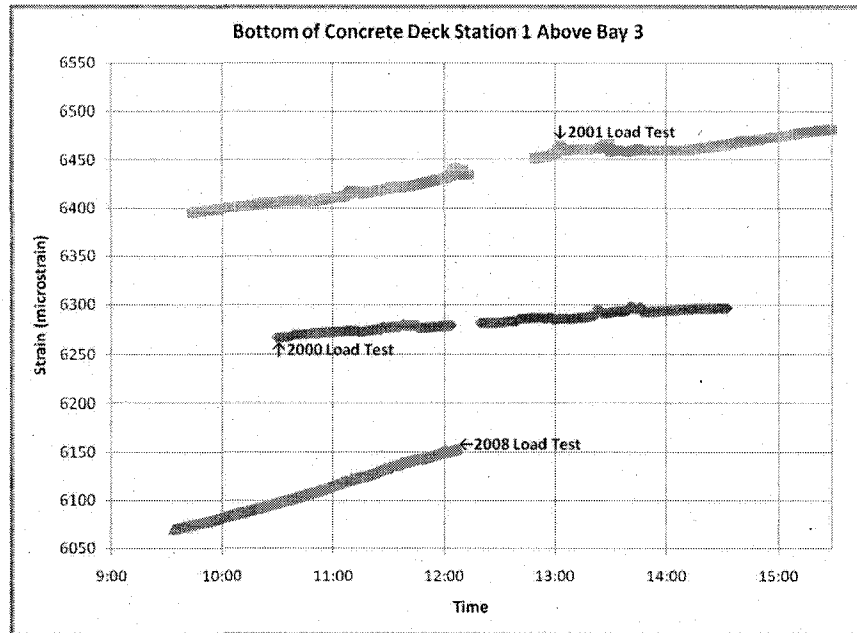


Figure 32: Bottom of concrete deck gauge station 1 above bay 3 strain readings for all three load tests

4.1.3 – Girder Data-to-Data Comparison

Figure 33, Figure 34, and Figure 35 show the strain values for the December 2000, August 2001, and April 2008 load tests in the HPC NEBT girders. The girder 5 top gauge shows that the strain values are bounded by the 2000 and 2001 data, indicating no excessive change in moment of inertia, area, or modulus of elasticity to warrant excessive strain or change in structural behavior.

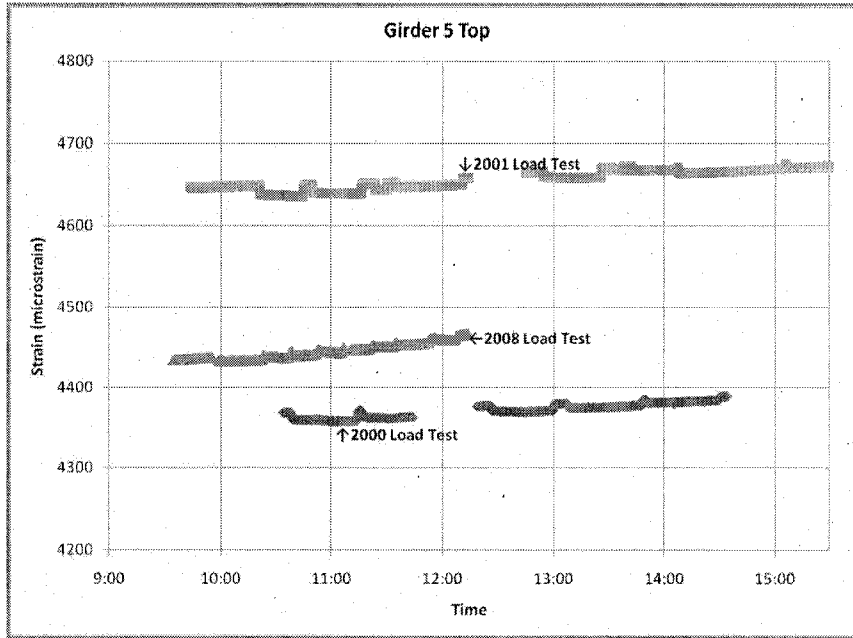


Figure 33: Girder 5 top gauge strain readings for all three load tests

The girder 4 top gauge shows again that the data is bounded by the previous two load tests suggesting no deterioration or change in structural behavior.

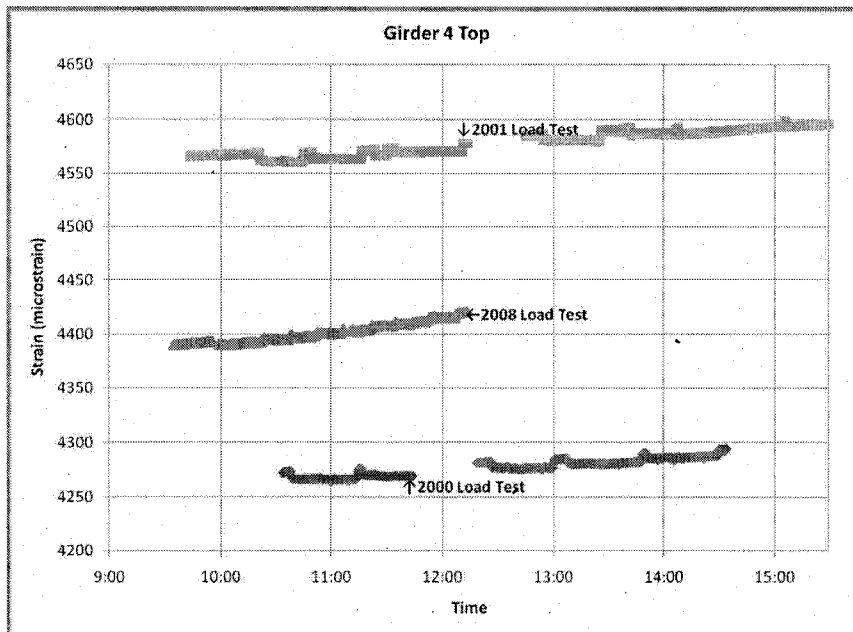


Figure 34: Girder 4 top gauge strain readings for all three load tests

The girder 3 top gauge shows the April 2008 strain values fell below both the December 2000 and August 2001 load test data, showing less strain and indicating no change in structural behavior that would warrant further investigation.

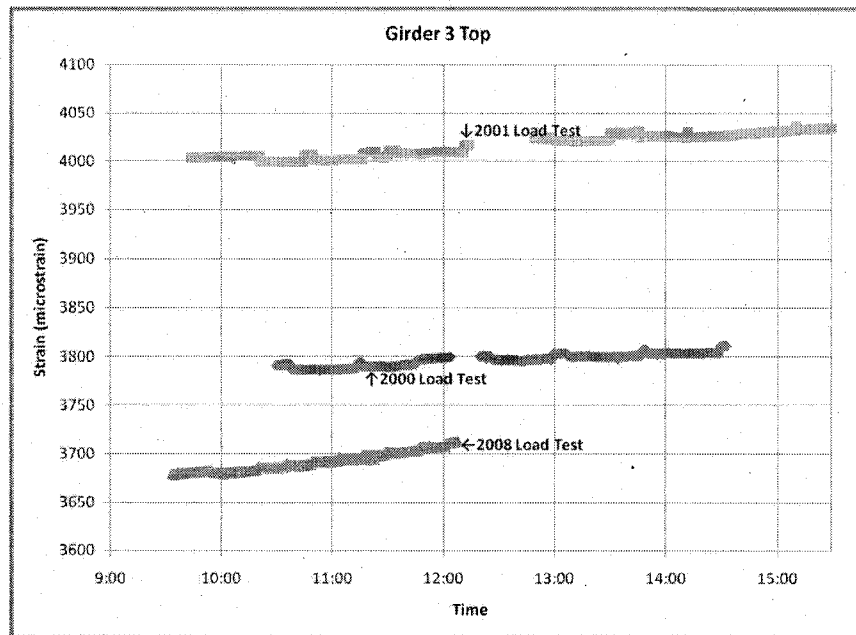


Figure 35: Girder 3 top gauge strain readings for all three load tests

4.2 – Discussion of Data-to-Data Comparison

All of the data-to-data comparisons show the structural behavior at RRB was not in excess. The data shows the April 2008 is either bounded by the previous two load tests or below. It is difficult to do a more comprehensive data-to-data comparison, because so many factors changed between the 2000/2001 and 2008 load tests: the gross weight of the truck used for the April 2008 load test was about half of the truck weight used in the previous two tests, the stopping locations between the 2000/2001 and the 2008 tests were similar but not exactly the same, temperature also continues to show its effect on the structural response of the bridge, the slopes of the lines from year to year seem to vary in some gauges looking at the data, and the

change in ambient temperature in the December 2000 load test was 6°F, while the change during the August 2001 load test was 16°F, and change during the April 2008 load test was 19°F. This temperature differential between the beginning and end of load test and resulting trend in the increasing slope of the strain lines can be seen in the data-to-data comparison graphs. Figure 36 provides a graphical representation of the ambient temperatures recorded during all three load tests by Bowman (2002) for the 2000 and 2001 load tests and by undergraduate researchers for the 2008 load test.

The change in temperature to slope relationship mentioned above and when discussing the CFRP data-to-data comparison is shown most in the CFRP strain gauges. The deck and girder sensors, while following a similar trend in different slopes do not correlate to the change in temperature over the duration during the load test as well as the CFRP gauges do.

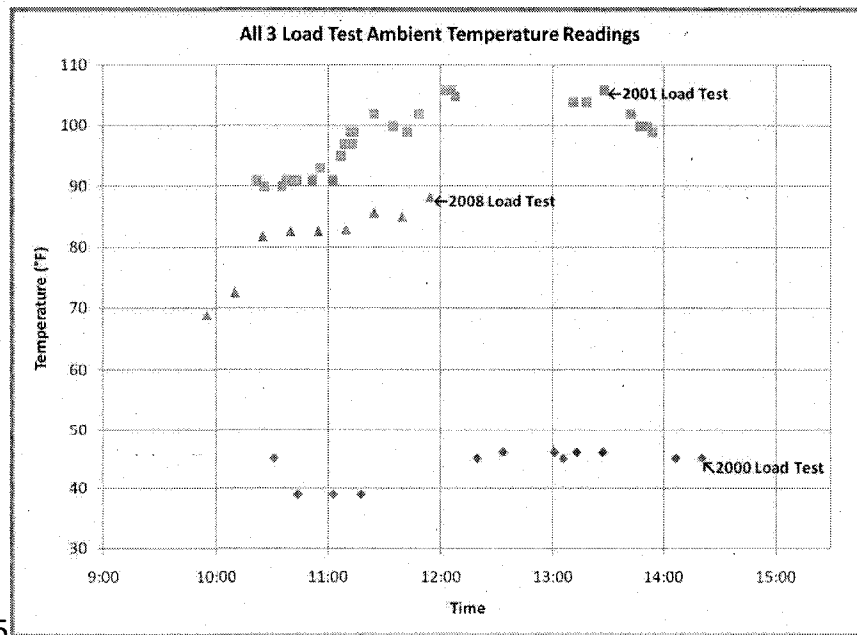


Figure 36: Ambient temperature readings for all three load tests

4.3 - Environmental Effects on Bridge Response

Just by taking a quick look at the data-to-data comparison of strain values, a big effect can be seen between the different load tests that cause the strains to be so different. Figure 37 shows the strain readings for girder 3 and girder 4 over the duration of the December 2000 load test. The graph shows peaks when the truck was on the bridge causing a change of about 6-microstrain. However, over the 4-hour duration of the load test there is a change of 20-microstrain.

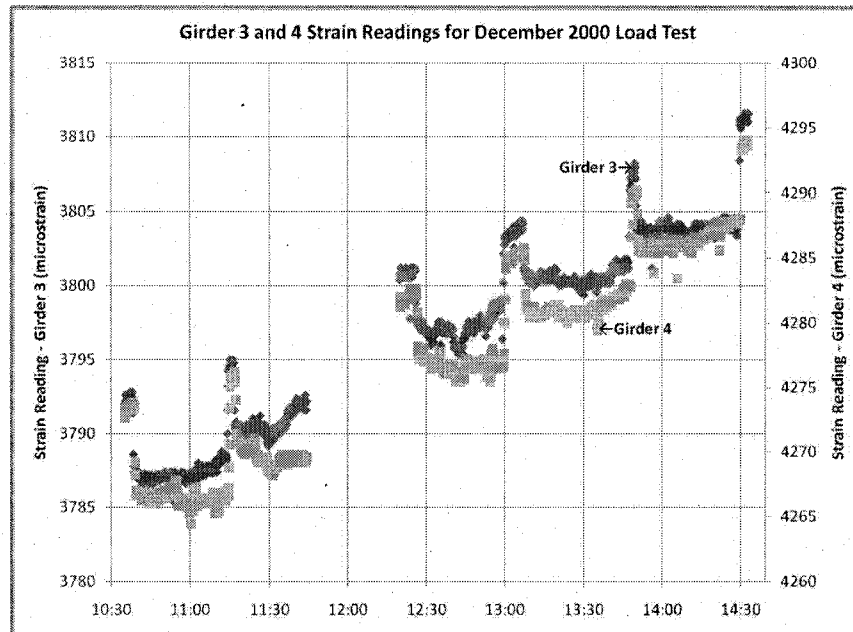


Figure 37: Strain readings from girder 3 and girder 4 over the duration of the December 2000 load test to show difference between thermal effects and load application

A similar trend is seen in the April 2008 load test data, even with the smaller truck load there was a change in strain due to load application of 3-microstrain while the change in strain during the 2.5-hour duration of the load test was around 25-microstrain. This shows an environmental effect, temperature, is masking the change due to a 19-ton, technically overloaded, truck passing over and resting on the bridge.

One benefit at RRB is temperature sensors are installed inside the bridge deck and girders. As discussed in the introduction, changing ambient temperature to material temperature is a source of research and ambiguity in SHM. At RRB, the temperatures of the deck can be measured directly and then correlated to strain values at any moment in time. Once it was determined the change in strain and structural response was heavily influenced by environmental effects, including temperature, it was decided that these effects must either be included in the SAP2000® model of the bridge or removed from the data to allow an accurate modeling of behavior and response for RRB.

4.3.1 – Removal of Strain Caused by Environmental Factors

One option for dealing with environmental strain, including thermal strain, was to remove it from the data, leaving strain caused solely by load application. Removing strain caused by environmental effects, including temperature, removes any ambiguity on what the values for material coefficient of thermal expansion are, how to accurately model the behavior of temperature and humidity, how to accurately capture that behavior, and any modeling errors associated with modeling temperature change. During the April 2008 load test, zero-load readings were included in the load test plan. These zero-load readings were included to record the impact of environmental effects during the duration of the load test. Due to time constraints, only three points were taken, two towards the beginning of the load test and one at the end. The zero-load reading meant the load truck and all traffic were not on the bridge, and the strain and survey measurements were taken. The purpose of these

three points is to see only change in strain or displacement on the bridge caused by a change in temperature.

One strain gauge from girder 3 and one strain gauge from girder 4 will be used in the demonstration on how environmental effects can be removed from the data. Figure 38 and Figure 39 show the girder 3 and girder 4 strain values, respectively, during the duration of the 2008 load test. A linear trend line is also shown, connecting the three zero-load points, which will be discussed further in the explanation.

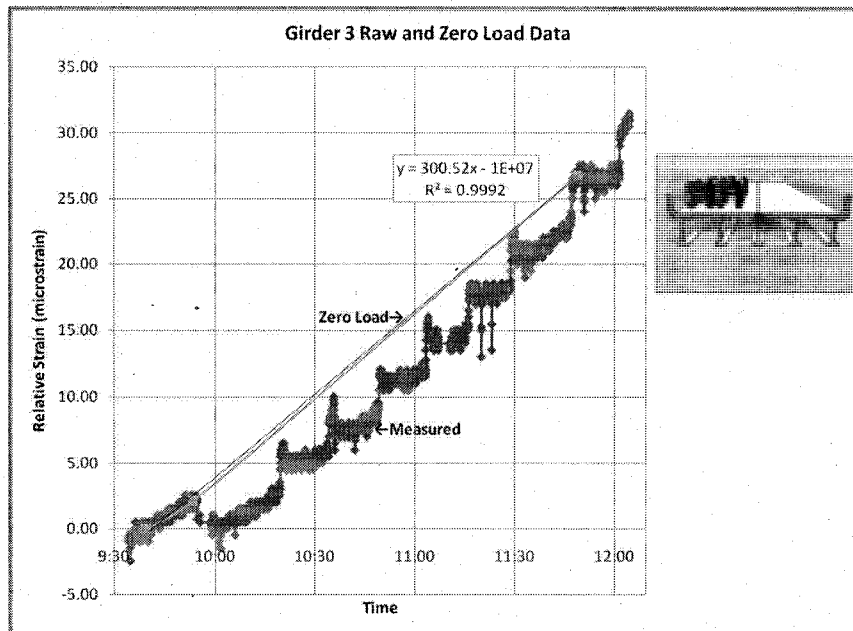


Figure 38: Girder 3 top sensor raw data from April 2008 load test, with three zero-load data points and trend line included

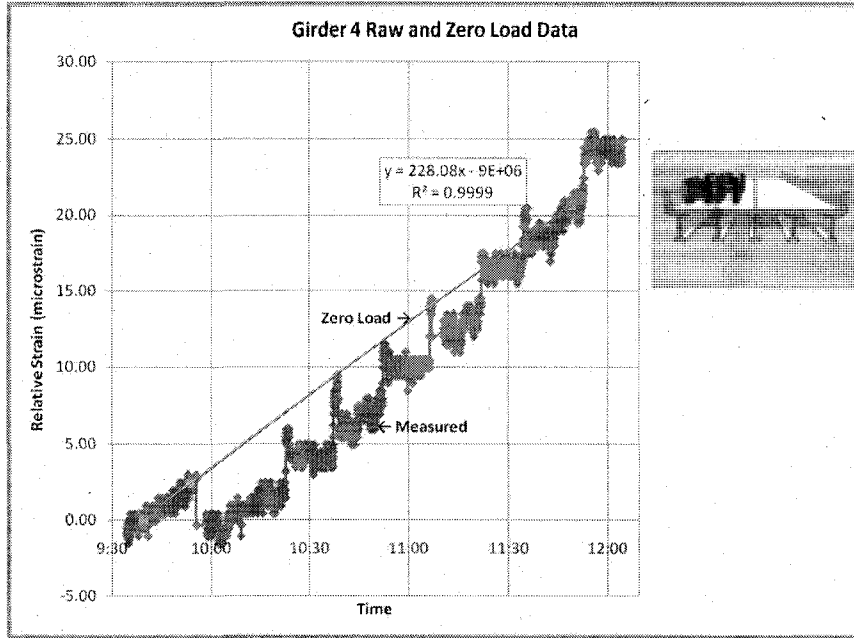


Figure 39: Girder 4 top sensor raw data from April 2008 load test, with three zero-load data points and trend line included

Table 9 shows the three times and coordinating strain values at the zero-load readings. From this point forward, all data will be plotted as relative strain for ease of comparison between conventional corrected, empirically corrected strain, and raw data. This means a point was chosen as a baseline, and all data was compared to that value for each gauge. The strain values in Table 9 are caused solely by the change in temperature since no load applied at those times. Once thermal effects are removed from the data, all three strain readings should read zero.

Table 9: Girder 3 and Girder 4 strain readings at point of zero-load

Relative Zero Points G3	
Time	Strain ($\mu\epsilon$)
9:39:30	0.00
9:53:30	2.12
11:49:30	26.80

Relative Zero Points G4	
Time	Strain ($\mu\epsilon$)
9:39:30	0.00
9:53:30	2.42
11:49:30	20.68

4.3.2 – Conventional Thermal Correction

The conventional thermal strain equation can be seen in Equation 2, where α is the linear coefficient of thermal expansion, ΔT is the change in temperature, L is the original length of the member, and δ_T is the algebraic change in length of the member (Hibbler, 2005).

Equation 2: Conventional thermal change in length equation (Hibbler, 2005)

$$\delta_T = \alpha \Delta T L$$

Bowman (2002) examined the difference between the compensated and non-compensated strain gauges. The coefficient of thermal expansion of the compensated gauge is similar to the substrate in which it is embedded. All of the gauges used in this research project are non-compensated, meaning a slight correction must be performed to remove the expansion of the gauge due to temperature change. Bowman (2002) obtained the equation for this correction from ROCTEST, seen in Equation 3.

Equation 3: ROCTEST correction equation (Bowman M. M., 2002)

$$\varepsilon_{LOAD} = (L_1 - L_0) + (\alpha_g - \alpha_s)(T_1 - T_0)$$

where,

ε_{LOAD} : Real strain, mechanic strain due to applied load
(relative strain)

L_1 : Reading from strain gauge

L_0 : Initial reading from strain gauge

α_g : Thermal expansion coefficient for the gauge (0, if gauge is not compensated)

α_s : Thermal expansion coefficient for substrate on which gauge is fixed (4.4×10^{-6} /°F (Bowman, 2002))

T_1 : Temperature reading of structure

T_0 : Initial temperature reading of structure

Equation 2 is used to calculate change in the structure as a whole. Equation 3 is used to provide a numerical quantification for the difference in thermal expansion of the stainless steel gauge material and the concrete in which it is embedded.

Using Equation 3, the internal temperature readings from the temperature sensors and taking the first zero-load reading for L_0 and T_0 , the conventional thermal correction is applied. The results from the correction can be seen in Figure 40 and Figure 41.

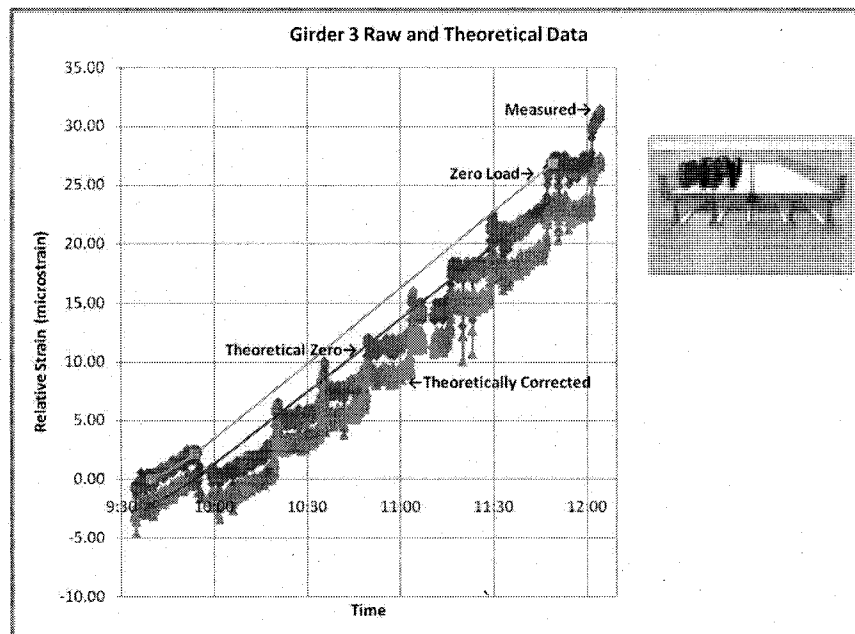


Figure 40: Girder 3 top sensor raw and theoretical data from April 2008 load test, with three zero-load data points and trend lines included

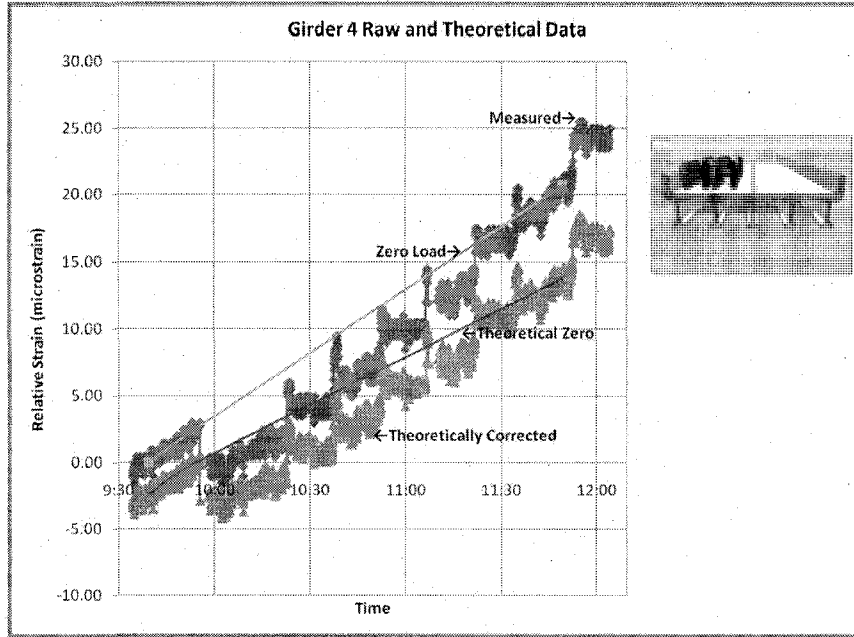


Figure 41: Girder 4 top sensor raw and theoretical data from April 2008 load test, with three zero-load data points and trend lines included

In the graphs above, it can still be seen that temperature effects are masking load application. Table 10 shows a similar table as shown before of the strain readings at the three zero-load times. There has been a reduction in strain values, however if all temperature effects were properly removed, these values should all read zero. Also, if the temperature effects were removed, the trend line for zero-load points shown in the graphs should lay along the x-axis (time axis).

Table 10: Girder 3 and Girder 4 conventionally corrected strain readings at point of zero-load

Conventionally Corrected Zero Points G3	
Time	Strain ($\mu\epsilon$)
9:39:30	-2.13
9:53:30	-0.02
11:49:30	23.77

Conventionally Corrected Zero Points G4	
Time	Strain ($\mu\epsilon$)
9:39:30	-2.39
9:53:30	-0.09
11:49:30	13.75

4.3.3 – Empirical Thermal Correction

Since the conventional thermal correction did not obtain the desired results, researchers investigated a more empirical method to remove temperature. This

method was fairly simple to formulate since there were three zero-load points recorded for the April 2008 load test. Using these three points, the data can be accurately corrected to remove temperature effects and show the bridge response caused only by applied loads. The idea behind the correction is simple and goes along with the desired results from the previous correction. The three zero-load strain values are desired to be zero and the slope of the trend line for the zero-load strain readings should be zero. Using these two basic ideas, the effects of the slope, temperature, can be removed from the data and all the desired results should be achieved.

Using statistical methods, a confidence interval (CI) of 95% on the mean reading during the zero-load times, the correction was applied and the results can be seen in Figure 42 and Figure 43. The previous correction data was included in these graphs to show the change in data.

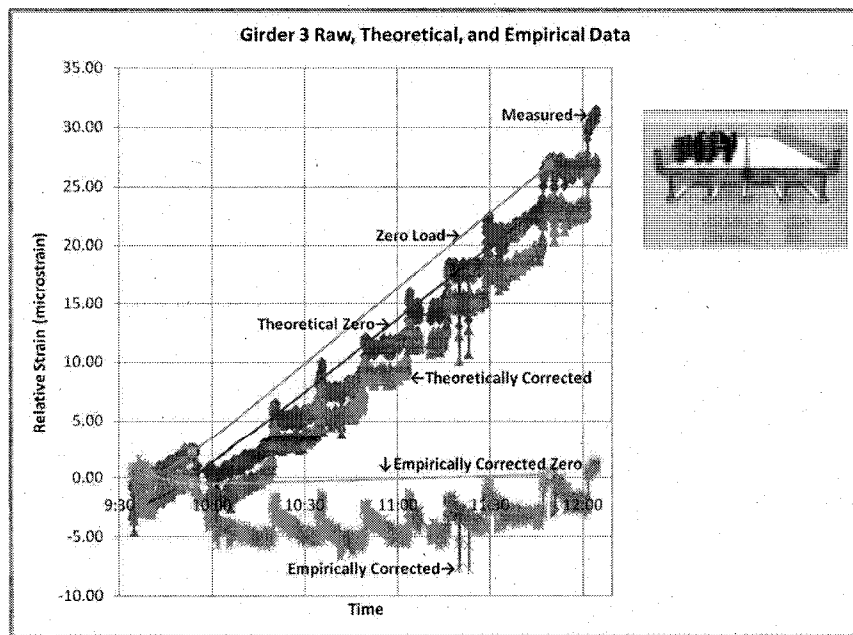


Figure 42: Girder 3 top sensor raw, theoretical, and empirical data from April 2008 load test, with three zero-load data points and trend lines included

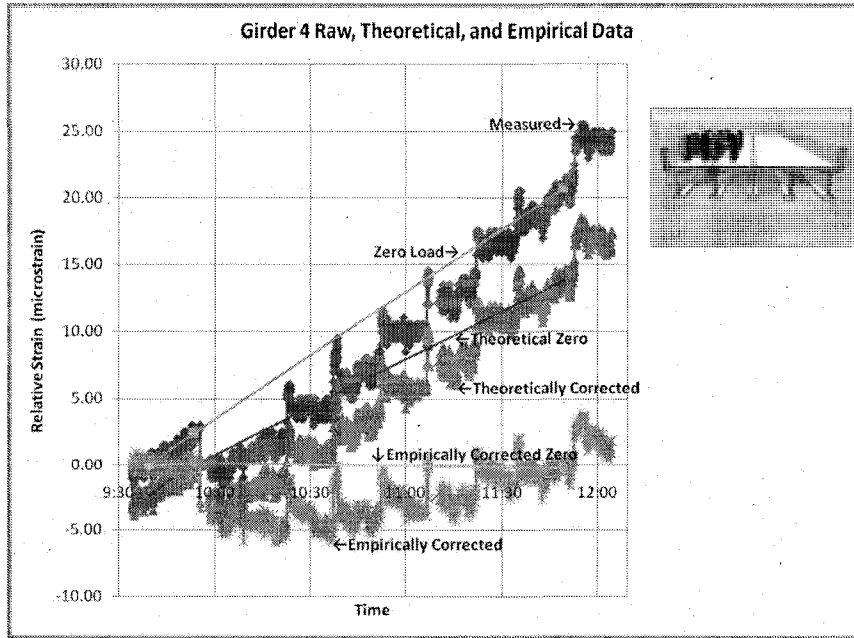


Figure 43: Girder 4 top sensor raw, theoretical, and empirical data from April 2008 load test, with three zero-load data points and trend lines included

These graphs show the reduced overall slope of the zero-load trend line as well as a much clearer visual representation of load application over the duration of the load test. Table 11 numerically confirms that the temperature was properly removed from the data, as the strain values are close to zero. If more zero-load points were taken, the accuracy of the technique would improve. This data looks like the expected response before it was seen how much of an effect temperature had on the structural response of the bridge.

Table 11: Girder 3 and Girder 4 empirically corrected strain readings at point of zero-load

Empirically Corrected Zero Points G3	
Time	Strain ($\mu\epsilon$)
9:39:30	0.42
9:53:30	-0.50
11:49:30	0.29

Empirically Corrected Zero Points G4	
Time	Strain ($\mu\epsilon$)
9:39:30	-0.13
9:53:30	0.15
11:49:30	-0.22

Further verification of the method can be seen in Figure 44 and Figure 45, where the truck position is included in the strain plots. There are two spikes seen in the data

between 11:00 and 11:30 where it was noted by researchers that two large 18-wheeler trucks passed over the bridge. This spike is seen higher on girder 3 than girder 4 because the truck passed over girders 1 and 2 which is adjacent to girder 3.

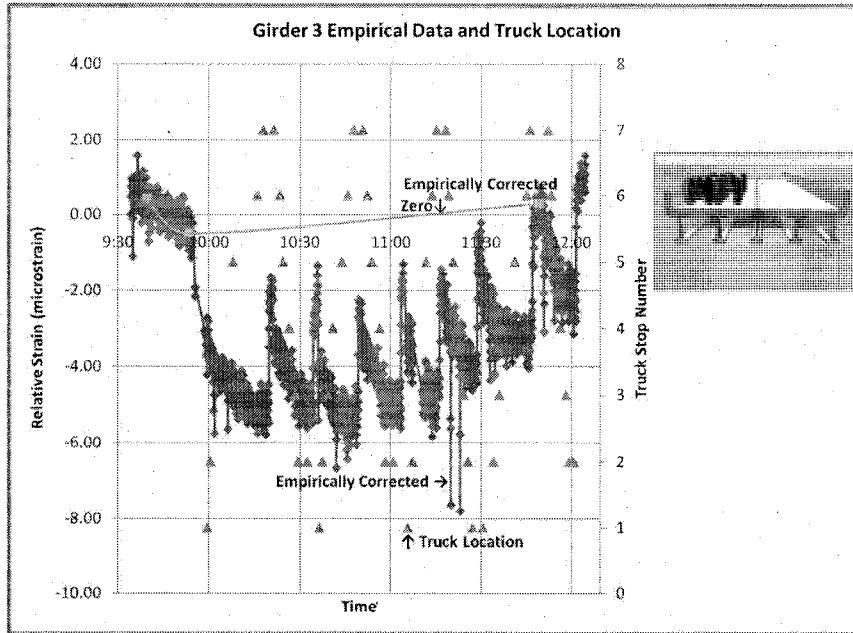


Figure 44: Girder 3 top sensor empirical data with truck position from April 2008 load test

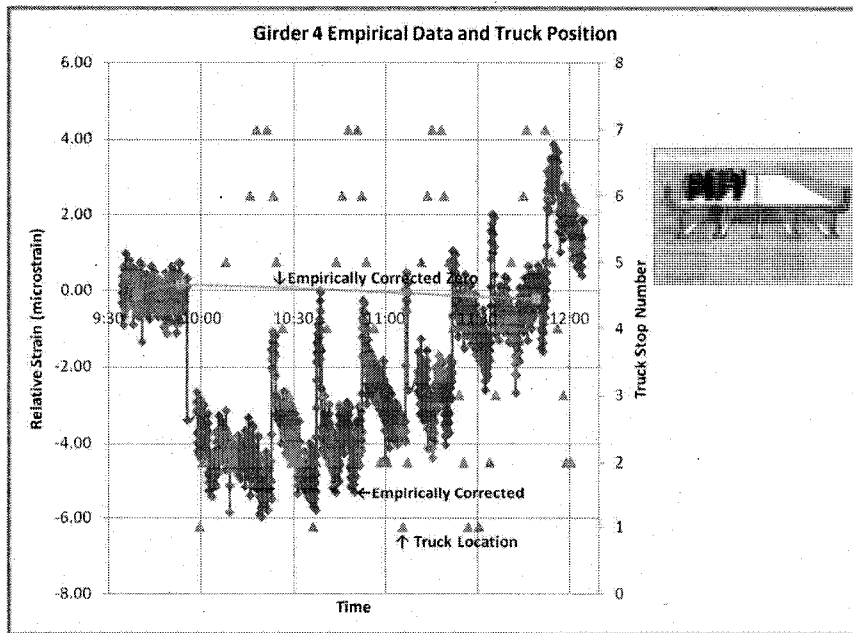


Figure 45: Girder 4 top sensor empirical data and truck position from April 2008 load test

4.3.4 – Discussion of Thermal Correction Techniques

A difference can be noted between the two sets of corrected data which after thinking about the method and reason for the correction is not so striking. The equation for the conventional correction requires a coefficient of thermal expansion. The value used in the analysis was the coefficient of thermal expansion for the high performance concrete where the gauge was installed. Like with any bridge component and the analysis of that component, applied loads are not just taken by one part of the bridge, they are taken by the entire bridge as a whole. Instead of calculating participation factors and a coefficient of thermal expansion for the entire bridge, empirical correction methods can successfully be used to remove temperature from the strain data.

The empirical correction more accurately reflects actual conditions at the bridge and removes unknown components associated with theoretical assumptions. Performing the empirical correction also takes into account all possible environmental effects that could cause a change in structural behavior at the bridge, such as humidity and even soil conditions as the temperature changes throughout the day. The empirical method can be done with little calculation and only requires having several zero-load readings included in the load test program. Once all temperature effects are properly accounted for in the load test data, a more effective model updating and parameter estimating process can take place.

Unfortunately, only the April 2008 load test took advantage of recording several zero-load readings during the load test. The December 2000 and August 2001

load test did have a zero-load reading, although not enough to get an accurate trend of temperature throughout the load test. For this reason, only the April 2008 load test data will be used to update the bearing pad stiffness values for the manual model updating portion of this research.

Figure 46 and Figure 47 show the raw and empirically corrected data along with the four load cases removed for manual model updating. These four load cases correspond to when the truck is located close to the center of the bridge and where survey measurements were recorded.

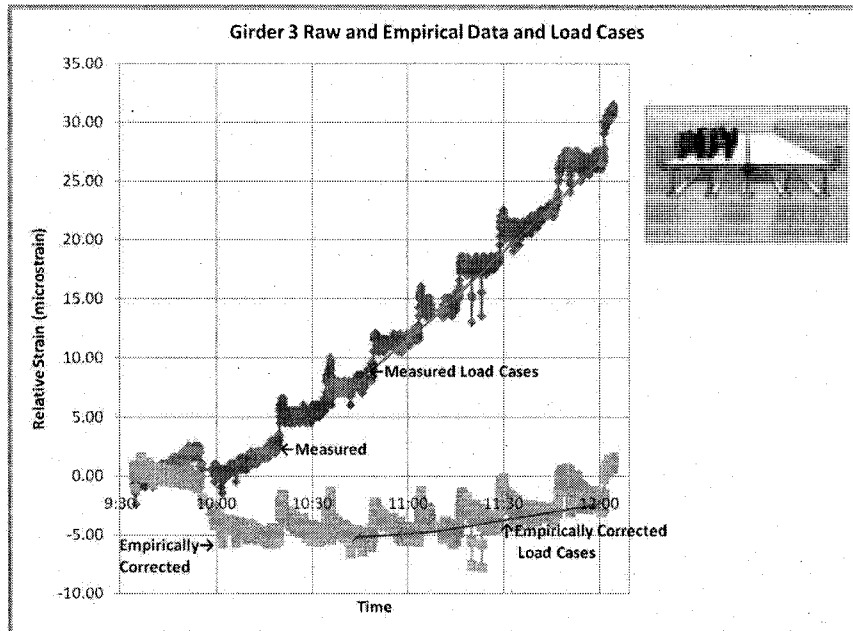


Figure 46: Girder 3 raw and empirical data with manual model updating load cases

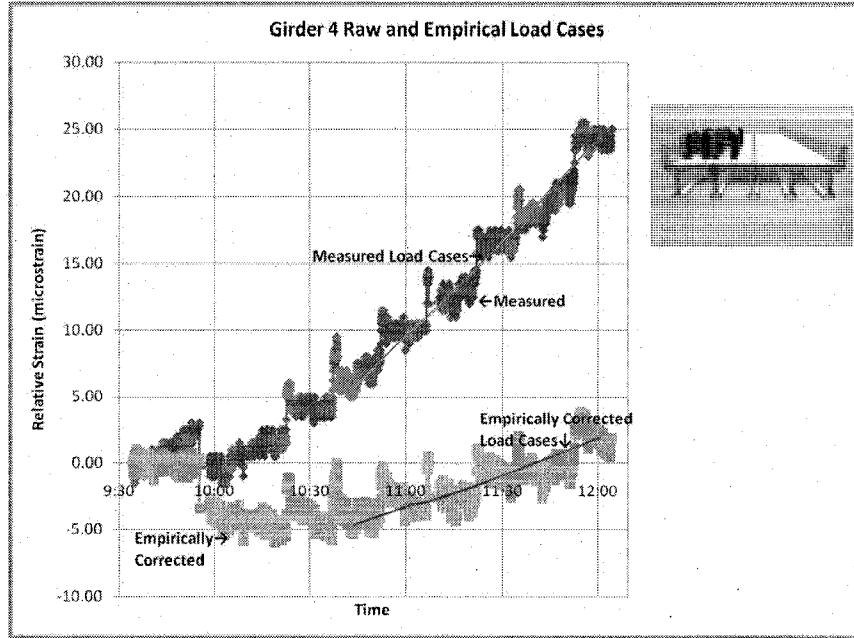


Figure 47: Girder 4 raw and empirical data with manual model updating load cases

A similar correction that was applied to the Girder 3 and Girder 4 sensors was also applied to the girder 5 top and girder 5 middle sensors. Figure 48 and Figure 49 show the raw, theoretical, and empirical data for girder 5 top and girder 5 middle sensors respectively.

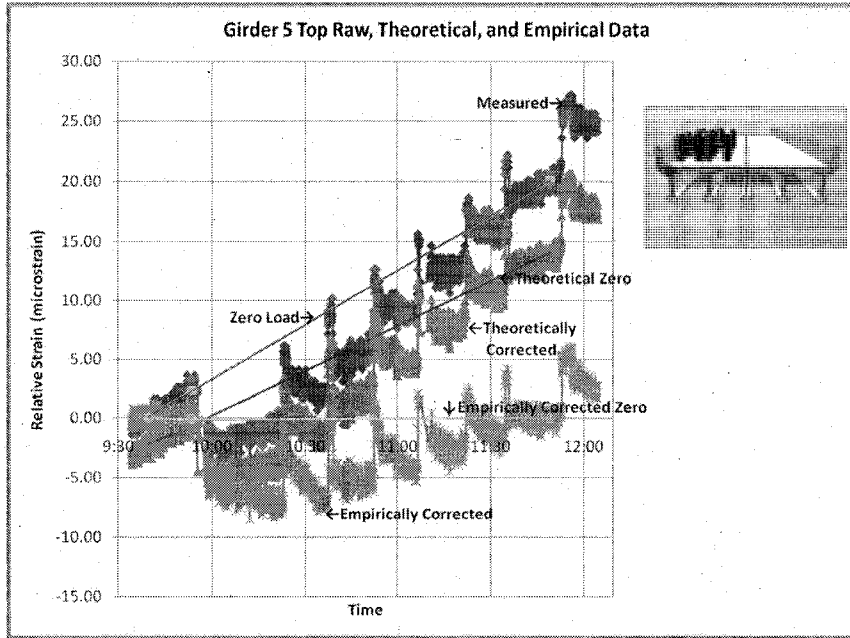


Figure 48: Girder 5 top row, theoretical and empirical Data from April 2008 load test, with three zero-load data points and trend lines included

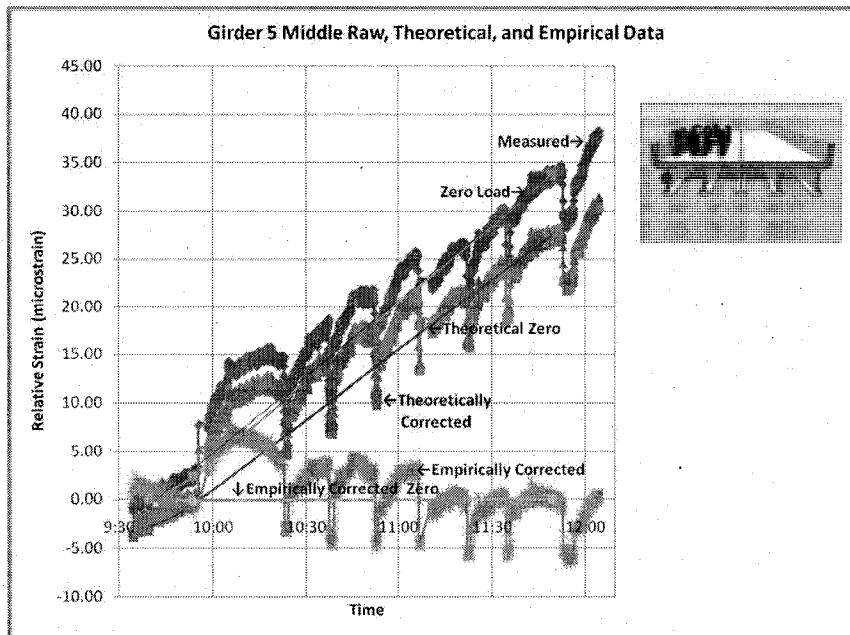


Figure 49: Girder 5 middle row, theoretical and empirical data from April 2008 load test, with three zero-load data points and trend lines included

Similar to the load cases pulled from the girder 3 and girder 4 empirically corrected data, four load cases at the same time were created from the girder 5 top and girder 5 middle empirically corrected data, see Figure 50 and Figure 51.

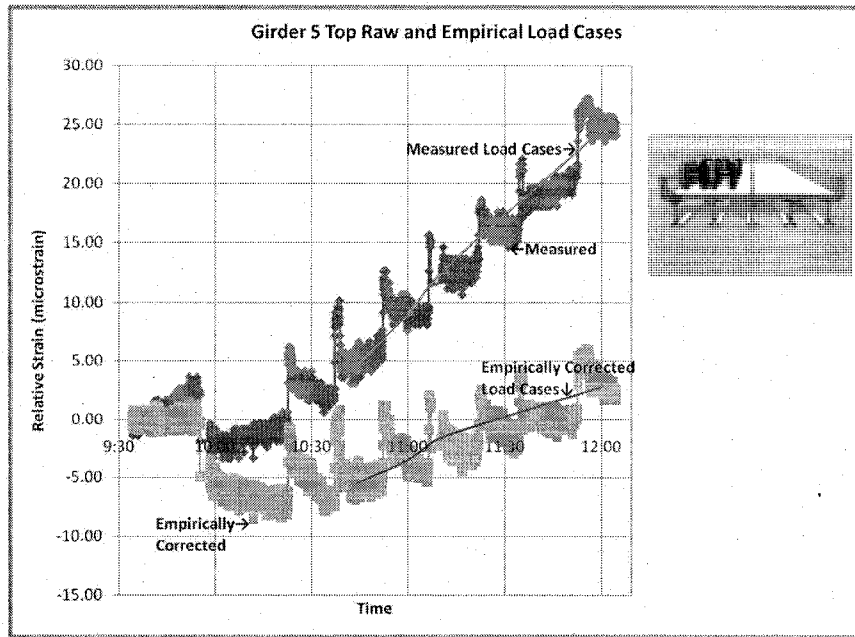


Figure 50: Girder 5 top raw and empirical data with manual model updating load cases

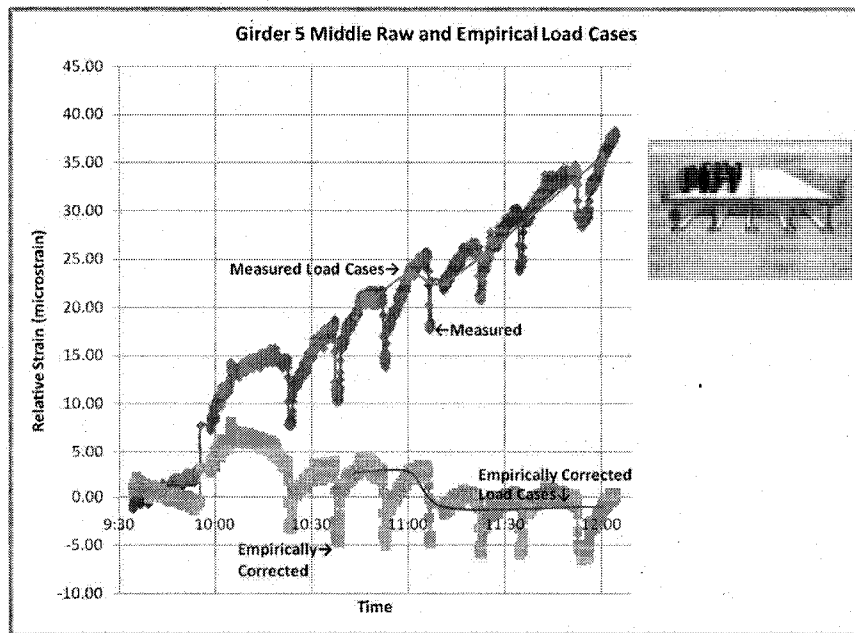


Figure 51: Girder 5 middle raw and empirical data with manual model updating load cases

4.3.5 – Interpretation of Results

In all of the measured data, it can be seen that there is a general positive slope in the line with consistent variations. These variations are times that the load test truck is on the bridge. The values spike back up to the zero-load line when the truck is driven off of the bridge, when it is turning around preparing for the next run. Figure 52 shows a snapshot, for example, from the girder 3 output. The graph shows the empirically corrected data which includes spikes due to traffic being allowed to pass between runs, strain values obtained from SAP2000® at the seven stop locations, and the empirical values at those same seven stop locations. Refer to Figure 17 for the stop locations on the bridge plan.

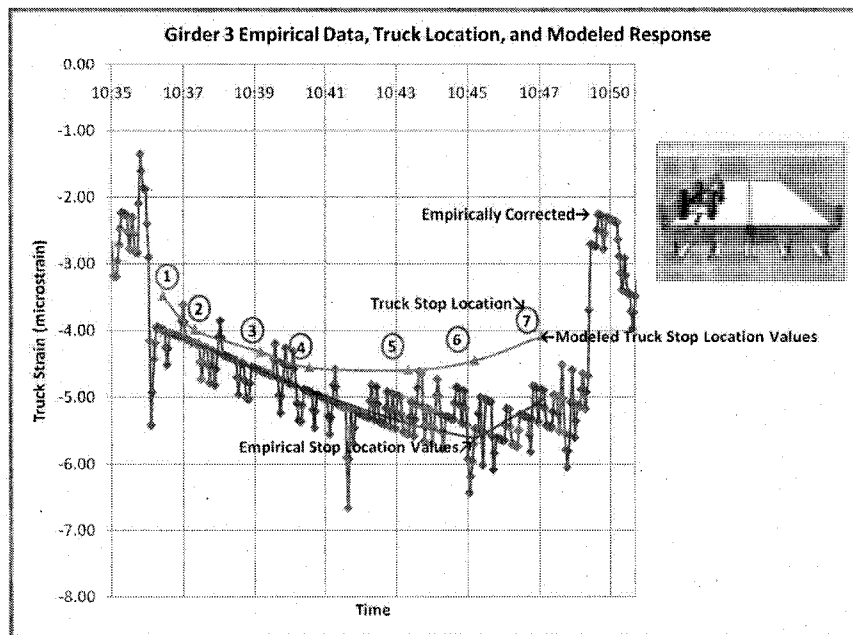


Figure 52: Truck run #3 snapshot for girder 3 with empirical data including traffic, modeled values at stop locations, and empirical values at stop locations

Between each stop location, traffic was allowed to pass on the opposite side of the load test truck which accounts for the spikes seen between the time which the

truck is stopped at each location. The linear trend for points two through four can be related back to the linear correction performed on the measured response data. The modeled strain values from stop five to stop seven reverse slope and go higher, which makes sense since the center of gravity of the truck has passed the centerline of the bridge past those points. This is seen in the empirical data, however not as much and that could be contributed to the linear correction not accurately capturing that portion of the data. If more zero-load readings were taken, it could be possible to perform a polynomial fit and therefore correction that would obtain a more accurate set of empirically corrected data.

CHAPTER V

MODELING PROTOCOL FOR ROLLINS ROAD BRIDGE

A goal of the Rollins Road Bridge Research Project is to create an analytical predictive monitoring based model to accurately capture the behavior of the bridge. While creating the model, researchers ensured usability was maintained and that tools available for the creation and use of the model were incorporated. Two different programs were looked at for modeling, GT Strudl® and SAP2000®. Specific structural properties such as carbon fiber reinforced polymers in the concrete deck, the New England Bulb Tee Girder, prestressing pattern, and the steel reinforced elastomeric bearing pad were included in the model. Five special topic studies were also done to verify results and ensure that the desired results were being achieved.

5.1 - Program Selection

Modeling is an important part of a value-added SHM program. A project goal was to pass a model along to the NHDOT for use in developing their internal SHM program. Due to this, it was important to use a modeling program that the personnel at the NHDOT were already familiar with. The NHDOT currently owns both GT Strudl® and SAP2000®. Therefore, these two programs were the two primary software

packages investigated for modeling RRB. GT Strudl® Version 28 was first used by the research group for this project.

One big draw to GT Strudl® in the beginning was the ability of the program to directly export the stiffness of modeled structures. GT Strudl® is a command driven program which leads to some advantages and disadvantages. The advantages include the ability to make changes to a text file, which would then be run to update the model instead of having to find specific nodes or elements in a graphical user interface (GUI) to change properties. Using the text file also presented some challenges; anything that needed to be modeled must be first written out or done in a basic GUI. Due to some difficulties in using GT Strudl®, SAP2000® was investigated further and it was determined that SAP2000® also has the capabilities to export the stiffness matrix of modeled structures.

SAP2000® contains an advanced programming interface (API) which would allow for a seamless integration between SAP2000® and a MATLAB® based parameter estimation program currently under development at UNH called MUSTANG (Model Updating SStructural ANalysis proGram). GT Strudl® does not have these API capabilities. MATLAB® and SAP2000® are also industry partners which also makes programming MUSTANG much easier. Another huge benefit of SAP2000® over GT Strudl® is contains the Bridge Information Modeler (BrIM™) which is a GUI, step-by-step wizard that allows user to construct a bridge model.

The BrIM™, a portion seen below in Figure 53, allows for an easy graphical creation of the bridge model. Users can decide whether to create a basic or complex

bridge model using the BrIM™. The BrIM™ also offers the NHDOT a friendly module that can be used for model creation of different bridge types. SAP2000® has the ability to view the model as a stick model or extruded, where the actual appearance and thickness of different elements are seen. This makes the model more visually appealing, adding value to the use of SAP2000®.

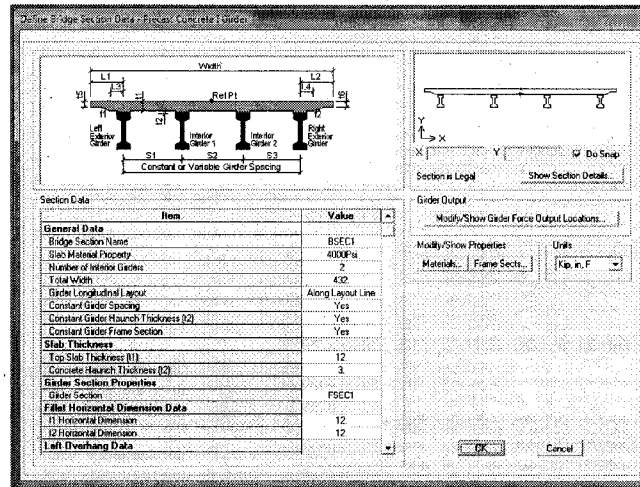


Figure 53: SAP2000® Bridge Modeler (SAP2000, 2007)

In the model creation portion of the BrIM™, the amount of discretization for size of shells in deck and amount of discretization in the girders are user defined variables. Once the base model is created using the BrIM™, the model can be modified through property and material definitions as seen fit to transform the model from a design model to a monitoring model. Benefits to using SAP2000® including usability, appearance, linkability between SAP2000® and MATLAB®, ease of creation, and a more advanced user interface made clear the selection of SAP2000®.

5.2 - Initial Modeling

The first analytical model of RRB was created in GT Strudl®, modeling the NEBT as frame elements and the deck as shell elements, as seen in Figure 54. The original plan was to put a considerable amount of time into node creation and load position correlating to the load test so that the weight of the truck can easily be transferred to the modeled deck through nodes. Nodes were specifically created at the point of truck load application. The material properties in the GT Strudl® model were user defined, but not applied easily. The need for several calculations to get the correct elements modeled correctly made it tedious, and then the element did not show up as a visual representation.

In order to model the NEBT section properly in GT Strudl®, wide flange section properties had to be modified to match that of the NEBT. There was also difficulty in trying to get the bridge deck and NEBT frame members to act in composite action. The use of “master” and “slave” joints was attempted, however that was not successful because the joints on the edges of the deck were not associated with a girder underneath, so they did not deform with the rest of this structure. During the time when the problem was being investigated, the decision to use SAP2000® was made. The time to create a comparable model using the SAP2000® BrIM™ took about 15 minutes while the first GT Strudl® model already had many hours already devoted to it.

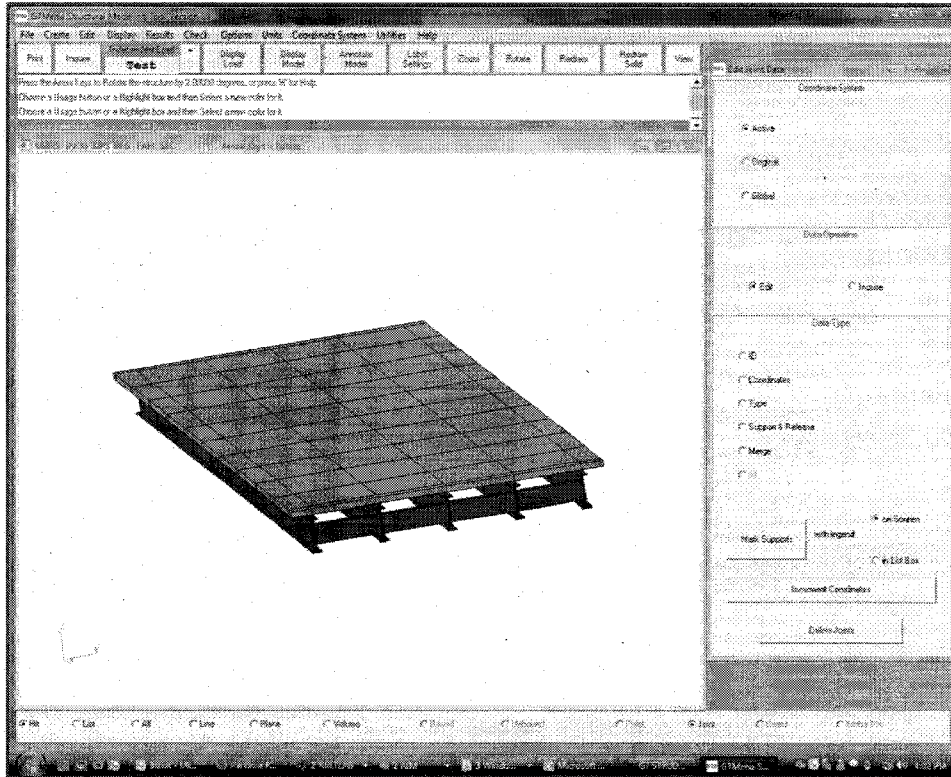


Figure 54: GT Strudl® bridge model (GT Strudl, 2007)

Using SAP2000® and the BrIM™, the end model was visually appealing, relatively easy to create, and results were accurately and easily obtained. The original plan for modeling was to create three models; model 1 having the girder as frame elements and the deck as shell elements, model 2 having the girder as frame elements and the deck as brick elements, and model 3 having the girder and the deck modeled as brick elements.

5.3 - Modified Modeling Plan

Once the research project was underway, the initial model planned was refocused on including specific elements and environmental impacts. The goal of creating a usable model for the NHDOT SHM program was still maintained, however the focus of that model was slightly modified. The first model, GT Strudl® model, was

used for comparison between the software programs. The second model was created using the BrIM™ in SAP2000®.

Once the design based model was created using the BrIM™ to a degree of satisfaction, the bridge modeler was turned off, allowing researchers take full control of element properties included in the model. The use of the BrIM™ takes full advantage of all the research done by Computer & Structures, Inc. (CSI) for the creation of the base bridge model and then allows researchers to build upon that model to reach the final goal. Structural components included in this monitoring model were prestressing tendons in the girder, CFRP reinforcement in the deck, the bridge rail, and boundary conditions modeled as springs with prescribed stiffness.

5.3.1 – Modeling the CFRP Reinforce Concrete Deck

The deck was modeled using design plans for RRB and measured distances (Bowman M. M., 2002). No as-built drawings were available for this bridge deck, so between Bowman's (2002) data and the design plans, researchers felt fairly confident in the dimensioning for the deck. CFRP reinforcement in the deck was included once the bridge modeler was turned off and the type of finite elements used for the bridge deck was changed from shell elements to layered shell elements. The deck of RRB contains two layers of CFRP reinforcement, one above and one below the centroid of the deck section.

In order to correctly model the CFRP material, the material specifications, modulus of elasticity, and density were obtained from previous work (Bowman M. M., 2002) (Trunfio, 2001). The thickness of the CFRP throughout the entire width of the

deck was maintained to keep the correct moment of inertia in the transformed section and having the ability to model it in SAP2000®. Since the layered shell material was throughout the entire thickness, not just present every 6-inches, the modulus of elasticity was transformed to capture the same behavior as it is placed in the bridge. The modification was achieved by taking a ratio between the actual area of CFRP in the cross section and the modeled area and then reducing the modulus of elasticity for the layer. A graphical representation of the steps list above can be seen in Figure 55 and calculations are contained in Appendix A – CFRP Reinforcement Calculations. Figure 56 shows the SAP2000® shell section layer definition window and how the material properties, distance, and thickness were specified.

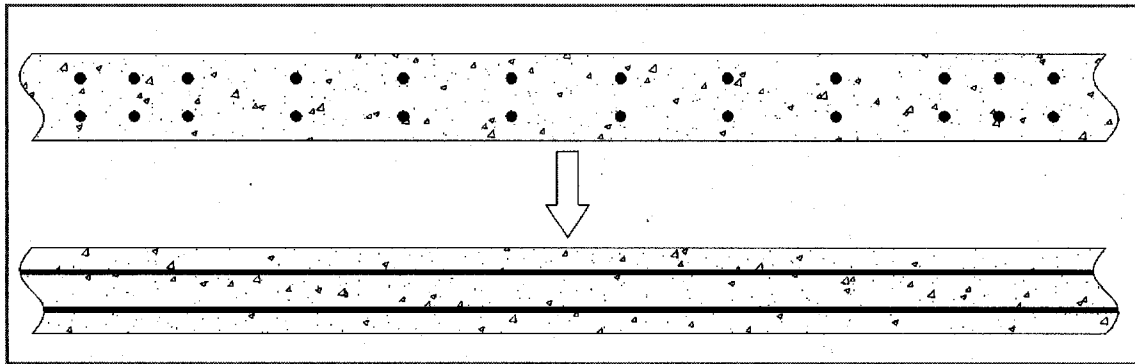


Figure 55: Graphical representation of how CFRP is modeled as layered shell element

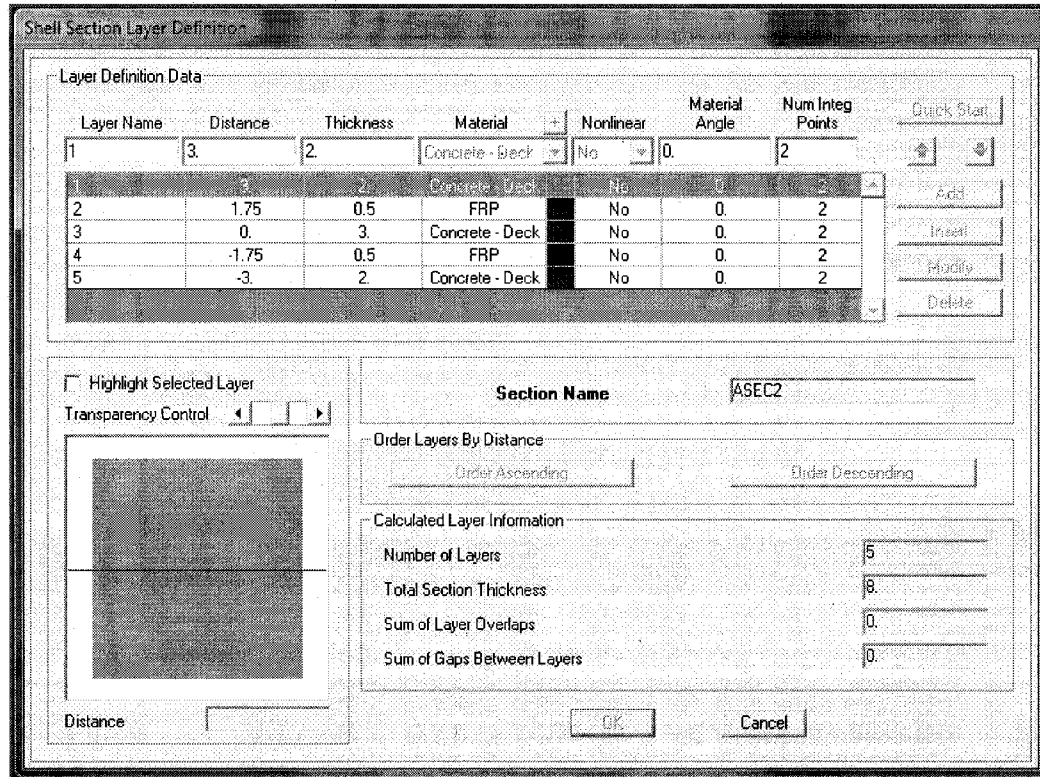


Figure 56: Layered shell properties for RRB deck (SAP2000, 2007)

5.3.2 – Modeling the Prestressed/Precast/HPC NEBT Girders

The SAP2000® BrIM™ contains preloaded concrete girder sections. Those sections can be used or modified depending on the properties of the girder located at the bridge. This was one big benefit to using SAP2000®, and it contains all of these different options which makes model easy for all bridges, not only RRB. GT Strudl® does not have the capabilities to import such sections into the program, the company was contacted and they explained that it was not under the scope of their program. Figure 57 shows the preloaded AASHTO PCI bulb tee included in the BrIM™ with the modified dimensions to match that of the NEBT.

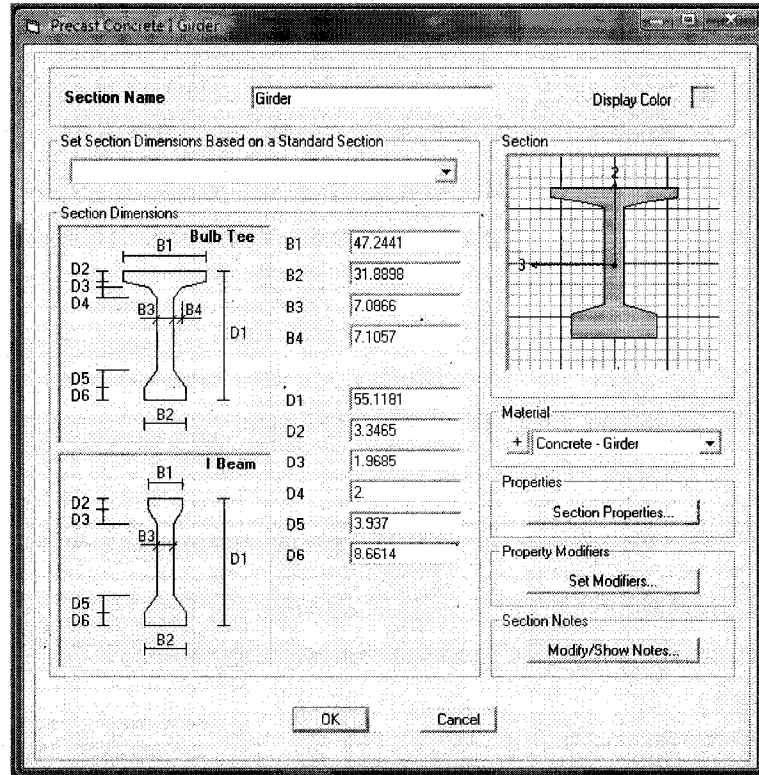


Figure 57: Preloaded NEBT section in SAP2000®

Prestressing tendons were included in the RRB model to accurately capture the bending behavior of the girders. SAP2000® has the ability to add strand patterns, see Figure 58. The two deflection point pattern used at RRB was one of the many options in the BrIM™. The design plans were used for all of the stressing, arrangement, and steel specification information. Losses were calculated using the AASHTO Bridge Code (AASHTO, 2004). The use of these values was validated through *NCHRP Report 496* which looked at the actual losses at RRB and compared them with losses calculations using AASHTO (Tadros & Al-Omaishi, 2003). During fabrication, special care was taken to ensure that the strand pattern was accurately laid out, as prescribed in the plans, and researchers were present at time of prestressing and pouring of the precast girders to ensure compliance. Due to the research driven nature of this project, there

was extra control in all aspects of construction, which allows researchers a high level of confidence that the bridge was constructed as designed and specified.

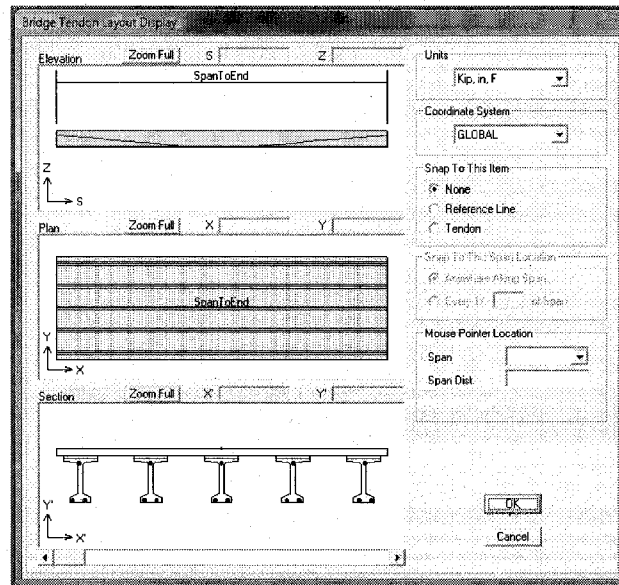


Figure 58: SAP2000® bridge tendon layout (SAP2000, 2007)

5.3.3 – Modeling the Steel Reinforced Elastomeric Bearing Pad

Steel reinforced elastomeric bearing pads support the Rollins Road Bridge on the abutments which transfer all loads into the ground. The bearing pads have three different possible directions of motion, as seen in Figure 59, caused by axial load, shear forces, and rotation.

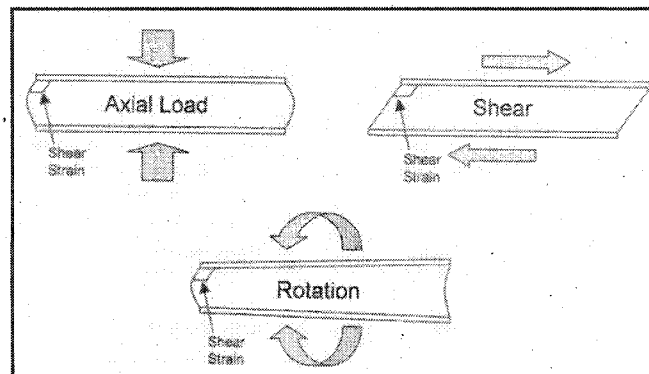


Figure 59: Deformations of a laminated elastomeric bearing pad (Stanton, Roeder, Mackenzie-Helwein, White, Kuester, & Craig, 2008)

The steel reinforced elastomeric bearing pads were a focus of this research, because there is not a conventional equation to calculate the horizontal stiffness, which will be discussed in detail in this section. Visual inspection showed no cracking or deterioration in the deck or girders. Representatives from D.S. Brown, Inc. have stated that the elastomeric bearing pads have a service life of up to 75-years. Research has been conducted beyond the initial research performed by AASHTO on both the axial and rotational stiffness of steel reinforced elastomeric bearing pads in order to develop bearing pad stiffness (Stanton, Roeder, Mackenzie-Helnwein, White, Kuester, & Craig, 2008). This research and physical testing, has resulted in two equations, seen in Equation 4 that can be used to calculate axial and rotational stiffness for one layer of the elastomer. Combining the layers of elastomer and steel together results in an overall stiffness for the bearing pad (Stanton, Roeder, & Mackenzie-Helnwein, 2004). Calculations of the bearing pad stiffness can be seen in Appendix C – Calculation of Reinforced Elastomeric Bearing Pad Stiffness.

Equation 4: Axial and rotational stiffness of one layer of elastomer (Stanton, Roeder, & Mackenzie-Helnwein, 2004)

$$K_a = \frac{P}{\Delta_a} = \frac{EA(A_a + B_a S^2)}{t}$$

$$K_r = \frac{M}{\theta_r} = \frac{EI}{t}(A_r + B_r S^2)$$

A total of ten, 16-inch diameter, steel reinforced elastomeric bearing pads are installed at RRB, one at each end of each girder. The bearing pads allow slight vertical compression while allowing the beam to rotate. Modeling spring boundary conditions, via links, in SAP2000® is also fairly simple. The BRIM™ allows for several different types

of boundary conditions to be used, from traditional fixed or pinned connections, to user defined links. When links are used, the user is allowed to specify stiffness in all directions, as seen in Figure 60. Links are used because they can be updated in the model updating process and more accurately capture the behavior of the actual bearing as opposed to a pinned or fixed condition. In the U2 directions (translation parallel to the abutment) a stiffness of $1.000E+09$ is used to show fixity in those directions and in the R1 and R3 directions (rotation about a line normal to the abutment and about a vertical line) a stiffness of $1.000E-09$ is used when rotational stiffness is not included. These values are specified instead of using the option to be fixed or free in the SAP2000® program window because using those options caused numerical instability in the analysis. Using values that accurately represent fixed and free did not cause the numerical instability but essentially gave the same response.

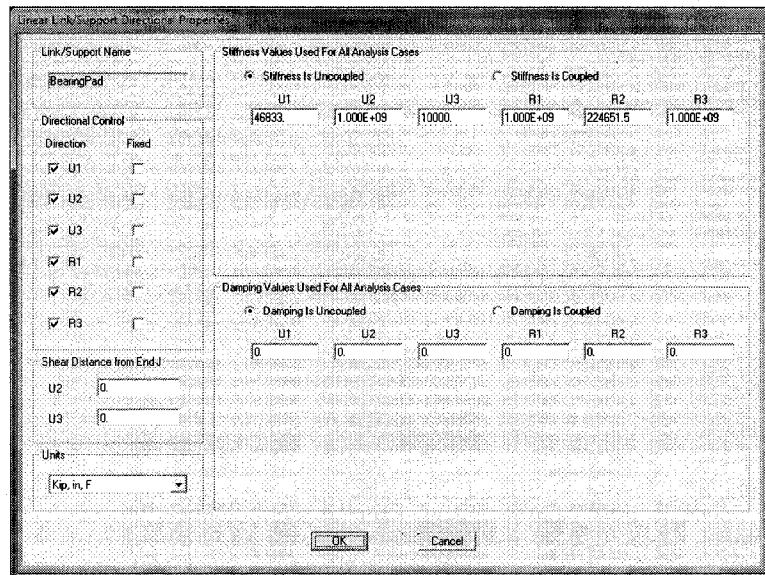


Figure 60: Stiffness parameters for modeled reinforced elastomeric bearing pad (SAP2000, 2007)

Stanton et al. (2008) has equations to calculate axial and rotational stiffness of the elastomeric bearing pads, however does not provide equations for the calculation

of horizontal stiffness caused by shear effects. That value is what was used in the manual parameter estimation exercise for this research.

5.3.4 – Modeling the Bridge Rail

The bridge rail at Rollins Road Bridge is a cast-in-place concrete rail. The use of concrete bridge rails is replacing the conventional aluminum/steel guardrail for NHDOT bridges. The rail will be modeled as a frame element and connected to the bridge deck through links since, as seen in Figure 61, it is connected to the bridge deck using stainless steel reinforcement.

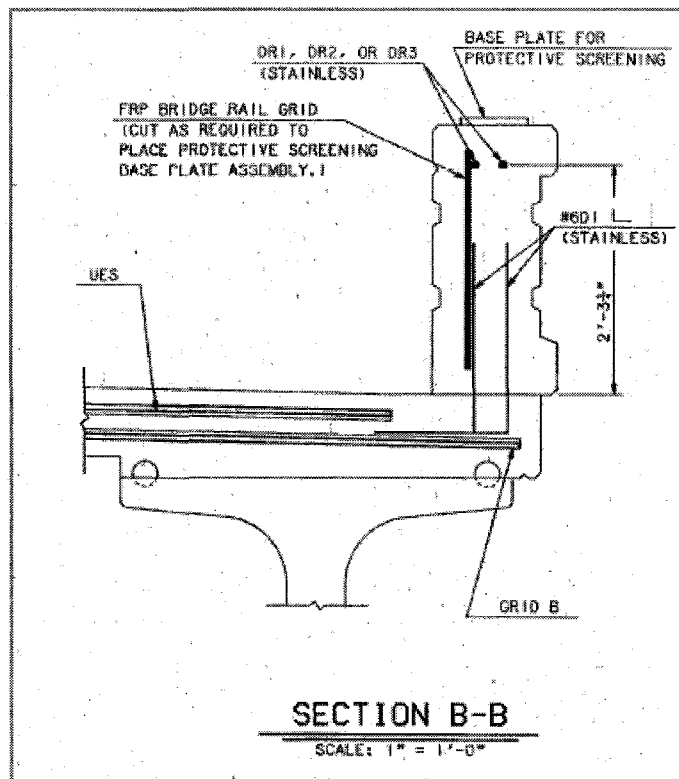


Figure 61: Section view of bridge rail connection to bridge deck (NHDOT Bureau of Bridge Design, 1999)

5.4 - Special Topic Studies

Five special topic studies were conducted during this research project. Special studies are meant to examine specific, smaller issues that affect modeling. The studies

try and ensure that the behavior is being properly captured or help find a more universal way of doing a process that makes modeling easier. Special studies tie into the goal of maintaining model usability while enhancing capabilities. The five studies include hand calculations to verify the SAP2000® model, hand calculations to verify strain obtained from the SAP2000® model, looking at the stiffness matrix export from SAP2000®, looking at an easier way for load application, and looking at the different ways to apply thermal load in the model

5.4.1 – Hand Calculation Verification of SAP2000® Model

The structural properties included in the model are known to a high degree. However, including these structural properties without any verification would make that data blindly valid. Several steps were taken to verify the bridge was being properly modeled, and the desired results were being extracted from the analysis. To do this verification, hand calculations were performed using structural analysis and bridge design techniques to obtain numerical results to then compare to the SAP2000® output. The model that was used in these hand calculations and modeled separately from the RRB model in SAP2000® was a reduced model. The model was reduced for ease of hand calculation, and because this is a verification. The hand calculations would be tedious to verify the entire bridge model, however if individual components are verified, it can be assumed that the model as a whole is performing as desired.

This reduced model maintained the geometry of RRB was simply supported and did not have the prestressing forces. The prestressing loads and strand pattern were known to a high degree of certainty. In hand calculations, as assumed with the NDT

load test, the bridge remains in the linear elastic range which also simplifies calculations. The CFRP remained in the model for hand calculations to ensure it was modeled properly using transformed sections. The base material for the transformed section was the girder concrete, and the deck and CFRP were transformed. In the hand calculations, a point load of 100-kips was placed at the midspan of the transformed section. A similar load was placed in the SAP2000® model, discretizing the point load along the width of the bridge deck to total the 100-kips put in the hand calculations. All of the hand calculations can be seen in Appendix D - Calculations for Model Verification. Both deflection and strain measurements were calculated and compared to the SAP2000® model. The results of the hand calculation versus SAP2000® can be seen in Table 12.

Table 12: Hand calculations and SAP2000® model comparison for deflection and strain

	Hand Calculated	SAP2000® Model	% Difference
Deflection <i>inches</i>	0.253	0.243	1.94%
Strain <i>microstrain</i>	24.9	25.7	3.21%

With this information, as well as all of the details included in the model listed above, researcher had a high confidence in the accuracy of the model of RRB.

5.4.2 – Obtaining Strain from SAP2000® Model

In order to compare the data from the SAP2000® model to the measured response, an important calculation had to be performed. The output from the beam elements, the girders, in SAP2000® is only displacements, axial force, bending moment, and shear. These outputs values must then be translated into strain.

Initially, researchers used axial force and bending moment in the girder and then using the geometry of the girder transformed those values into strain. After a close examination of these values, it was determined that they did not accurately capture the composite action, between slab and girder, occurring at the bridge.

Several other methods to get strain were thought of, including re-modeling the entire bridge using solid elements, in which strains can be taken directly. However that method would require entirely remodeling the bridge in a much more difficult fashion, reducing the usability of the model. It was finally determined that the displacement of the deck and girder could be manipulated to find strain values. Since the behavior exhibited by the bridge is within the linear elastic range of the material, it can be assumed that the strain is linearly varying throughout the depth of the bridge. Using this principle the deflection, both x and y, values from SAP2000® can be extruded for the nodes that comprise the deck above the sensor location, as well as the nodes that comprise the girder at sensor location. Once these values are obtained, and the initial values are known, strain at the deck level and girder center line can be calculated, and then linear interpolation allows finding the exact strain value at the depth of the strain gauge. Figure 62 shows a basic diagram on how strain is calculated. Knowing the new and original length of both elements, the difference between new and original length over the original length equals the strain value at the deck and girder levels. This can then be transformed to any depth in the bridge cross section. Sample calculations to obtain actual strain values can be seen in Appendix E – Strain Calculations.

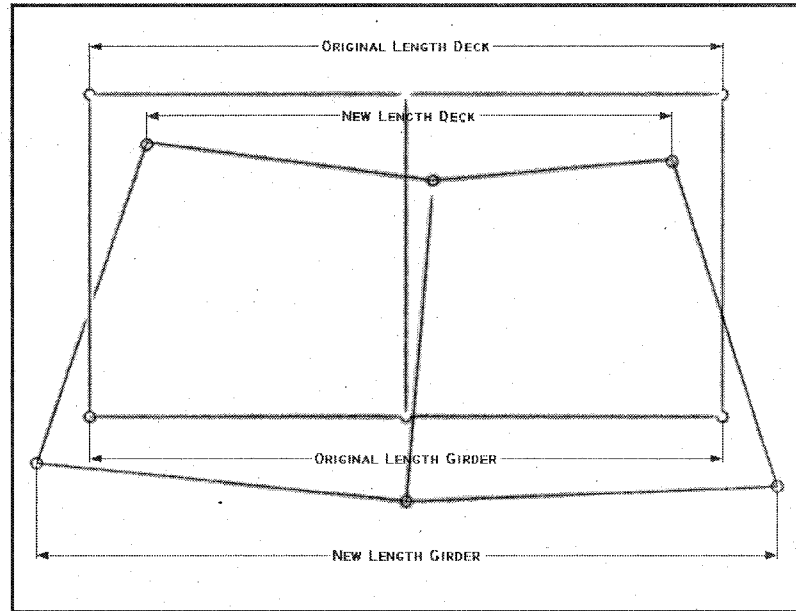


Figure 62: Strain calculation diagram

5.4.3 – Stiffness Matrix Export

The capability for SAP2000® to export the stiffness matrix of models was an important characteristic for choosing SAP2000®. This special topics study was done to verify the output from SAP2000® compared with conventional stiffness calculations. This was done by comparing the SAP2000® output to hand calculations using matrix structural analysis techniques. A simple cantilever beam was modeled in SAP2000® with a distributed load. The same cantilever beam was analyzed using matrix structural analysis, and the results were compared. An illustration of the cantilever beam and both hand (MATLAB®) and SAP2000® outputs can be seen in Figure 63.

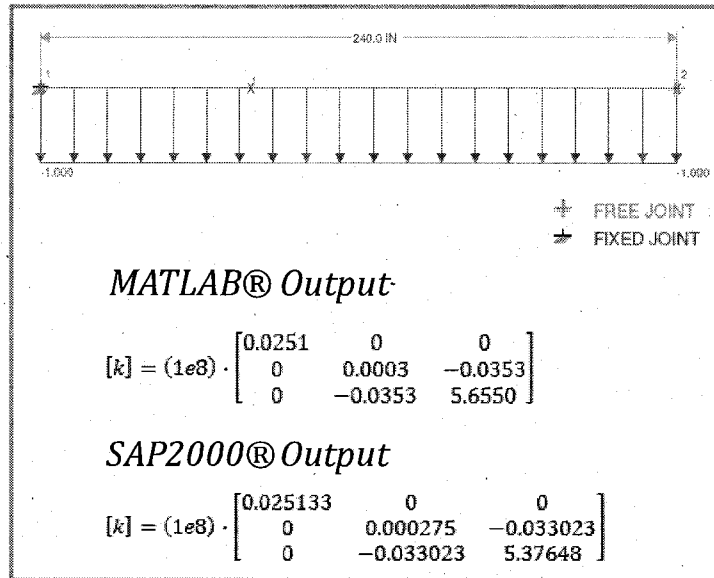


Figure 63: Modeled cantilever beam with MATLAB® and SAP2000® stiffness matrix output

The output from both methods compare within a reasonable accuracy. This matching of stiffness matrices will allow for the programmers of MUSTANG to take full advantage of the exported stiffness matrix from SAP2000®. This tie eliminates the need for a parameter estimation program to develop its own stiffness matrix. It also takes full advantage of the time and research taken place for the development of SAP2000® to model such integrate structures and export the stiffness matrix.

5.4.4 – Load Application

Typical load application is achieved by applying a load to a node in the model. The BrIM™ has a predetermined pattern for creating joint locations in the bridge model, not necessarily where the truck will be. A similar problem was seen in the GT Strudl® model, and the solution was to place nodes where there was a point of load application. That led to confusing creation of shell elements to get a solid deck. There could be an infinite number of different locations for load application during a load

test that may not necessarily already be a point. Typical load application is done by a truck, which in reality are applying the wheel loads over an area. Trying to get these loads modeled properly on the shell elements proved to be a challenge.

If a finite element mesh was created and the area loads were applied to this separate mesh, resultant forces could be calculated at points of actual node locations on the bridge. A fine mesh, using 3-inch spacing, was created to obtain the force resultants. Once this mesh was created, it could be moved to any place on the bridge to find resultant forces. This universal method proved to be useful during the analysis portion of this research project, allowing loads to be applied in different locations on the bridge depending on the specific load case. Once the mesh was moved to the area of load application, the equivalent area loads were applied to the mesh model, and the two existing nodes on the deck were selected as boundary conditions in the mesh model. This was done for all areas of load application and the mesh model was run. The resulting reaction forces from the mesh model were then applied to the deck nodes, as seen in Figure 64.

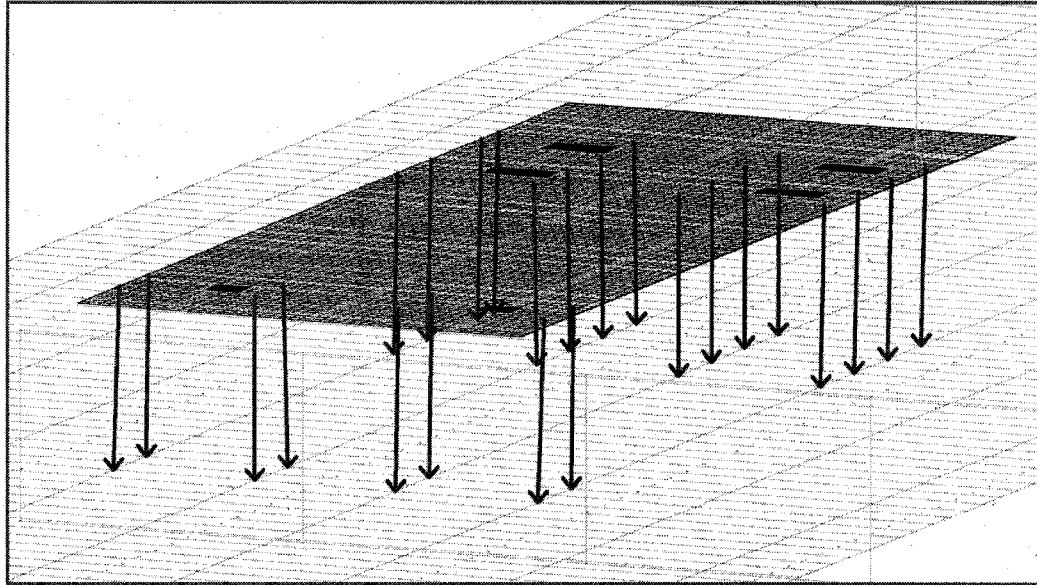


Figure 64: Truck load mesh to bridge deck graphic

The use of force resultants can be done because the focus of the load tests was to look at the overall effect on the bridge. The sensors used in the analysis were in the girders, so local effects from the truck wheels were not of concern. It also takes full advantage of using the BrIM™, while still being universal enough to apply loads to existing nodes at any location on the bridge. Future analysis and load tests at UNH will use this method.

5.4.5 – Thermal Load Application

A special topics study was performed by an undergraduate research assistant, Jake Carmody, to validate the behavior of a beam under thermal loading in SAP2000®. Jake performed typical hand calculations to determine the displacement of a uniform beam. He then used those hand calculations as a benchmark to compare two SAP2000® models. Jake modeled the beam as a shell element and solid elements. The displacement calculated from hand calculations was 0.0264-inches, the shell element

beam had a displacement of 0.0277-inches, and the solid element beam had a displacement of 0.0265-inches. All well within a 5% difference which is acceptable for these types of calculations. Figure 65 shows an example SAP2000® output for the analysis done during the temperature special study.

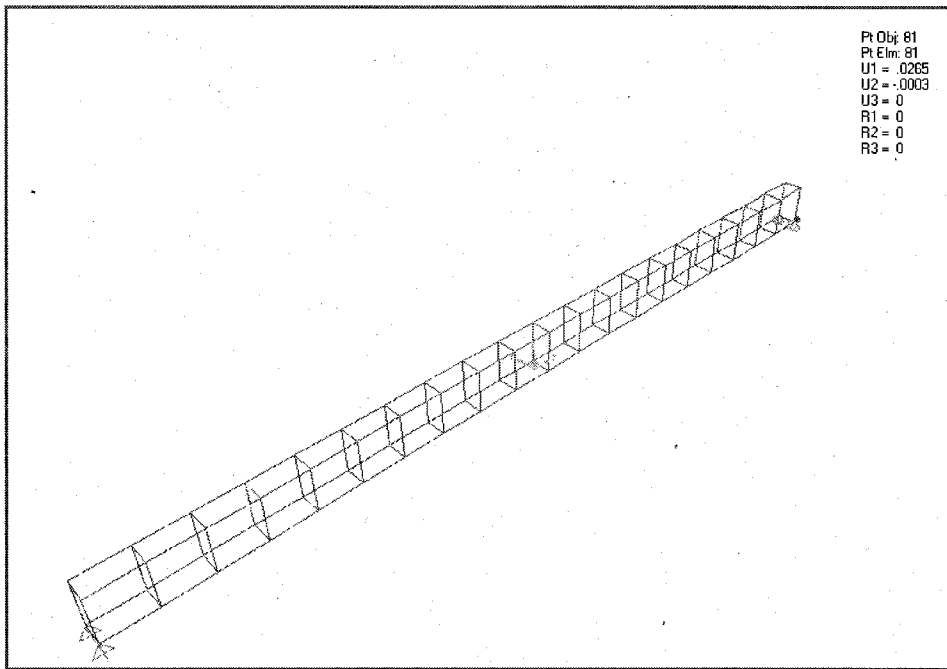


Figure 65: Sample output from SAP2000® for temperature special study

5.5 - Use of Rollins Road Bridge Load Test Data

The Rollins Road Bridge provides an invaluable field lab and research facility to collect structural response data. The original 2000 testing and instrumentation programs for RRB did not include long-term SHM. For this reason, there was difficulty using the previous load test data since initial strain values were not known. Since initial strain values were unknown, it was hard to determine the change in behavior from an “initial” state to the state during the load test. The definition of initial is also an arbitrary choice. There really is no time in the bridge’s life that can be used as an

initial state since it is not created perfectly in a vacuum. If a strain reading right before the bridge was opened to traffic was obtained, that could have been used as the initial reading providing all environmental factors were also recorded. Since the 2008 load test was created for the purpose of structural health monitoring, researchers included three zero-load points which allowed the temperature data and all other environmental effects to be removed from the load test data, which made the comparison between load test data and model analysis results data possible.

5.6 – Three-Year Analysis of Rollins Road Bridge Load Test Data

Analysis was attempted using all three years of data to capture the global response. However the results showed that environmental factors such as temperature and humidity had such a large effect and the lack of initial readings for the strain gauges made a proper comparison of the data to the analytical model difficult. The results from this attempt can be seen in Appendix F – First Analysis of Rollins Road Bridge Load Test Data for All Three Years. Researchers determined that using all three years of data was not practical due to lack of critical information, however the correction of the 2008 load test data would provide that critical information.

5.7 – 2008 Analysis of Rollins Road Bridge Load Test Data

The analysis of the condition of Rollins Road Bridge through model updating was performed using the corrected 2008 load test data and the SAP2000® model to perform condition assessment on the steel reinforced elastomeric bearing pads.

Correcting the data allowed researchers to see structural response caused solely by applied truck load and removed ambiguity caused by environmental factors, as seen in Figure 66. The 2008 load test data was corrected for temperature effects, as seen in Section 5.4 - Special Topic Studies. With this correction, a change in strain due to applied load became the focus. In order to properly compare this with the analytical model, a procedure had to be developed in order to look at the same thing in the model that was now being observed in the data.

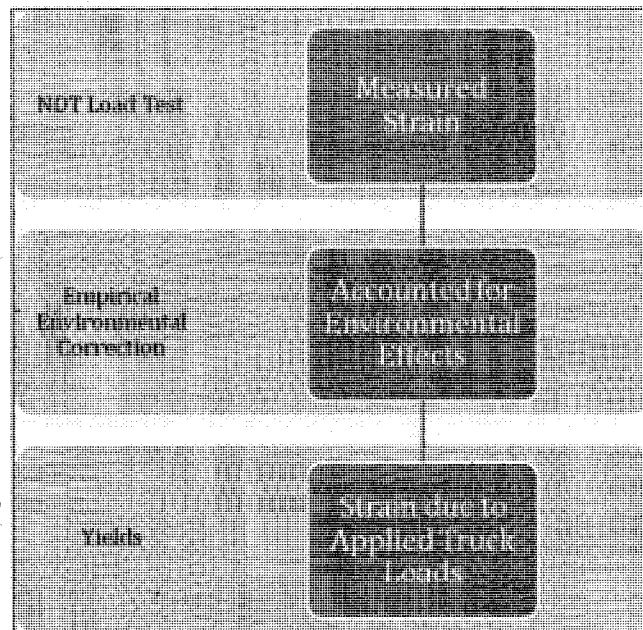


Figure 66: Measured strain to strain due to applied truck load diagram

5.7.1 – Establishing a Running Benchmark for SAP2000® 2008 Model

Since temperature and environmental effects were removed from the measured data set, the strain values are only due to the applied truck load. In order to have the SAP2000® model reflect this same condition, two models had to be created. The reason for these two models is because prestressing forces in SAP2000® are modeled as a force, not a behavior. The modeled CFRP is modeled in a way that the

behavior is captured when an analysis is run, however the prestress load case must be run in order to capture the behavior of the prestressing forces. Due to this, prestress and dead load were modeled for one model while prestress, dead, and applied truck loads were modeled in another model. Figure 67 shows how two models were created, and the difference between those resulted in strain due to applied truck load, matching the output from the measured data.

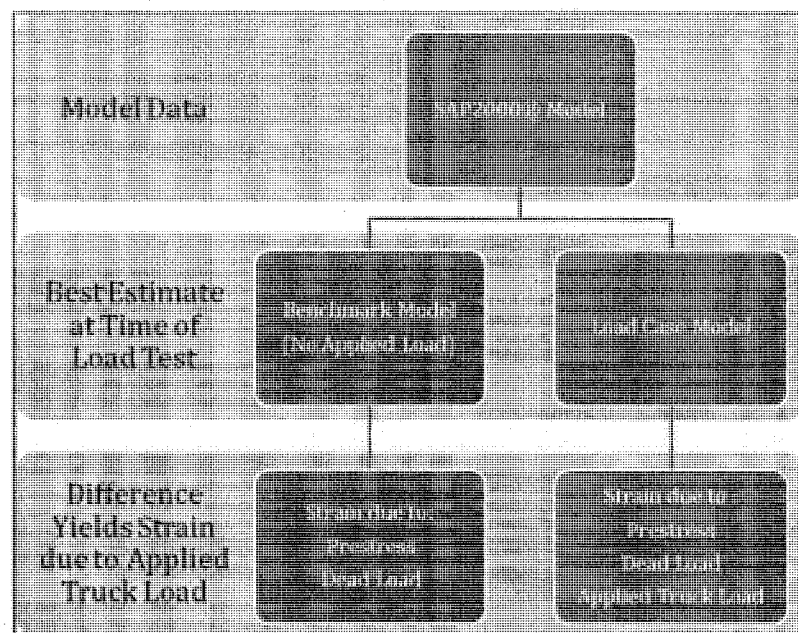


Figure 67: SAP2000® modeled strain data to strain due to applied truck load

This benchmark model had all structural components modeled as the best estimate at current bridge conditions. Calculations of bearing pad stiffness were maintained, and since the bridge is in such good structural conditions, researchers have a high degree of confidence in modeled structural parameters such as area, modulus of elasticity, and moment of inertia. The strain values from the model are determined through techniques described in Section 5.4 - Special Topic Studies.

Since the condition assessment was performed on the elastomeric bearing pads, the stiffness values were modified in the model to match the measured behavior. Since researchers wanted to examine the change in behavior from a zero-load state to an applied load state, the modeled response had to be compared back to a zero-load state, benchmark, model with the same bearing pad stiffness as the applied load model. For each set of bearing pad stiffness case, a benchmark model was created and benchmark strain values were obtained.

5.7.2 – Established Model Loads

The applied truck loads are simple to establish in the model, the wheel weights are known, weighed at the RRB test site, the location of the truck is dependent on the load case being analyzed, and using the truck mesh the loads are applied to the nodes of the model. Using the measured wheel weights and truck load mesh, node loads are calculated and applied to the SAP2000® model in four different load cases, depending on the location of the truck.

5.7.3 – Established Measured Response Values

Once the measured data was corrected for temperature, as mentioned in Section 4.3.3 – Empirical Thermal Correction, a small bit of analysis had to be performed to get the strain readings into compared strain data. The times at which the load case occurred were noted, and pulled from the corrected data set. This resulted in about 25 data points, per sensors, for the time the truck was at that position. A 95% confidence interval was then performed on the mean of those

numbers, to determine if the data was within acceptable limits. The strain gauge tolerance was set to ± 0.40 -microstrain (Bowman M. M., 2002). All variation in the data was well within 0.25-microstrain over the one to five minute period of recording, which was determined to be acceptable by researchers. Table 13 shows the resulting measured strain values for the load test data with environmental factors removed.

Table 13: 2008 measured strain values corrected for environmental effects

	<i>Channel 32</i> <i>Girder 3</i> <i>Top</i>	<i>Channel 3</i> <i>Girder 4</i> <i>Top</i>	<i>Channel 5</i> <i>Girder 5</i> <i>Middle</i>	<i>Channel 6</i> <i>Girder 5</i> <i>Top</i>
2008 LC1	-5.21	-4.67	2.85	-5.59
2008 LC2	-4.88	-3.21	2.82	-3.44
2008 LC3	-4.58	-2.59	-1.11	-1.46
2008 LC4	-2.39	1.85	-0.99	2.81

5.8 – Load Test Data to SAP2000® Comparison

With corrected data from the field measurements, data from the SAP2000® model, and a running benchmark SAP2000® model, the change in strain reading between the SAP2000® model and the running benchmark was determined and could be compared with the empirically corrected strain value in the manual model updating process seen in Chapter VI: Manual Model Updating. This data will also be used for full scale parameter estimation and model updating exercise once MUSTANG is fully developed by a fellow graduate student researcher, John Welch at UNH.

CHAPTER VI

MANUAL MODEL UPDATING

There are open source parameter estimation programs, such as PARAmeter Identification System Software (PARIS©) from Tufts University and Damage Identification and MODal aNalysis for Dummies (DIAMOND) from Los Alamos Labs (Sanayei, 1997) (Los Alamos National Laboratories, 1997). This research specifically looked at PARIS©. MUSTANG (Model Updating STructural ANalysis proGram) is currently under development at UNH and will be able to handle the shell and solid elements, along with being tied to SAP2000®. The objective for the RRB required shell elements for accurately modeling of the bridge span. The exported stiffness matrix from SAP2000® on the RRB model was a 7704 square matrix, resulting in 59 million values. With a matrix this size, it is not possible to do successful parameter estimation without an automated program. Another graduate student research assistant will use the model and data with MUSTANG. For the focus of this research project, manual parameter estimation will be performed to show how the process works on a local level which will then be taken to the global level when MUSTANG is running.

6.1 – Three Data/Model Comparisons

There were a total of three comparisons done on using the data obtained from the RRB. The first analysis which did not provide the desired results can be seen in Appendix F – First Analysis of Rollins Road Bridge Load Test Data for All Three Years. The second and third analysis were done on the 2008 load test data that had been corrected for environmental factors, as described in Section 4.3 - Environmental Effects on Bridge Response. The second analysis looks at the effects of modifying the horizontal stiffness value in the model in order to obtain a match to measured structural response. In the second analysis the vertical and rotational stiffness values of the elastomeric pads were also modified to see the effect on the model response. Once the data SAP2000® model matched the measured response, the third analysis shows the importance of included specific structural properties in the RRB SAP2000® model. This is by removing those structural parameters that were included to show what the response would be if they were not included in the analysis. The MUSTANG Research Project will examine the values of structural parameters such as area, moment of inertia, and modulus of elasticity using the data obtained from this research project.

For second analysis of the 2008 model all structural components, CFRP, prestressing, and bridge rail, were kept in the model. Manual parameter estimation is performed on the RRB model, specifically on the bearing pads, by modifying the stiffness in three directions, vertical stiffness (z-direction, compression), horizontal stiffness (x-direction, shear), and rotation about the abutment (ry-direction, rotation).

All bearing pad stiffness values were kept consistent for all 10 bearing pads in the model, which can be referred to as grouping (Sanayei, Imbaro, McClain, & Brown, 1997). The axial and rotation stiffness values that were calculated in Section 5.3.3 – Modeling the Steel Reinforced Elastomeric Bearing Pad, were kept constant for the final case when the horizontal stiffness values was changed to get a match between change in model response and change in measured data. Separately modifying stiffness values will be a focus of the runs in MUSTANG as part of future work. Parameters such as modulus of elasticity and moment of inertia for specific elements will also be included in the parameter estimation. However, for the scope of this research project those properties were not examined in the manual parameter estimation.

6.1.1 – Analysis of Modifying Bearing Pad Stiffness

Table 14 shows the five different support conditions (SC) used in second manual model updating analysis. The vertical stiffness values and horizontal are modified in the first four cases, and the fifth case shows that modification of the horizontal stiffness value must be done in order to get the change in model strain to match the measured change in strain. The error of ± 0.40 -microstrain shown in the error bars for the measured strain corresponds to the accuracy of the gauges as set when installed. The manual model updating results can be seen in Figure 68, Figure 69, Figure 70, and Figure 71.

Table 14: Manual model updating cases and corresponding bearing pad stiffness values for second analysis

	Vertical Stiffness (kips/in)	Rotational Stiffness (kips/rad)	Horizontal Stiffness (kips/in)
Support Condition 1	46833	224651.5	fixed
Support Condition 2	46833	free	fixed
Support Condition 3	fixed	free	fixed
Support Condition 4	46833	fixed	fixed
Support Condition 5	46833	224651.5	10000

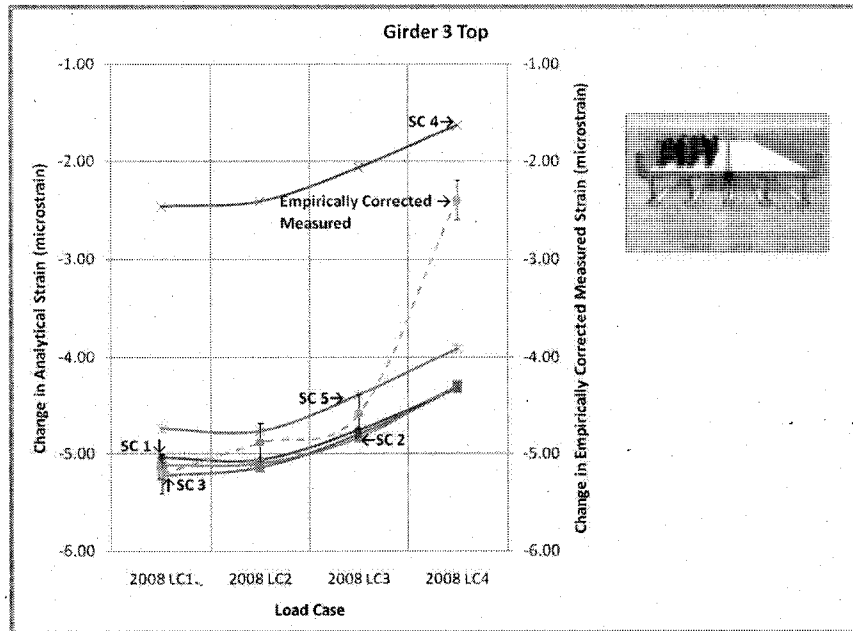


Figure 68: Manual model updating using girder 3 top strain sensor

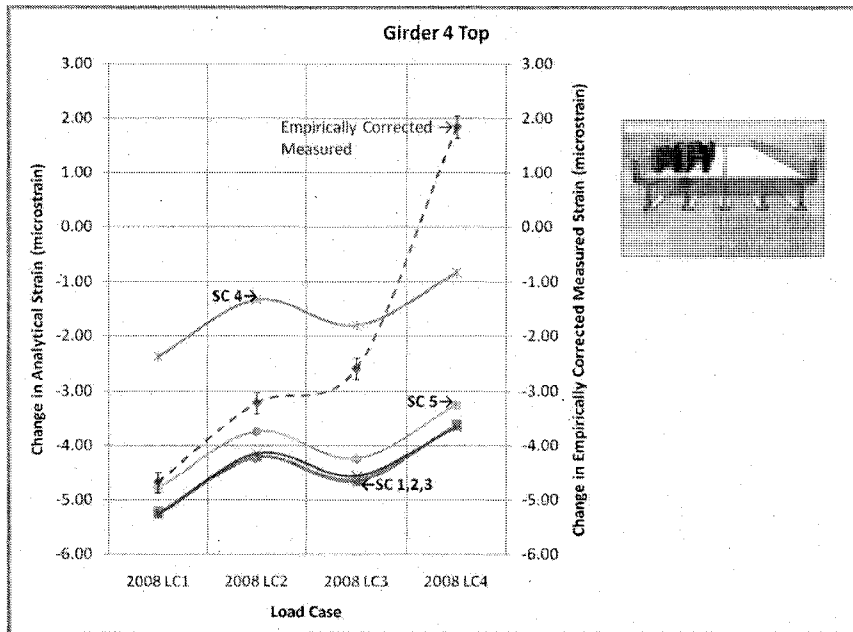


Figure 69: Manual model updating using girder 4 top strain sensor

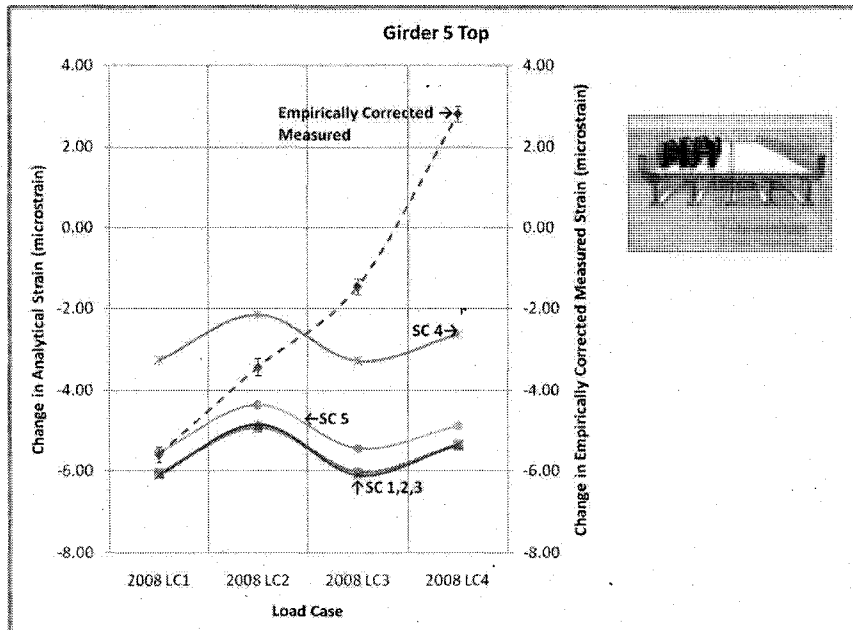


Figure 70: Manual model updating using girder 5 top strain sensor

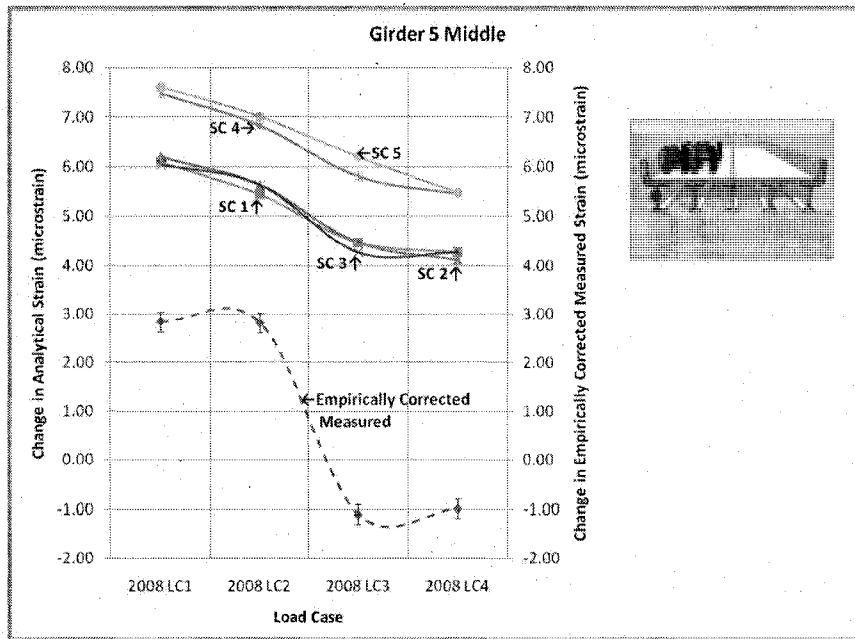


Figure 71: Manual model updating using girder 5 middle strain sensor

The figures above show how by changing the bearing pad stiffness, updating the model, the response of the model matches that of measured structural response. The model response matches the measured response fairly well in support condition 5 when the horizontal bearing pad stiffness value is modified from the fixed condition. Further analysis using a parameter estimation and model updating program will be able to get a more precise value by varying each component independently as part of an algorithm to obtain the optimal conditions. There is a shift in girder 5 middle which could suggest a change in the location of the neutral axis. For girder 3, girder 4, and girder 5 top the change in the model trends follow the change in measured strain trends.

While examining strain is viewed to be a more accurate method for manual parameter estimation when compared to deflection measurements since there is a larger opportunity for human error and the reference dependent nature of deflection

measurements; the deflection measurements that were taken during the 2008 load test were also used as a way to validate the strain response seen in the figures above. Figure 72, Figure 73, and Figure 74 show the modeled deflection compared with the measured deflection. The deflections typically fall within the error bars for the measured response which gives researchers more confidence in the results obtained from the strain comparisons for manual model updating. The outliers could be associated with the variability in the survey measurements due to non-optimal conditions as previously discussed.

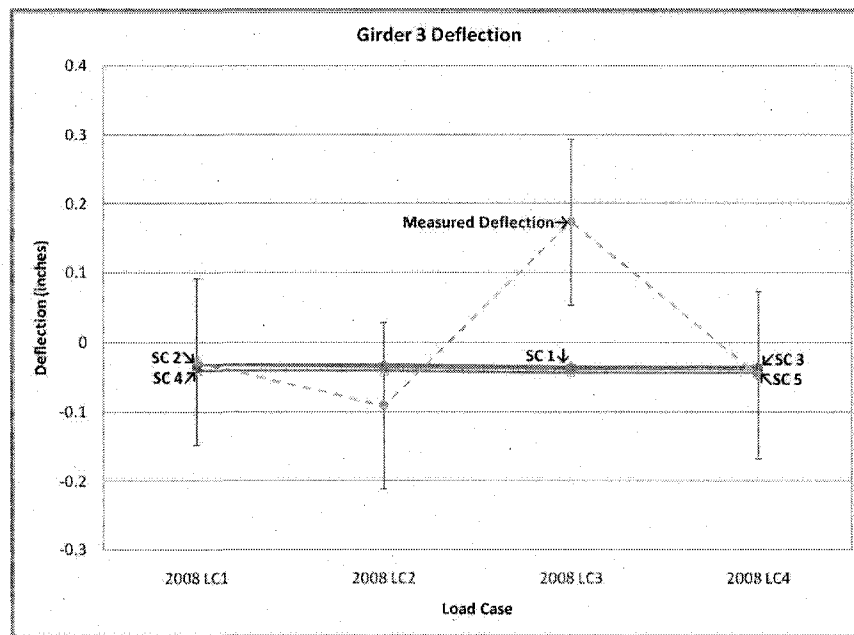


Figure 72: Manual model updating verification using girder 3 deflection measurements

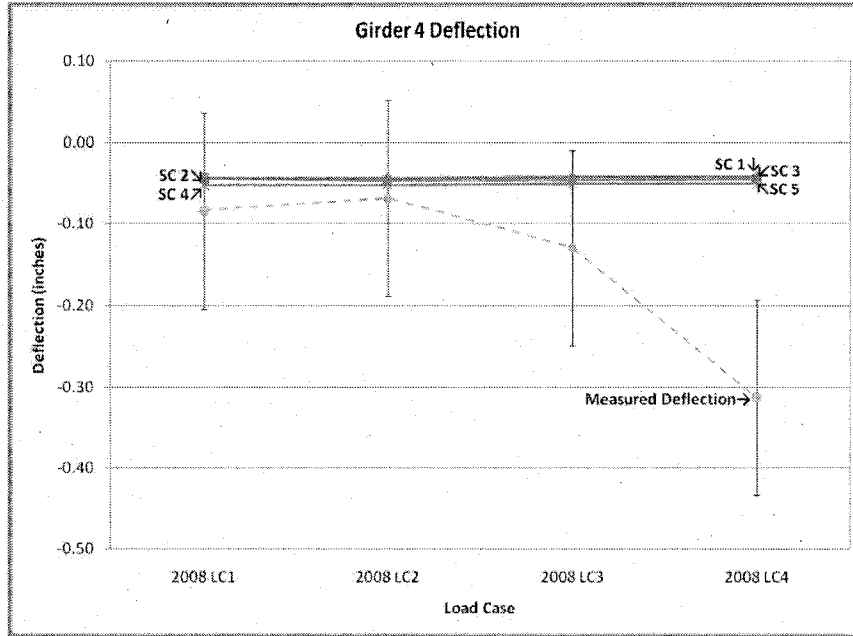


Figure 73: Manual model updating verification using girder 4 deflection measurements

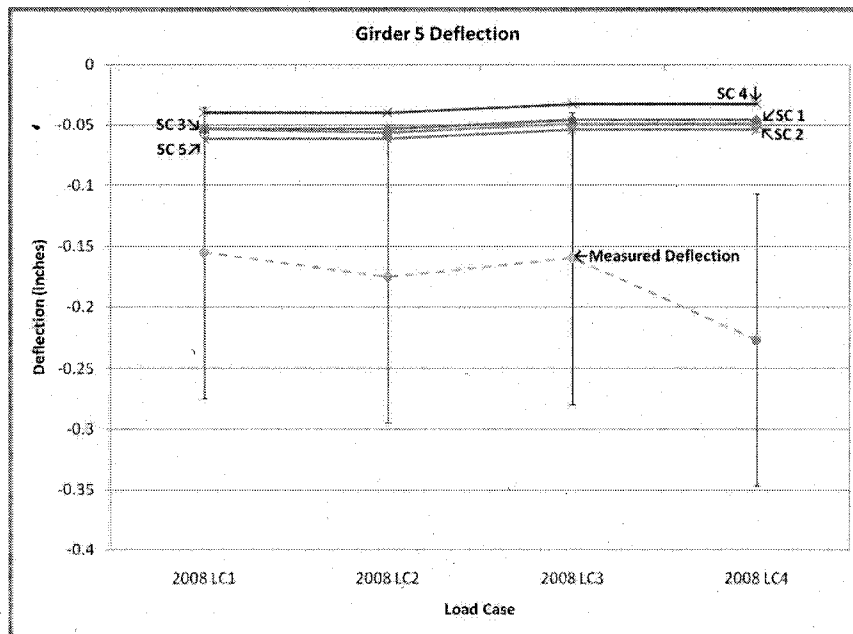


Figure 74: Manual model updating verification using girder 5 deflection measurements

6.1.2 – Analysis of Removing Specific Structural Elements

The bearing pad stiffness obtained from the above analysis, support configuration 5 now benchmark, will be kept constant in the next analysis of modeled

response. Table 15 shows the four cases that will be used to show the effect of specific parameters in the model. Structural parameters such as CFRP, prestressing, and bridge rail will be removed from the SAP2000® model, and the response will be seen in Figure 75, Figure 76, Figure 77, and Figure 78.

Table 15: Manual model updating cases and corresponding bearing pad stiffness values for third analysis

	Vertical Stiffness (kips/in)	Rotational Stiffness (kips/rad)	Horizontal Stiffness (kips/in)
Benchmark	46833	224651.5	10000
No CFRP	46833	224651.5	10000
No Prestress	46833	224651.5	10000
No Bridge Rail	46833	224651.5	10000

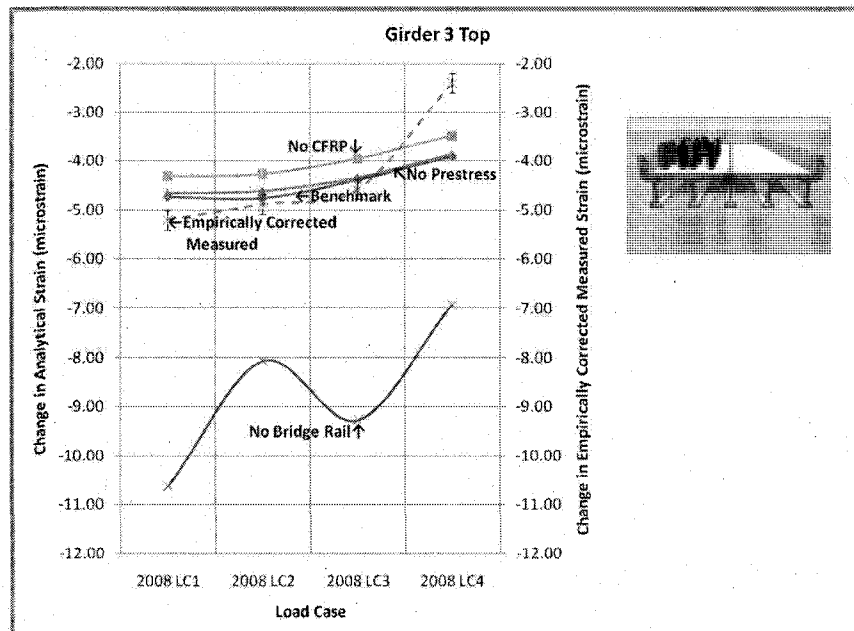


Figure 75: Manual model updating using girder 3 top strain sensor

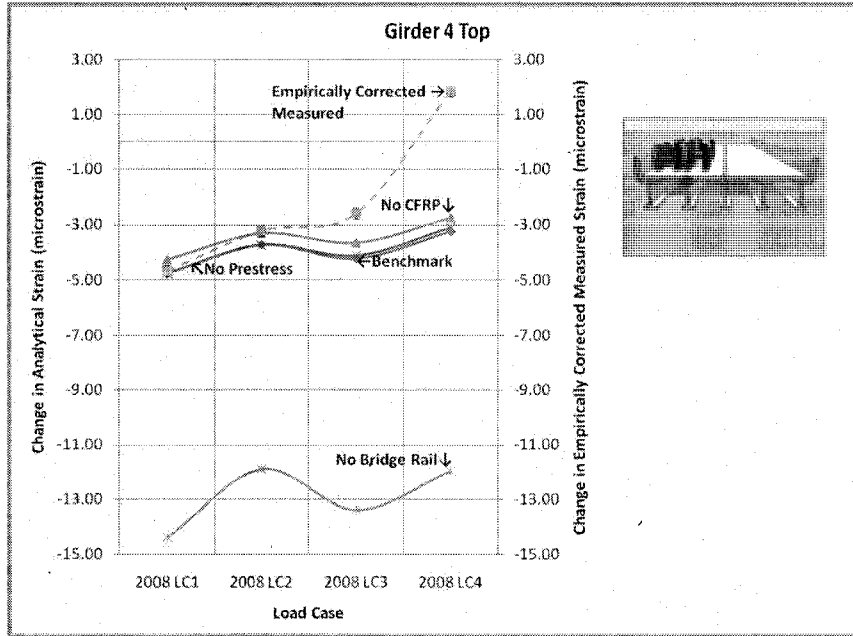


Figure 76: Manual model updating using girder 4 top strain sensor

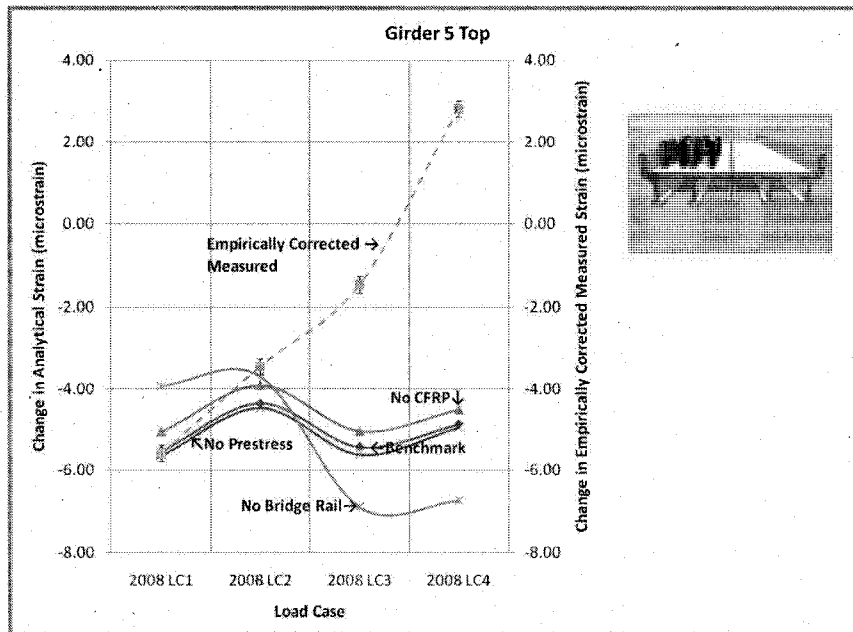


Figure 77: Manual model updating using girder 5 top strain sensor

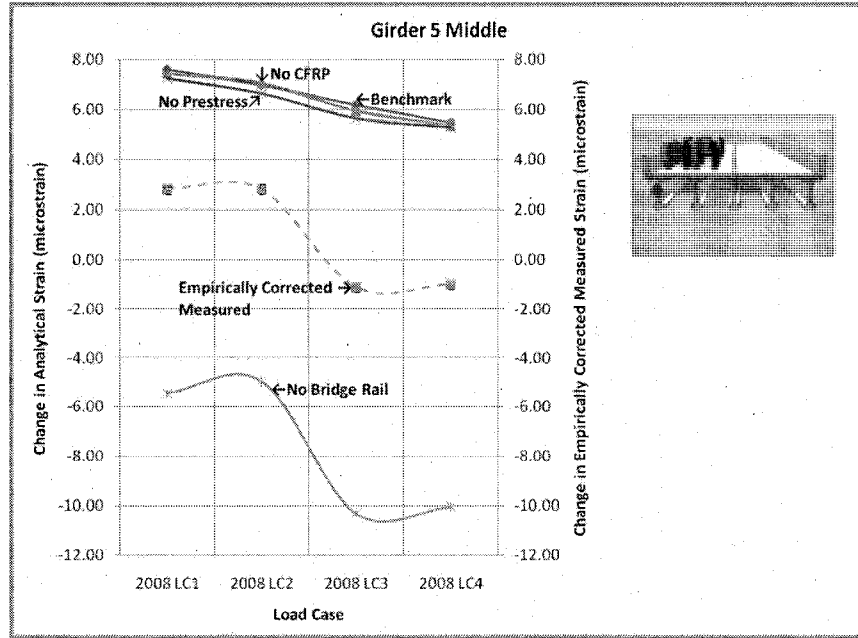


Figure 78: Manual model updating using girder 5 middle strain sensor

These results show that not including the bridge rail in the model had significant effects on the change in measured response of the bridge model. Removing prestress and/or CFRP had a smaller effect in change of strain but it must also be remembered that this is a change in strain, so the benchmark model for the base also has no CFRP or prestress which explains why the values appear to be similar.

As with the second analysis case, deflection measurements were also shown for a second comparison and validation. Figure 79, Figure 80, and Figure 81 show the deflection comparison done for the third analysis case.

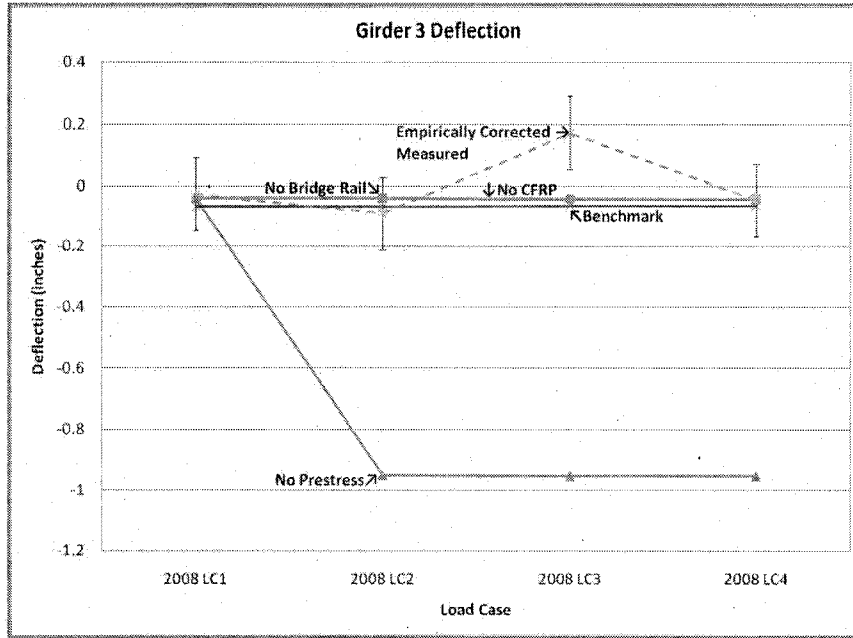


Figure 79: Manual model updating comparison using girder 3 deflection measurements

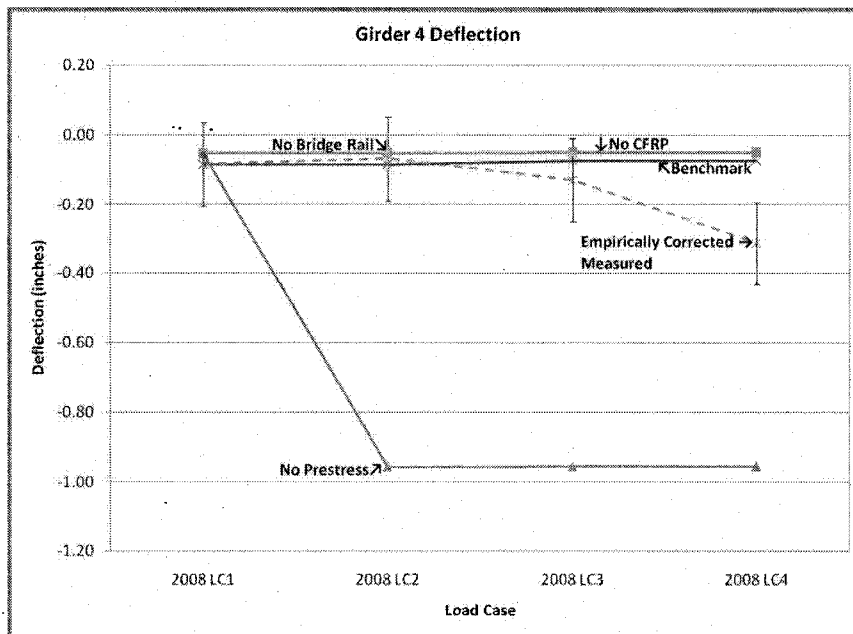


Figure 80: Manual model updating comparison using girder 4 deflection measurements

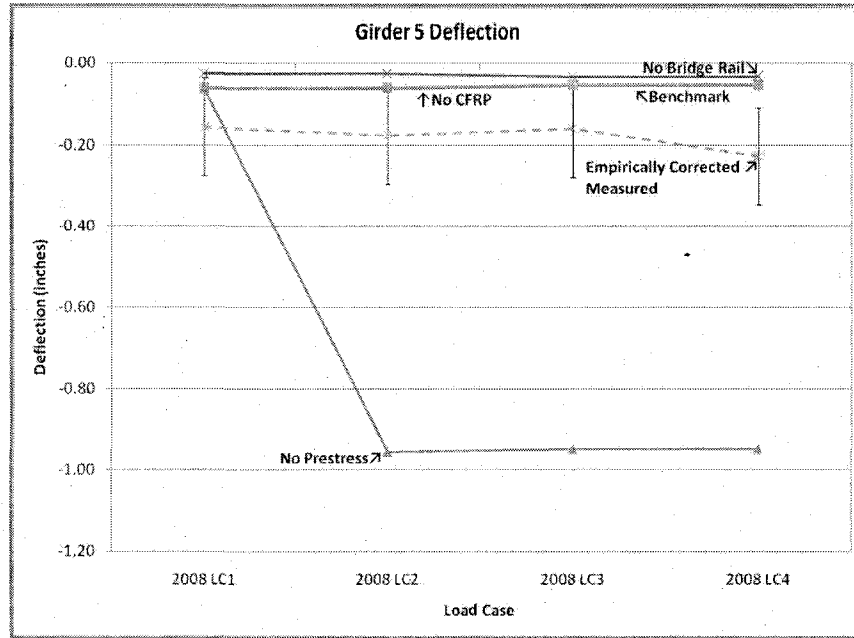


Figure 81: Manual model updating comparison using girder 5 deflection measurements

In the deflection comparison it can be seen that not having the prestress produced the biggest change when compared to measured response. Removing CFRP and the bridge rail had less of an effect, however it can still be noted.

6.2 – Discussion of Manual Parameter Estimation Results

To reiterate, the only gauges used in the SHM program for RRB were the gauges embedded in the HPC girders. These gauges are oriented in the longitudinal direction and capture the global structural response of the bridge given the loadings. Using only the girder gauges also limits the computations to a reasonable limit for the scope of the Rollins Road Bridge Research Project. The 2000 and 2001 load test were not geared towards SHM and proved to be not as useful as the 2008 load test which was specifically designed for SHM purposes. Including three zero-load points allowed

researchers to remove strain due to change in environmental factors and perform manual model updating on the structural model to match the measured response.

6.3 – Conclusions on Manual Parameter Estimating Results

The results from the manual parameter estimation show that the change in measured structural response could match the change in modeled response by modifying the horizontal stiffness of the elastomeric bearing pad. The final bearing pad stiffness ended up being 46,833-kip/in in the axial direction (k_a), 10,000-kip/in in the horizontal direction (k_h), and 224,651-kips/rad for rotation (k_r). Figure 82 and Figure 83 show a quantification of the bearing pad stiffness values used as compared to a roller, pinned, and fixed connection. This is only to show the effects of the spring on an example 40-foot beam with a 10-kip point load, not the actual bridge configuration. The axial and horizontal stiffness remained as calculated since there was nothing to suggest otherwise, and the horizontal direction was modified to get the structural response to match. According to Stanton et al. (2008), there are no standard calculations for the horizontal stiffness value.

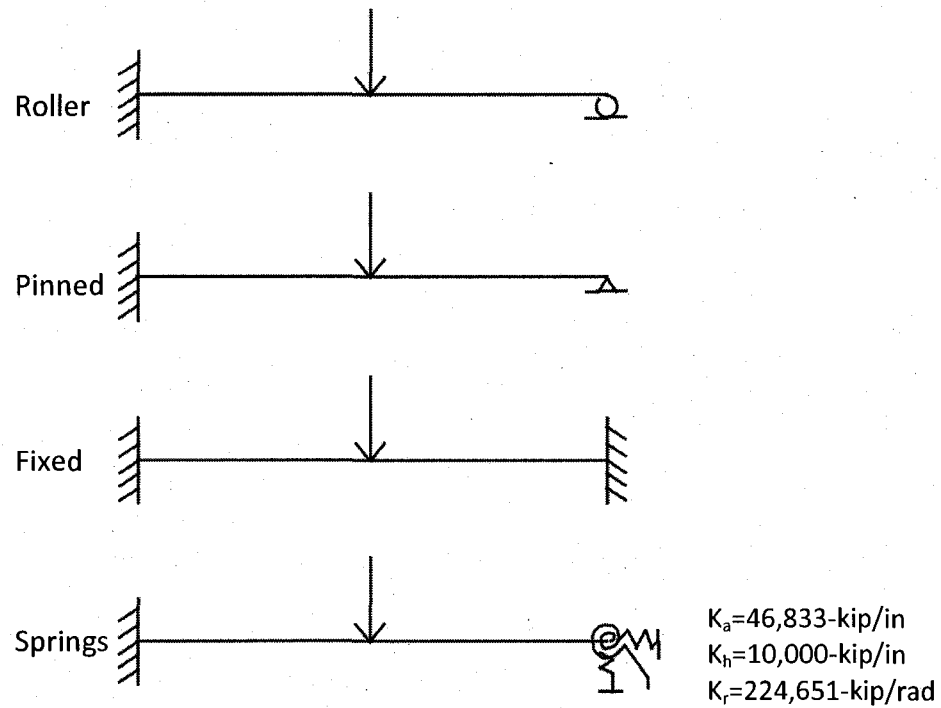


Figure 82: Quantification of bearing pad stiffness examples

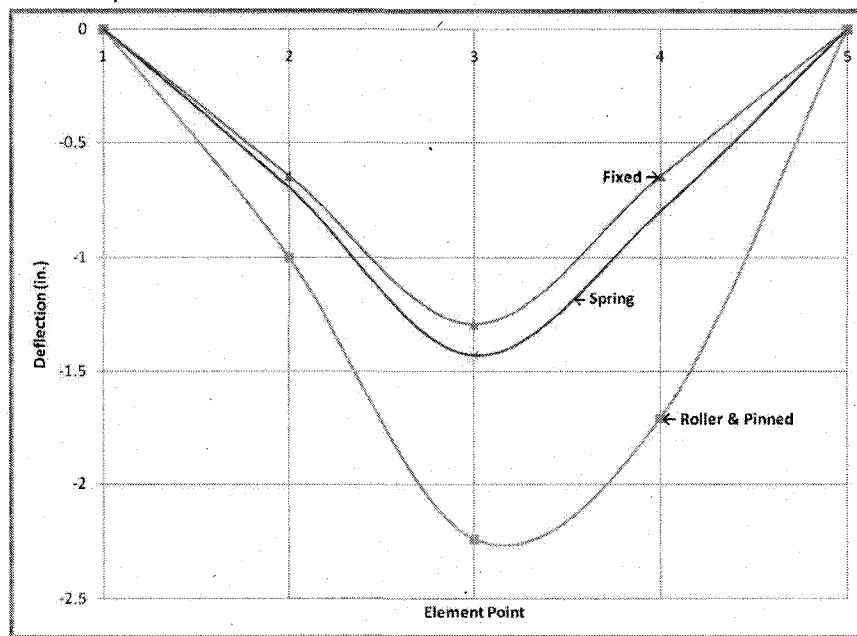


Figure 83: Quantification of bearing pad stiffness results

When this model is run through MUSTANG, structural parameters such as moment of inertia, modulus of elasticity, and individual bearing pad stiffness

properties can be modified to see the effect on the modeled response. Including the abutment and ground conditions into the model and then running parameter estimation could also give insight into the structural response exhibited by the bridge in the field. A good way to see if the abutments are affecting the structural response would be to take survey measurements during the load test and throughout the year to see how the abutments are moving. This could then be correlated to changes in structural response of the bridge.

6.4 – Variations in Data

Several things may be noted in the results for both strain and deflection comparison. In the strain comparisons for girder 3 top, girder 4 top, and girder 5 top there seems to be a large variation between the third and fourth load case. This variation could be due to the fact that the linear correction applied tended to deviate from the data the further it went into the load test. This is because it was a linear correction done using only three data points, two recorded towards the beginning of the load test and only one recorded towards the end. In the strain comparisons for the second analysis have support conditions one through three being grouped very close together in most cases. This can be due to the fact that if the stiffness conditions are examined closely, the ones that would have the greatest effect on the bridge response are either not changed at all or only changed by a small amount while keeping the horizontal stiffness fixed.

The deflection comparison shows the variation inherent with the type of survey measurements and survey conditions that were present during the load test, i.e.

having the measuring rod in a lift bucket. It would be optimal to take more measurements and be able to perform statistical operations on the data to remove any outliers or values obtained that are not what is actually occurring in the field, instead of just one measurement point.

In the third analysis the strains from the benchmark, no CFRP, and no prestress are also grouped in the same area. This is because the numbers in the graph are change in response, with respect to a benchmark that has the same conditions as the truck load model. The biggest change with not including the bridge rail, in both the truck load model and the benchmark model for that situation, can be attributed to a change in the load and configuration of the bridge. The third analysis deflection readings follow a similar group with the benchmark, no CFRP, and no bridge rail being grouped together while the no prestressing model shows significant deviation. This is obviously due to the effects of camber on the dead and applied load not being included in the deflection measurements.

6.5 - Optimal Conditions

As seen with the parameter estimation, and the not so successful initial parameter estimation run as seen in Appendix F – First Analysis of Rollins Road Bridge Load Test Data for All Three Years, it is important when doing a load test for SHM, to design the load test with that in mind. Also, if a better initial value was known for the strain readings on the bridge it might have been possible to perform successful parameter estimation in the initial analysis. However, not knowing the initial values of strain, exact environmental factors, and being able to properly model all of those

environmental factors made doing the initial analysis challenging. As seen in the second analysis, being able to remove environmental effects from the measured response data and not having to worry about the initial gauge value, proved to be useful in the model updating of the RRB SAP2000® model.

CHAPTER VII

STRUCTURAL HEALTH MONITORING, PARAMETER ESTIMATION, AND MODEL UPDATING

The Rollins Road Bridge Research Project has created a model that captures the behavior of the RRB. This model has undergone minor manual model updating to calibrate the model to the observed in the structural behavior. Some trends in the behavior of the model can be observed, however the values are still not exactly where they should be. This was to be expected since only minor model updating was done. MUSTANG will be used to do a full-scale parameter estimation using the model created and the post-processed data analyzed in this research project.

7.1 - Parameter Estimation

The parameter estimation that will be performed on the RRB SAP2000® model includes investigating boundary conditions as well as other structural parameters that affect the stiffness of the structure, such as moment of inertia, area, and modulus of elasticity. Parameter estimation uses measured data and a comparative, predictive model to give validity to both the model and the data. Once the parameters are

updated and behaviors match, the difference between the design parameters and estimated parameters can be used to show the change in state of the structure.

When a structure is designed, several things are assumed to be known such as modulus of elasticity (E), moment of inertia (I), boundary conditions, torsional rigidity (GJ) and area (A). In the design phase, if finite element models are used, the assumed EA , EI , GJ , and design loads are applied to that model. Finally displacements and rotations are calculated. Parameter estimation is, in some senses, the inverse to direct structural analysis. The existing structure is known, with initially assumed EA , EI , and GJ . Experimental loads are applied, through nondestructive test techniques, and the response of several degrees of freedom are measured. Through the use of a model, the response data, and parameter estimation software the information is combined and actual EA , EI , and GJ of the structure are determined. Figure 84 shows a graphical representation of the process of parameter estimation.

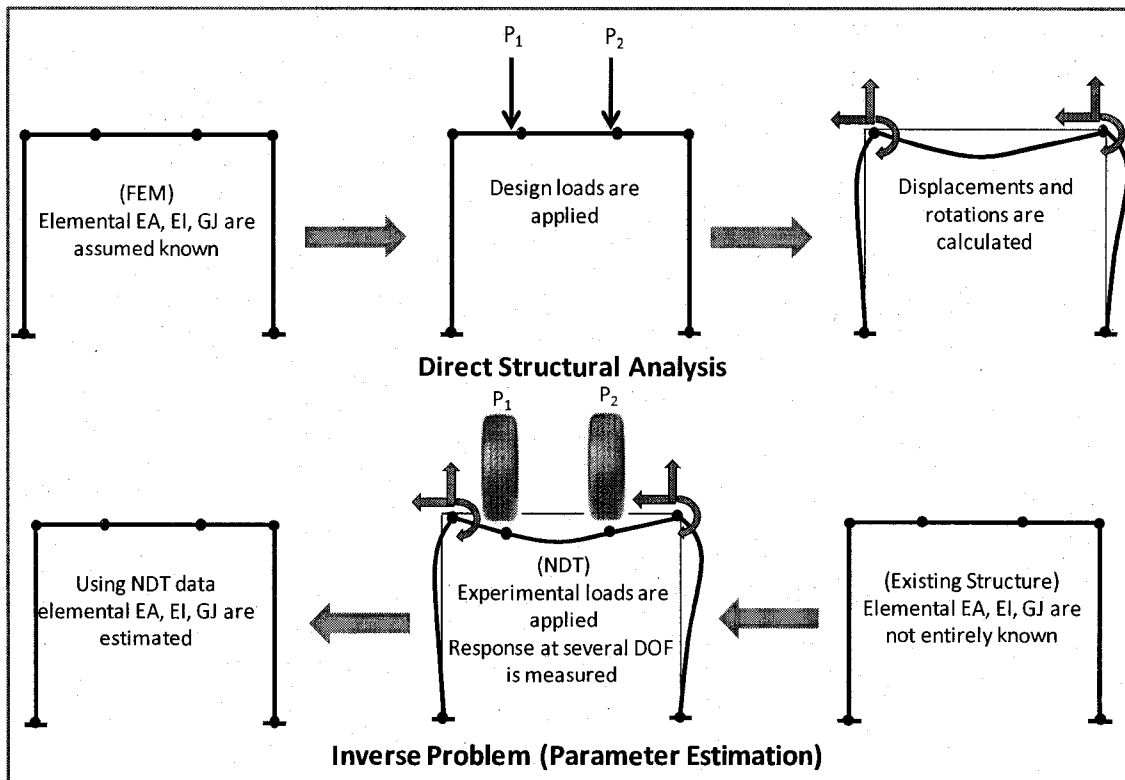


Figure 84: Graphical representation of parameter estimation (Sipple, 2008)

Once this parameter estimation has been performed on the RRB model, researchers and the NHDOT will have an up-to-date model of actual conditions at RRB. This model could easily be used for special permitting.

During a special permitting operation that took place in Norco, Louisiana on the Bonnet Carré Spillway Bridge, Bridge Diagnostics, Inc. and researchers from the University of South Carolina used a calibrated, essentially parameter estimated, model to match response caused by a superload passing over the bridge. This model successfully predicted the response and results showed that the approach of using a model was the same as the typical load rating procedure. An added benefit of using the model was being able to see the global structural response instead of analyzing beams with distribution factors (Grimson, Commander, & Ziehl, 2008).

7.2 - Central Artery Parameter Estimation

Parameter estimation and model updating has been successfully performed by researchers at UNH that are involved in the Rollins Road Bridge Research Project. This parameter estimation was done on a research project conducted by Tufts University in conjunction with the University of New Hampshire and Geocomp Corporation.

A part of the Central Artery/Tunnel project in Boston, MA was removing the existing six-lane, steel frame Central Artery viaduct to be replaced with a cut-and-cover tunnel. To allow for the viaduct to remain in service during tunnel construction, the existing foundations were underpinned using steel frame bents. Once the tunnel was opened, the demolition of the viaduct took place which removed the roadway and left the steel underpinning frames exposed for a short time. While these underpinning frames were exposed and prior to demolition, researchers from Tufts, UNH, and Geocomp performed two nondestructive tests, one a moment frame and the other braced frame. Strain, rotation, and displacement measurements were taken during the test in which the frame was loaded using a crane with a load cell between the crane cable and the structure. Results from this test, as well as a model created in GT Strudl®, were combined and used in the parameter estimation, PARIS© (Santini-Bell, Sanayei, Brenner, Sipple, & Blanchard, 2008), see Appendix G – Nondestructive Testing for Design Verification of Boston’s Central Artery Underpinning Frames and Connections .

Parameter estimation was successfully performed using PARIS© (Sanayei, 1997), estimating the stiffness of the moment connections in the moment frame. It

was possible to use PARIS© for this exercise since the model was created using entirely frame elements, which PARIS© has full capabilities of using. The model was created in GT Strudl® to determine geometry, and then those properties were transferred over to PARIS©'s internal FEM protocol. The parameter estimation was run through PARIS©, the updated connection stiffness values were obtained. Those values were put into a separate GT Strudl® model and the analysis was run again to confirm the measurements from PARIS©.

This was an exercise in this research project to determine how parameter estimation can be performed using a FEM and NDT results. The fixed connections in the moment frame had a numerical stiffness value of 9.28×10^7 in-kips/radian which matches the idea that they had infinite stiffness, and therefore fixity (Santini-Bell, Sanayei, Brenner, Sipple, & Blanchard, 2008). The lessons learned from this exercise is serving as input in the programming of MUSTANG and aid in the analysis of the RRB SAP2000® model once MUSTANG is fully functional.

The process for the Central Artery/Tunnel Project ran fairly smoothly, however it did not take full advantage of the powers of the structural analysis program, GT Strudl®. Everything that was manually inputted into PARIS© was already modeled in GT Strudl®. This is the reason why researchers at UNH are currently developing a program that links the power and intelligence a structural analysis program, SAP2000®, with a parameter estimation program similar to PARIS© called MUSTANG.

7.3 - Current Ongoing Research at UNH – MUSTANG

During the permitted process of the Bonnet Carré Spillway Bridge, it took 3,276 strain comparisons from 28 strain gauges and 117 load cases, three truck paths with 39 stop positions to calibrate the model before it was used to match response caused by the superload (Grimson, Commander, & Ziehl, 2008). This entire process, instead of being done by hand or manual model updating, could be done using an automated program such as MUSTANG.

MUSTANG uses the modeling power and capabilities of SAP2000® to get all of the connectivity tables, joint locations, boundary conditions, element types, material properties and stiffness matrices used for parameter estimation. MUSTANG will take full advantage of the SAP2000® Advanced Programming Interface (API) to make linking MUSTANG with SAP2000® easier. The program and research into linking the two programs is being performed at the University of New Hampshire by John Welch.

7.4 - Structural Health Monitoring Program

An efficient SHM takes full advantage of the modeling done by designers through upgrading the design model to a monitoring model. Visual inspection information can be incorporated into the model as well as load test programs. This can allow structural response data from nondestructive testing to provide an invaluable resource for bridge owners. This data satisfies needs of bridge owners including determining serviceability and load capacity, investigating the reliability of the structure, and giving a record, through models, of the progression of the health of

the bridge. This information may also be able to provide insight into the how long the bridge will operate at current capacities.

Ensuring all new bridge construction project have a SHM component in the design of the bridge, whether that be including sensors in the girders or tilt meters installed after construction, will provide invaluable insight into the health of bridges well into the future. There has been talk with the NHDOT to include a SHM layer in their current GIS system, allowing officials to know, at a glance, which bridges are instrumented and have the capabilities of performing SHM. This GIS layer could go even a step further when linking up to the data acquisition and processing systems to alert the NHDOT if there is an abnormal structural response at one of their bridges. This will allow for a more efficient allocation of time and money which is already spread fairly thin for DOTs throughout the country.

Retrofitting existing bridges, or even just troubled bridges, may be able to offer the same benefits as instrumenting new construction, if not more. Instrumentation of aging bridges could allow bridge owners to see which bridge is most in need of structural repairs. With existing bridges, instrumentation incorporated into a GIS layer may also serve to provide an early warning for changes that could affect public safety.

RRB was instrumented for the IBRC to look at prestress losses and performance of the CFRP in the deck. This research project successfully took that instrumentation plan and used it to find the global structural response for SHM. This same process can easily be repeating on other bridges in the state of New Hampshire that have been

instrumented as part of the IBRC to examine structural behavior and eventually be included on a GIS layer linking the data acquisition and processing systems.

CHAPTER VIII

CONCLUSIONS, FUTURE WORK, AND RECOMMENDATIONS

8.1 – Key Observations

During the course of this research project there were several key observations made. Some of those observations include the large effect that temperature has on the relatively short span Rollins Road Bridge. Change in environmental conditions and the resulting change on the bridge must either be included in the modeled aspect or accounted for in the measured structural response data. The stiffness of the bearing pads was updated solely for the reason of experimentally determining the horizontal stiffness of the elastomeric reinforced bearing pad, the one stiffness value not given through experimentally verified equations. The linear correction can be seen when closely examining the measured response; however this does not capture all of the data, specifically towards the end of each run. Using more zero-load points and a parabolic correction could better correct the data and therefore capture a more accurate structural response caused by applied truck load. The effects of including the bridge rail can be seen when that element is removed during the third analysis. Another option to deal with the bridge rail would be to break up the element that

models the bridge so it is not modeled as a continuous bridge rail, which would more accurately reflect how it is cast on the bridge.

8.2 – Conclusions

The RRB load test data shows that the structural performance of the CFRP grid, concrete deck, and concrete girders matches the excellent rating from visual inspections. The strain values are either bounded by, or shown to be less than the two prior tests performed in December 2000 and August 2001. It is difficult to do an exact data-to-data comparison since testing conditions different from 2000/2001 to 2008. The difference between 2000/2001 and 2008 load tests included stopping locations and gross weight of the truck. The reason for the differences in stop locations was because the goal of the 2008 load test was to observe global response while the 2000/2001 load tests examined local response in the CFRP and deck. The performance of the CFRP was an important aspect of the project, however not the ultimate goal.

A monitoring model, with added specific structural components, was created to capture the behavior of the bridge. The effects of removing those components can be seen in the third analysis of the data. This model and the data from the load test is currently in a phase where it can be easily taken over by a fellow researcher, John Welch, to be used in the first major parameter estimation exercise of a parameter estimation program being developed at UNH called MUSTANG (Model Updating StrucTural ANalysis proGram).

As noted in the current bridge inspection report, there are no visible signs of deterioration or cracking, which caused the main focus of the parameter estimation to

be the horizontal stiffness of the elastomeric bearing pads. Visual inspections will continue to be performed at RRB, and once there is noted deterioration, the model will be easily updated to model that change in behavior. The modeling of structural deterioration will also allow that deterioration to be quantified as a reduction in area, moment of inertia, or modulus of elasticity instead of a note on an inspection report.

Environmental effects, including temperature changes, had a much larger effect on load test data than originally expected. The change in temperature throughout a three hour load tests overshadowed the effect of a 19-ton truck. Environmental effects can be easily removed if zero-load data points are included several different times in the load test program. Removing environmental effects through empirical methods allowed a normalization of the data without relying on theoretical calculations. All information used to remove temperature using the empirical method was determined by the bridge and current structural conditions at the exact time of the load test. The two previous load tests did not include zero-load data points which is why the manual parameter estimation was not performed on those sets of data. Subsequent tests should include enough of those points to be able to properly correct for environmental effects potentially using a parabolic or quadratic fit functions.

The empirical temperature correction proved to be beneficial. Performing the empirical temperature correction allowed for manual model updating to be successfully performed on the 2008 RRB SAP2000® model. The SAP2000® data converged with the measured structural response after only a few iterations, and will

be more precisely determined using MUSTANG. This manual model updating has shown that by changing structural properties of a monitoring based model, that analytical model can be matched to measured structural response.

8.3 – Future Work

The performance of the CFRP, bridge deck, and NEBT girders will continue to be monitoring by collecting long-term SHM data and the occasional load test. These load tests will be performed with all the knowledge gained from this load test, and will add an unknown amount of new knowledge to the testing program for RRB and SHM programs for the bridges of the state of New Hampshire. Parameter estimation and model updating will be performed on the RRB SAP2000® model in the spring of 2009 on MUSTANG. This model will be kept up-to-date when the next load test is done, and since the model has already been created more time and effort can be spent into ensuring all behavior experienced by the bridge is captured in the model. Post processing of load test data and model output will be refined, possibly using the SAP API and [B] transformation matrix to obtain directly without having to perform radius of curvature calculations.

This project has also raised questions on the modeling techniques and how results are obtained from the model. The abutment was not modeled in this project because it was decided that modeling would only be done to the bearing pads. It would be beneficial to see the results of manual or automated parameter estimation if the abutments and ground conditions were modeled. The model including abutments

could then be compared to the model for this research project to determine the cost benefit of modeling the abutments.

An eventual goal would be to eliminate looking for the change, and be able to get matching results. This will required significant research of all aspects of the structure that needs to be included in the model. This will also require knowing the initial reading for the strain gauges while the bridge is still in construction, before framework is removed and the bridge carries its own self weight. Environmental effects will also have to be measured. There is also the possibility of using weigh-in-motion sensors or closed-circuit video monitoring at the bridge to use everyday traffic as a load and then measure response from traffic loading.

There are now three different sets of load test data and continuous temperature and strain data collected specifically for the CFRP and bridge deck that can be closely analyzed to determine behavior of the CFRP and bridge deck. The data collection will continue as most of the problems associated with data collection have been resolved during this research project.

8.4 – Recommendations

Lessons learned in this project can be applied to an upcoming research partnership including UNH, NHDOT, Tufts University, Fay, Spofford, and Thorndike, Inc. (FST), and Geocomp Corporation. This project involves creation of an instrumentation plan, monitoring model, and testing of a new bridge with FST and NHDOT. This project is sponsored by the Project for Innovation (PFI) through the National Science Foundation (NSF). The structural behavior of the bridge will be more accurately

captured since the instrumentation plan will be designed around SHM. The PFI Project Bridge is currently in the design phase and the instrumentation plan will be designed with SHM as the focus. There will be multiple temperature sensors installed throughout the cross section of the bridge to obtain accurate readings of temperature to be able to apply the temperature as a gradient throughout the bridge, rather than just a thermal load applied to the surface.

During the load test, zero-load points should be taken from the first load test when the bridge is commissioned. This will give the opportunity to have a baseline established for the behavior of the bridge, the temperature and strain values recorded at commissioning will give a snapshot of the first moments in the service life of the bridge. All following data may then be compared to this snapshot in order to assess current conditions at the bridge, whether that is two years or 30 years down the road. There has also been discussion of installing traffic cameras on the bridge so this zero-load reading can be taken at any point by observing the bridge and remotely collecting data several times a month. This would allow observation of temperature trends throughout the year for the bridge to see how it behaves, and then compare that with data from different years to have a catalog on change to the bridge.

For future tests at RRB, more zero-load readings can be taken for a better trend line for temperature removal. There were also logistical issues with taking the deflection reading with the leveling rod, having a small lift bucket and having to make several different moves to get to each point. Having a larger bucket that can remain

up under the bridge and the surveyor just walk down the length of the bucket and be able to reach each survey point would make gathering deflection data easier.

The Rollins Road Research Project proved valuable for the amount of information obtained from doing one load test on an instrumented bridge. Most importantly, it showed that manual model updating can be performed on a monitoring based model to have the analytical results calibrated to the measured response. Doing the data analysis for the load test and having a comparative model to make the data analysis accountable to the model and vice-versa gives an aspect of accountability through a predictive model. The original thoughts on how the research group thought this project was going to be run changed throughout the process as things not to be important, number of elements, discretizations were not important and things that were not originally considered, accounting for temperature, modeling specific structural characteristics, became the focus of the research. Research projects involving SHM for bridges will take all the lessons learned from this project to further advance SHM programs.

WORKS CITED

- AASHTO. (2008). *Bridging the Gap - Restoring and Rebuilding the Nation's Bridges*.
- AASHTO. (2004). LRFD Bridge Design Specifications Third Edition. *14.5 Bridge Joints*, pp. 14-8.
- AASHTOWare. (2008). *AASHTOWare Catalog July 1, 2008 - June 30, 2009*. American Association of State Highway and Transportation Officials.
- Aktan, A. E., Farhey, D. N., Helmicki, A. J., Brown, D. L., Hunt, H. J., & Lee, K. L. (1997). Structural Identification for Condition Assessment: Experiment Arts. *Journal of Structural Engineering, ASCE*, 123 (12), 1674-1684.
- Bailey, J., & Murphy, K. (2008). The Effectiveness of Fiber Reinforced Polymers in Modern Day Bridge Building. *Eighth Annual Freshman Conference* (p. 5). Pittsburgh, PA: University of Pittsburgh.
- Bardow, A. K., Seraderian, R. L., & Culmo, M. P. (1997). Design, Fabrication and Construction of the New England Bulb-Tee Girder. *PCI (Precast/Prestressed Concrete Institute) Journal*, 29-40.
- Beal, D. (2008, September 9). Retrieved September 23, 2008, from Transportation Research Board of the National Academies:
<http://www.trb.org/TRBNet/ProjectDispaly.asp?ProjectID=2507>
- Bell, E. S., Sanayei, M., Javdekar, C. N., & Slavsky, E. (2007). Multiresponse Parameter Estimation for Finite-Element Model Updating Using Nondestructive Test Data. *Journal of Structural Engineering - ASCE*, 1067-1079.
- Benmokrane, B., El-Salakawy, E., El-Ragaby, A., & Lackey, T. (2006). Designing and Testing of Concrete Bridge Decks Reinforced with Glass FRP Bars. *ASCE Journal of Bridge Engineering*, 217-229.
- Bowman, M. M. (2002). *Load Testing of the Carbon FRP Grid Reinforced Concrete Bridge Deck on the Rollins Road Bridge, Rollinsford, New Hampshire*. Durham, NH: University of New Hampshire.
- Bowman, M. M., Yost, J. R., Steffen, R. E., & Goodspeed, C. H. (2003). Diagnostic Testing and In-Service Performance Monitoring of a CFRP Reinforced HPC Bridge Deck. *Second New York City Bridge Conference - Recent Developments in Bridge Engineering* (pp. 361-371). New York, NY: Bridge Engineering Association.
- Branco, F. A., & Mendes, P. A. (1993). Thermal Actions for Concrete Bridge Design. *Journal of Structural Engineering*, 119 (8), 2313 -2331.
- Brownjohn, J. M., Moyo, P., Omenzetter, P., & Chakraborty, S. (2005). Lessons from monitoring the performance of highway bridges. *Structural Control and Health Monitoring*, 12:227-244.
- Choquet, P., Juneau, F., & Bessette, J. (2000). New generation of Fabry-Perot fiber optic sensors for monitoring of structures. *SPIE's 7th Annual International Symposium on Smart Structures and Materials*. Newport Beach, CA.
- Computer Structures, Inc. (2007, October). *CSI Analysis Reference Manual for SAP2000®, ETABS®, and SAFE™*. Berkeley, California, USA.

- El-Salakawy, E., Benmokrane, B., & Desgagne, G. (2003). Fibre-reinforced polymer composite bars for the concrete deck slab of Wooton Bridge. *Canadian Journal of Civil Engineering* , 30.
- Farhey, D. N. (2005). Bridge Instrumentation and Monitoring for Structural Diagnostics. *Structural Health Monitoring* , 301-318.
- Farhey, D. N. (2007). Quantitative Assessment and Forecast for Structurally Deficient Bridge Diagnostics. *Structural Health Monitoring* , 39-48.
- FISO. (2008). *EFO Strain Sensor Product Data Sheet*. Retrieved August 18, 2008, from http://www.fiso.com/modules/AxialRealisation/img_repository/files/documents/2007/MC-00086%20R6_PDS_EFO.pdf
- Fu, G., Feng, J., & Dekelbab, W. (2003). *NCHRP Report 495 - Effect of Truck Weight on Bridge Network Costs*. Washington, D.C.: Transportation Research Board.
- Grimson, J. L., Commander, B. C., & Ziehl, P. H. (2008). Superload Evaluation of the Bonnet Carre Spillway Bridge. *Journal of Performance of Constructed Facilities - ASCE* , 22 (4), 253-263.
- GT Strudl. (2007). *Version 29* . Georgia Tech - CASE Center.
- Guan, H., Karbhari, V. M., & Sikorsky, S. C. (2007, August). Long-term Structural Health Monitoring System for a FRP Composite Highway Bridge Structure. *Journal of Intelligent Material Systems and Structures, Vol. 18* , 809-823.
- Haenni. (2008). Retrieved November 2008, from HAENNI Wheel Load Scales, a division of Baumer Borudon Haenni AG: <http://www.haenni-scales.com/e/>
- Hearn, G. (2007). *NCHRP Synthesis 375 - Bridge Inspection Practices*. Washington, D.C.: Transportation Research Board.
- Hibbler, R. C. (2005). 4.6 Thermal Stress. In *Mechanics of Materials - Sixth Edition* (pp. 154-158). Upper Saddle River, New Jersey: Prentice Hall.
- Howell, D. A., & Shenton III, H. W. (2006). System for In-Service Strain Monitoring of Ordinary Bridges. *Journal of Bridge Engineering - Vol. 16, No. 6* , 673-680.
- Karbhari, V. M., Chin, J. W., Hunston, D., Benmokrane, B., Juska, T., Morgan, R., et al. (2003). Durability Gap Analysis for Fiber-Reinforced Polymer Composites in Civil Infrastructure. *Journal of composites for construction* , 7 (3), 238-247.
- Los Alamos National Laboratories. (1997). DIAMOND. Los Alamos, New Mexico.
- Moorty, S., & Roeder, C. W. (1992). Temperature-Dependent Bridge Movements. *Journal of Structural Engineering* , 118 (4), 1090-1105.
- National Climatic Data Center. (n.d.). *Snowfall - Average Total in Inches*. Retrieved August 18, 2008, from <http://lwf.ncdc.noaa.gov/oa/climate/online/ccd/snowfall.html>
- NHASCE. (2006). *2006 Report Card for New Hampshire's Infrastructure*. NHASCE.
- NHDOT Bureau of Bridge Design. (2007). *Bridge Inspection Report - Rollinsford 091/085*. NHDOT.
- NHDOT Bureau of Bridge Design. (1999, July). Rollins Road Bridge Over B&M Railroad and Main Street Plans.
- NHDOT . (2008, August 5-6). *New Hampshire bridges and related maintenance issues*. Northeast Bridge Preservation Partnership Meeting, Worcester, Massachusetts.

- Nystrom, H. E., Watkins, S. E., Antonio, N., & Murray, S. (2003). Financial Viability of Fiber-Reinforced Polymer (FRP) Bridges. *Journal of management in engineering* , 19 (1), 2-8.
- Office of Bridge Technology. (2008, August 18). *IBRC - Bridge*. Retrieved from FHWA: <http://www.fhwa.dot.gov/bridge/ibrc/>
- Peeters, B., & De Roeck, G. (2001). One-year monitoring of the Z24-Bridge: environmental effects versus damage events. *Earthquake Engineering and Structural Dynamics* , 30 (2), 149-171.
- Petroski, H. (2007, August 4). Learning from bridge failure. *Los Angeles Times* .
- Phares, B. M., Rolander, D. D., Graybeal, B. A., & Washer, G. A. (2000). Studying the Reliability of Bridge Inspection. *Public Roads* , 64 (3).
- Robert-Nicoud, Y., Raphael, B., Burdet, O., & Smith, I. F. (2005). Model Identification of Bridges Using Measurement Data. *Computer-Aided Civil and Infrastructure Engineering* (20), 118-131.
- Sanayei, M. (1997). *PARIS - PARAMeter Identification System*©. Medford, MA: Tufts University.
- Sanayei, M., Bell, E. S., Javdekar, C. N., Edelmann, J. L., & Slavsky, E. (2006). Damage Localization and Finite-Element Model Updating Using Multiresponse NDT Data. *ASCE Journal of Bridge Engineering* , 11 (6), 688-689.
- Sanayei, M., Imbaro, G. R., McClain, J. A., & Brown, L. C. (1997). Structural Model Updating Using Experimental Static Measurements. *Journal of Structural Engineering* , 792-798.
- Santini-Bell, E., Sanayei, M., Brenner, B., Sipple, J., & Blanchard, A. (2008). Nondestructive testing for design verification of Boston's Central Artery underpinning frames and connections. *Bridge Structures - Assessment, Design and Construction* , 4 (2), 87-98.
- SAP2000. (2007). Version Advanced 11.0.7. Berkely, California, USA: Computer and Structures, Inc.
- Sipple, J. (2008, April 26). *2008 Structures Congress Presentation*. Vancouver, BC.
- Sohn, H., Dzwonczyk, M., Straser, E. G., Kiremidjian, A. S., Law, K. H., & Meng, T. (1999). An Experimental Study of Temperature Effect on Modal Parameters of the Alamosa Canyon Bridge. *Earthquake Engineering and Structural Dynamics* , 879-798.
- Stanton, J. F., Roeder, C. W., & Mackenzie-Helnwein, P. (2004). *Rotational Limits for Elastomeric Bearings Appendix F*. Washington: Transportation Research Board.
- Stanton, J. F., Roeder, C. W., Mackenzie-Helnwein, P., White, C., Kuester, C., & Craig, B. (2008). *NCHRP Report 596 - Rotational Limits for Elastomeric Bearings*. Washington, D.C.: Transportation Research Board.
- Tadros, M. K., & Al-Omaishi, N. (2003). *NCHRP Report 496 - Prestress Loss in Pretensioned High-Strength Concrete Bridge Girders*. Washington, D.C.: TRB.
- Taly, N. (1998). *Design of Modern Highway Bridges*. New York: McGraw-Hill.
- The D.S. Brown Company. (2008, October 09). *The D.S. Brown Company Corporate Website*. Retrieved from <http://www.dsbrown.com/>

- Trunfio, J. P. (2001). *Experimental Testing for the use of Carbon FRP Grids in the Rollins Rd. Bridge, Rollinsford, NH*. Durham, NH: University of New Hampshire.
- U.S. Department of Transportation. (2006). *2006 Status of the Nation's Highways, Bridges, and Transit - Conditions and Performance*.
- Wipf, T. (1991). Use of tilt sensing equipment for monitoring long-term bridge movement. *Canadian Journal of Civil Engineering* , 1033-1046.

APPENDICES

APPENDIX A – CFRP REINFORCEMENT CALCULATIONS

Actual of CFRP through cross-section

$$A_{actual} = 10.86in^2$$

If CFRP was in a layer throughout entire cross-section

$$A_{desired} = 202.5in^2$$

Transform moment of inertia to maintain thickness of material

$$E_{equivalent} = \frac{E_{actual}}{\eta}$$

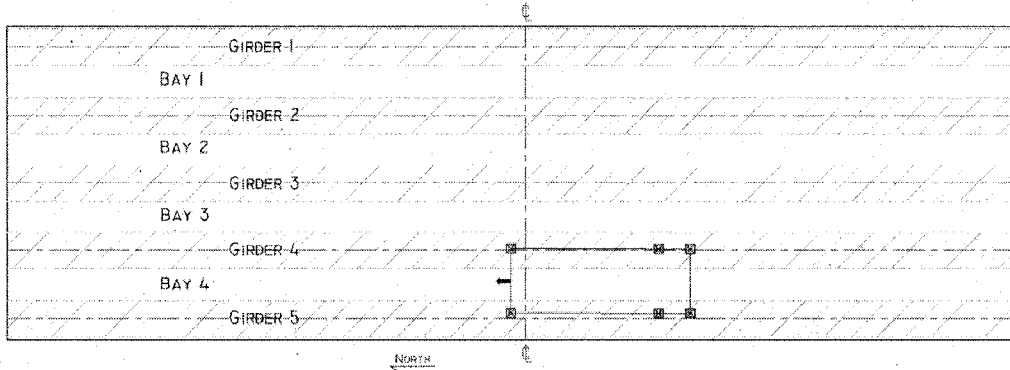
$$\eta = \frac{A_{desired}}{A_{actual}} = \frac{202.5in^2}{10.86in^2} = 18.646$$

$$E_{equivalent} = \frac{104000ksi}{18.646} = 557.75ksi$$

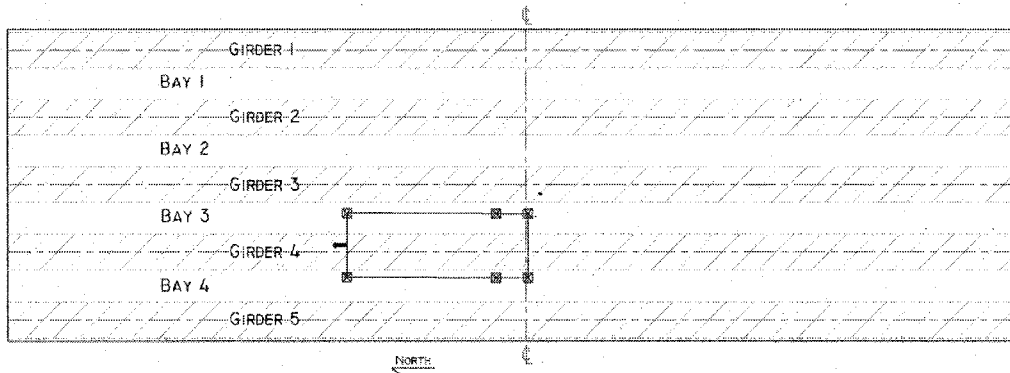
APPENDIX B – LOAD CASES FOR ALL YEARS

2000 Load Cases

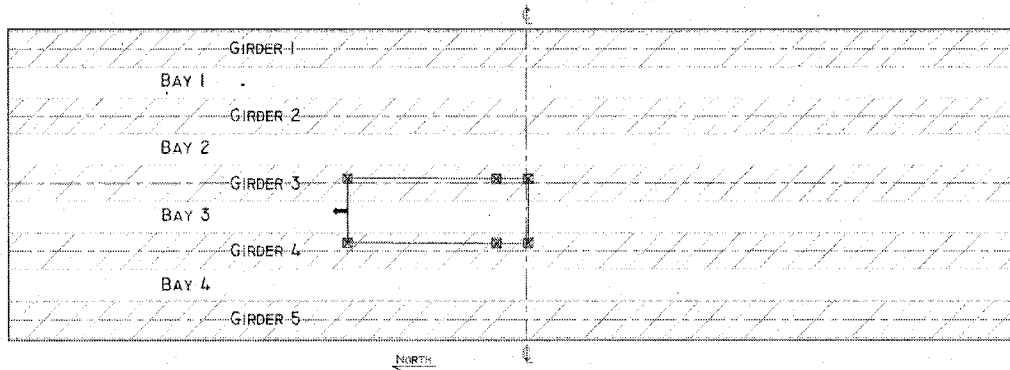
Load Case 1



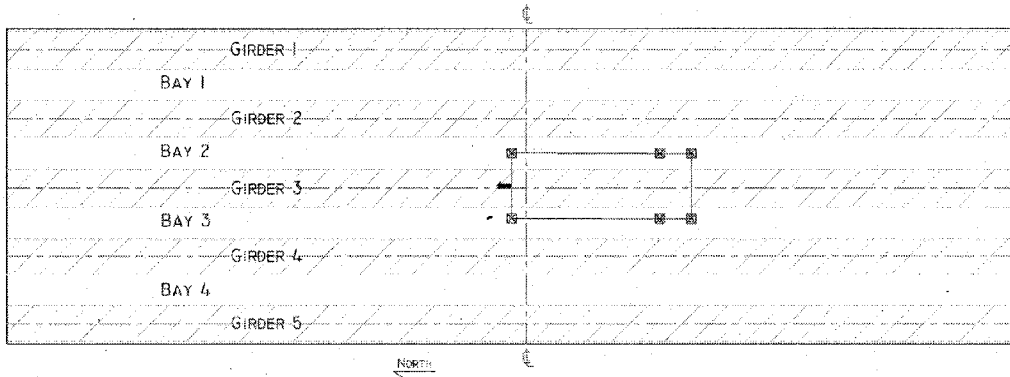
Load Case 2



Load Case 3

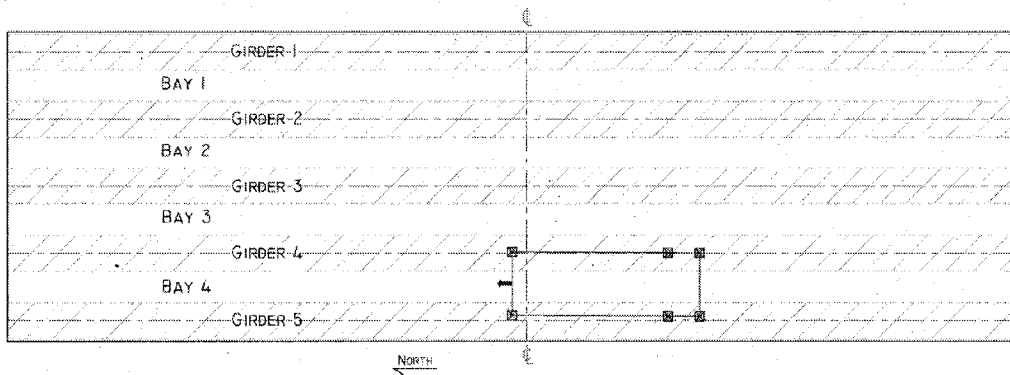


Load Case 4

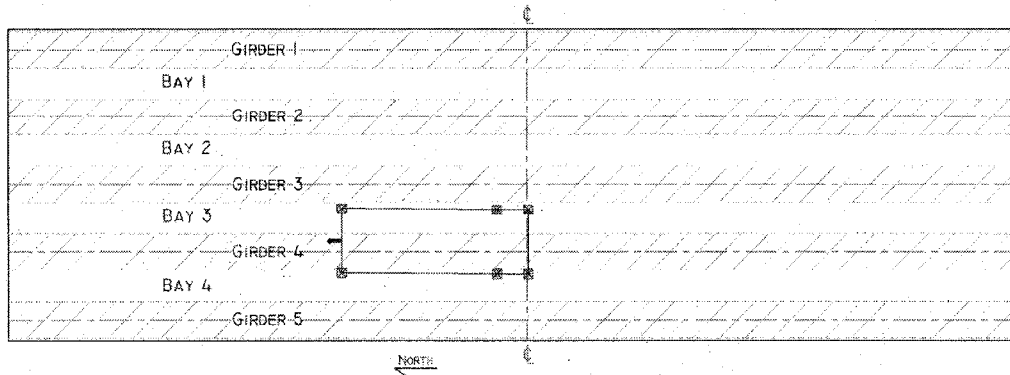


2001 Load Cases

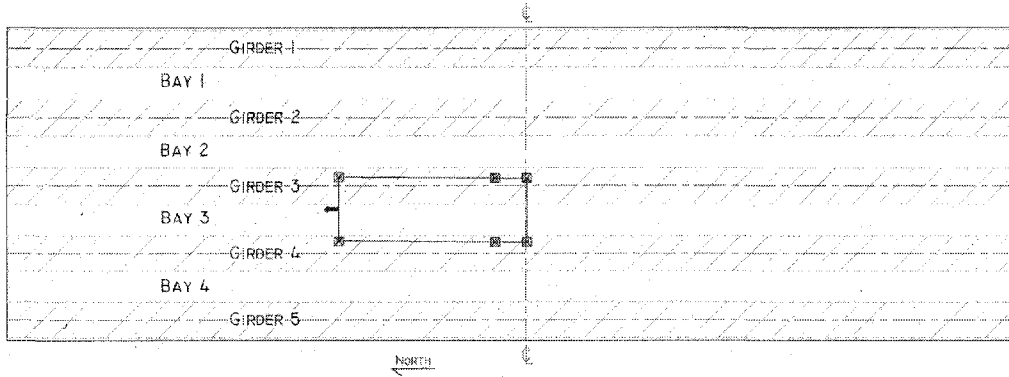
Load Case 1



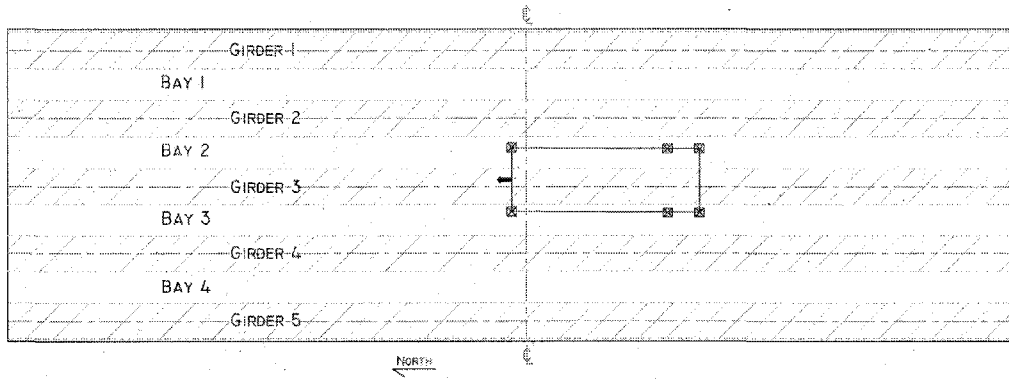
Load Case 2



Load Case 3

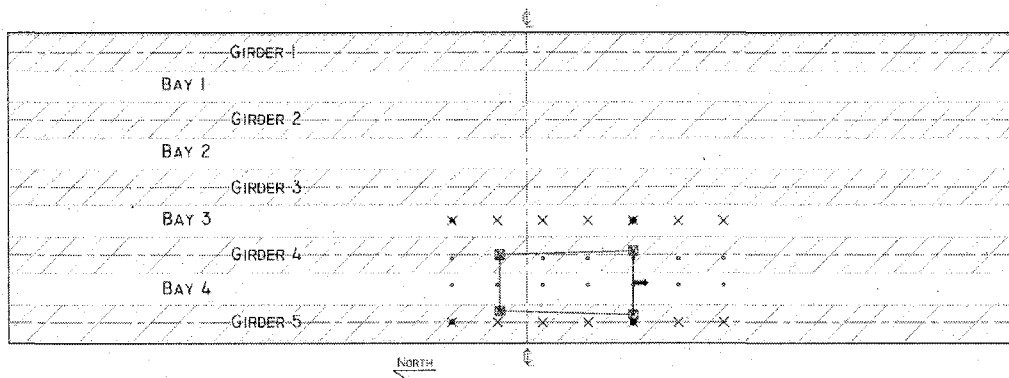


Load Case 4

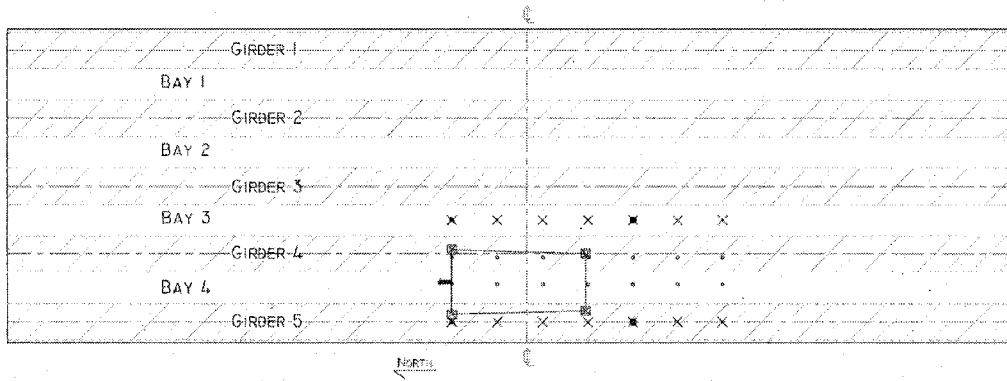


2008 Load Cases

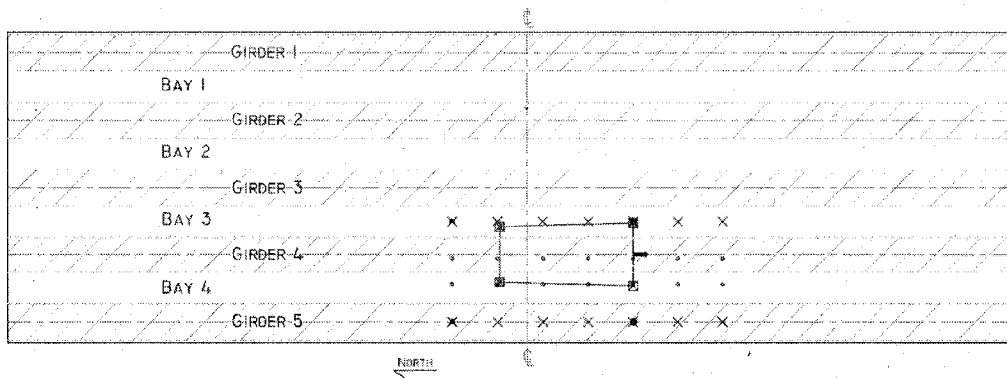
Load Case 1



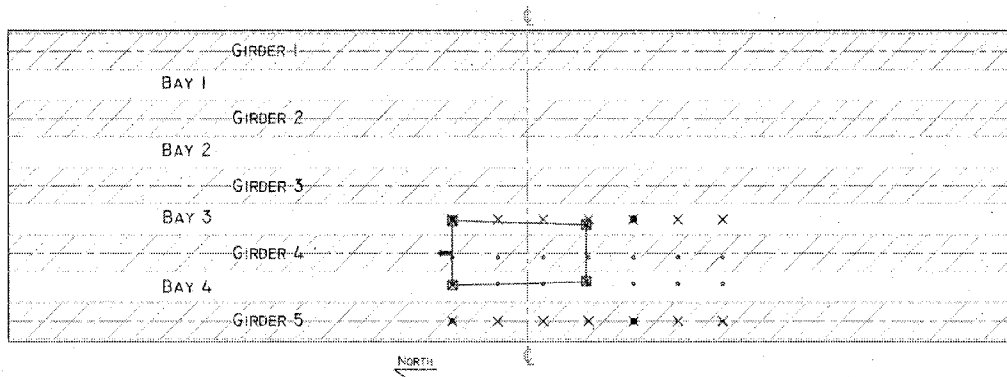
Load Case 2



Load Case 3



Load Case 4



APPENDIX C – CALCULATION OF REINFORCED ELASTOMERIC BEARING

PAD STIFFNESS

All calculations in this equations and table values taken from Stanton, Roeder, & Mackenzie-Helnwein, NCHRP Report 596 - Rotational Limits for Elastomeric Bearings

$$S = \text{Shape Factor} = \frac{\text{Loaded Plan Area}}{\text{Perimeter Area Free to Bulge}}$$

$$\text{Loaded Plan Area} = \left(\frac{16\text{in}}{2}\right)^2 * \pi = 201\text{in}^2$$

$$\text{Perimeter} = 16\text{in} * \pi = 50.3\text{in}$$

$$\therefore S = 4.00$$

$$\lambda = S \sqrt{\frac{3G}{K}}$$

$G = \text{Shear Modulus}$

$K = \text{Bulk Modulus}$

$$\begin{aligned} G &= 0.1300\text{ksi} \\ K &= 363\text{ksi} \\ \therefore \lambda &= 0.1312 \end{aligned}$$

$$\begin{aligned} G &= 0.200\text{ksi} \\ K &= 464\text{ksi} \\ \therefore \lambda &= 0.1438 \end{aligned}$$

$$\begin{aligned} G &= 0.1300\text{ksi} \\ K &= 464\text{ksi} \\ \therefore \lambda &= 0.1160 \end{aligned}$$

$$\begin{aligned} G &= 0.200\text{ksi} \\ K &= 363\text{ksi} \\ \therefore \lambda &= 0.1627 \end{aligned}$$

$$\lambda_{\text{average}} = 0.1384$$

$$B_a = 2.1 \text{ (from graph)}$$

$$B_r = 0.7 \text{ (from graph)}$$

$$K_a = \frac{EA(A_a + B_a S^2)}{t}$$

$$A_a = 1$$

$$E = 3 * G = 3 * 0.1300\text{ksi} = 0.390\text{ksi}$$

$$t = \frac{5}{8} \text{ in}$$

$$K_a = 4341 \frac{\text{kips}}{\text{in}}$$

$$t = \frac{1}{2} \text{ in}$$

$$K_a = 5426 \frac{\text{kips}}{\text{in}}$$

$$\text{Total} = 36,899 \frac{\text{kip}}{\text{in}}$$

$$E = 3 * G = 3 * 0.200 \text{ksi} = 0.600 \text{ksi}$$

$$t = \frac{5}{8} \text{ in}$$

$$K_a = 6678 \frac{\text{kips}}{\text{in}}$$

$$t = \frac{1}{2} \text{ in}$$

$$K_a = 8348 \frac{\text{kips}}{\text{in}}$$

$$\text{Total} = 56,767 \frac{\text{kip}}{\text{in}}$$

$$\text{Total}_{\text{average}} = 46,832$$

$$K_a = \frac{EI}{t} (A_r + B_r S^2)$$

$$I = \frac{1}{4} \pi \left(\frac{16 \text{in}}{2} \right)^4 = 3217 \text{in}^4$$

$$E = 3 * G = 3 * 0.1300 \text{ksi} = 0.390 \text{ksi}$$

$$t = \frac{5}{8} \text{ in}$$

$$K_r = 24490 \frac{\text{kips}}{\text{rad}}$$

$$t = \frac{1}{2} \text{ in}$$

$$K_r = 30613 \frac{\text{kips}}{\text{rad}}$$

$$\text{Total} = 208,168 \frac{\text{kip}}{\text{rad}}$$

$$E = 3 * G = 3 * 0.200 \text{ksi} = 0.600 \text{ksi}$$

$$t = \frac{5}{8} \text{ in}$$

$$K_r = 24490 \frac{\text{kips}}{\text{rad}}$$

$$t = \frac{1}{2} \text{ in}$$

$$K_r = 47097 \frac{\text{kips}}{\text{rad}}$$

$$\text{Total} = 241,135 \frac{\text{kip}}{\text{rad}}$$

$$\text{Total}_{\text{average}} = 224,652 \frac{\text{kip}}{\text{rad}}$$

APPENDIX D - CALCULATIONS FOR MODEL VERIFICATION

Hand verification of SAP2000® Rollins Road Bridge Bridge Model

Assumptions:

No dead load

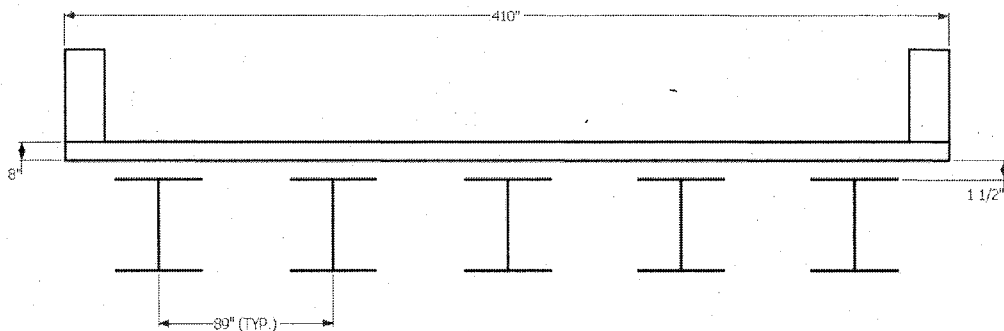
No prestressing force

No temperature effects

Simply supported

No bridge rail in stiffness

Bridge cross section:



Material Properties:

Bridge Deck

$$f'_c = 6000psi$$

$$E = 57\sqrt{f'_c} = 57\sqrt{6000psi} = 4415ksi$$

Girder

$$f'_c = 8000psi$$

$$E = 57\sqrt{f'_c} = 57\sqrt{8000psi} = 5098ksi$$

$$I = 146.5 * 10^9 \text{mm}^4 \left(\frac{(1\text{in})^4}{(25.4\text{mm})^4} \right) = 351968 \text{in}^4$$

$$A = 553 * 10^3 \text{mm}^2 \left(\frac{(1\text{in})^2}{(25.4\text{mm})^2} \right) = 857 \text{in}^2$$

CFRP

$$E = 10400 \text{ksi}$$

$$\text{Area in 111in section} = 2.976 \text{in}^2$$

$$\text{Total length of reinforced area} = 410\text{in} - (2 * 2.5\text{in}) = 405\text{in}$$

$$\frac{405\text{in}}{111\text{in}} = 3.65$$

$$3.65 * 2.976 \text{in}^2 = 10.86 \text{in}^2$$

Transform Section

Base material is concrete in girder

$$n_{\text{deck}} = \frac{E_{\text{girder}}}{E_{\text{deck}}} = \frac{5090 \text{ksi}}{10400 \text{ksi}} = 1.155$$

$$\text{Equivalent width of deck} = \frac{\text{Actual}}{n} = \frac{410\text{in}}{1.155}$$

If CFRP was solid across cross section – for ease of transforming section and using

SAP2000® layered shell elements

$$A = 10.86 \text{in}^2$$

$$\frac{10.86 \text{in}^2}{0.5} = 21.7 \text{in} \Leftarrow \text{Width}$$

$$n_{\text{CFRP}} = \frac{E_{\text{girder}}}{E_{\text{CFRP}}} = \frac{5090 \text{ksi}}{10400 \text{ksi}} = 0.489$$

$$\text{Equivalent width} = \frac{21.7 \text{in}}{0.489} = 44.3 \text{in}$$

Moment of inertia for section

$$I = \Sigma(I_o + Ad^2)$$

$$I_{deck} = \frac{1}{12}(355in)(8in)^3 = 15150in^4$$

$$I_{CFRP_1} = I_{CFRP_2} = \frac{1}{12}(44.3in)(0.5in)^3 = 0.462in^4$$

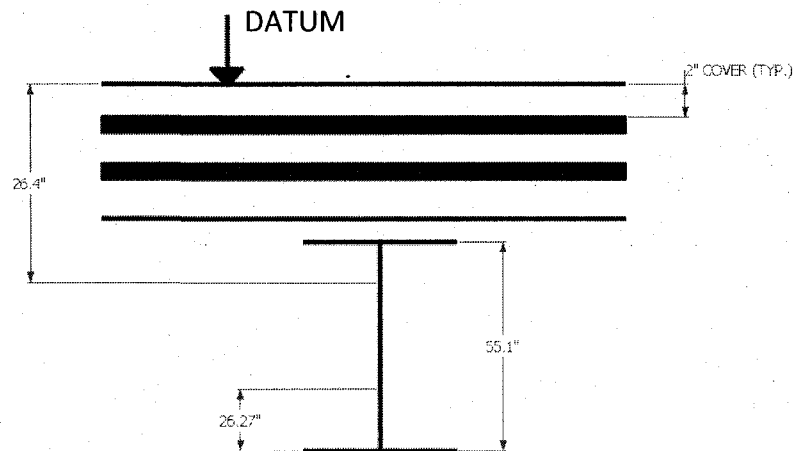
$$I_{girder} = 351968in^4$$

$$A_{deck} = (355in)(8in) = 2841in^2$$

$$A_{CFRP_1} = A_{CFRP_2} = (44.3in)(0.5in) = 22.15in^2$$

$$A_{girder} = 857in^2$$

Centroid for area:



$$\bar{y} = \frac{\Sigma A_i y_i}{\Sigma A_i}$$

$$y_{deck} = 4in$$

$$y_{CFRP_1} = 2.25in$$

$$y_{CFRP_2} = 5.75in$$

$$y_{girder} = 8in + 1.5in + (55.1in - 26.27in) = 38.33in$$

$$\begin{aligned}
 y &= \frac{(2841in^2 + 4in) + (22.15in^2 + 2.25in) + (22.15in^2 + 5.75in) + 5 * (857in^2 + 38.33in)}{2841in^2 + (2 * 22.15in^2) + (5 * 857in^2)} \\
 &= \frac{175785}{7170} = 24.52in
 \end{aligned}$$

$$\begin{aligned}
 I &= [15150in^4 + (2841in^2 * (24.5in - 4in)^2)] \\
 &\quad + [0.462in^4 + (22.15in^2 * (24.5in - 2.25in)^2)] \\
 &\quad + [0.462in^4 + (22.15in^2 * (24.5in - 5.75in)^2)] \\
 &\quad + 5[351968in^4 + (857in^2 * (24.5in - 38.33in)^2)] \\
 &= 1210887in^4 + 10975in^4 + 7796in^4 + 2577404in^4 \\
 &= 3807062in^4
 \end{aligned}$$

$P = 100kips$ at center of bridge

$$\Delta = \frac{PL^3}{48EI} = \frac{100kips(1340in)^3}{48 * 5098ksi * 3807062in^4} = 0.258in$$

From SAP2000®

$$\Delta = 0.253in$$

Find moment at center

$$\begin{aligned}
 M_{max} &= \frac{PL}{4} = \frac{100kips * 1340in}{4} = 33500in * kips \\
 \frac{33500in * kips}{5} &= 6700in * kips = 558ft * kips
 \end{aligned}$$

Calculating Strain Values

Assuming still within linear elastic range

$$\sigma = \frac{My}{I}$$

$$\sigma = E\varepsilon$$

Look at top gauge, down 2.5in from top of girder

y = distance from centriod to depth of gauge

$$\text{Depth to center} = 26.4in$$

$$\text{Depth to gauge} = 8in + 1.5in + 2.5in$$

$$26.4in - 12in = 14.4in$$

$$\sigma = \frac{33500in * kips(14.4in)}{3807062in^4} = 0.1267ksi$$

$$\varepsilon = \frac{\sigma}{E} = \frac{0.1267ksi}{5098ksi} = 24.9\mu\varepsilon$$

From SAP2000®

$$\text{strain} = 25.7\mu\varepsilon$$

APPENDIX E – STRAIN CALCULATIONS

Sample calculation for one strain sensor, girder 5

x,y Notation	Point	Undeformed X-Coordinate	Undeformed Y-Coordinate
1	g5-d1	658.074	-176
2	g5-g1	658.074	-176
1	g5-d2	670	-176
2	g5-g2	670	-176
1	g5-d3	681.926	-176
2	g5-g3	681.926	-176

x,y Notation	Point	Deformed X-Coordinate	Deformed Y-Coordinate
1	g5-d1	658.0762350	-4.8103190
2	g5-g1	658.0757090	-12.3103190
1	g5-d2	669.9999410	-4.8108300
2	g5-g2	669.9998850	-12.3108300
1	g5-d3	681.9236500	-4.8104460
2	g5-g3	681.9240630	-12.3104460

$$\text{Azimuth} = \arctan \left(\frac{(g5 - g1)_{xcord} - (g5 - d1)_{xcord}}{(g5 - g1)_{ycord} - (g5 - d1)_{ycord}} \right)$$

$$\text{Gauge Point}_x = \text{Deformed X Coordinate} + (\text{Depth to Gauge} * \sin (\text{Azimuth}))$$

$$\text{Gauge Point}_y = \text{Deformed Y Coordinate} + (\text{Depth to Gauge} * \cos (\text{Azimuth}))$$

Point	Depth to Gauge	Azimuth	Gauge Point Coordinates	
			x	y
g5-t1	-13.5	7.0133E-05	658.075288	-18.310319
g5-t2	-36.118	7.0133E-05	658.073702	-40.928319
g5-t3	-13.5	7.4667E-06	669.999840	-18.310830
g5-m1	-36.118	7.4667E-06	669.999671	-40.928830
g5-m2	-13.5	-5.5067E-05	681.924393	-18.310446
g5-m3	-36.118	-5.5067E-05	681.925639	-40.928446

$$\text{Strain} = \frac{\text{New Length} - \text{Original Length}}{\text{Original Length}}$$

APPENDIX F – FIRST ANALYSIS OF ROLLINS ROAD BRIDGE LOAD TEST

DATA FOR ALL THREE YEARS

Modeling Temperature Effects

Special care was taken to include the coefficient of thermal expansion into the material properties for all materials used the model. Experimental coefficients of thermal expansion were obtained from Martha Bowman who performed tests on concrete samples.

Benchmark Data for Data Set and SAP2000 Model

To go from 120,000 data points to a more manageable data set, some data reduction was required. The four load cases previously discussed were created for all three years, resulting in a total of 12 load cases run throughout the analysis. At every predetermined truck stop, the truck sat at the location for approximately a minute. These one minute time intervals corresponding to load cases were removed from the large data set. From this reduced data, material temperatures were separated and transformed to thermal loads. This transformation of temperature measurements to thermal loads involved comparing the data to the benchmark data set, and finding the difference and therefore thermal load. The strain values for the load cases were also grouped together and will be examined when manual parameter estimation is discussed in

Establishing the Benchmark Data Set

The earliest recorded data, with no loading, was recording at the start of the December 2000 load test. At that time, the strains in the bridge were caused by self weight, environmental effects, and prestressing loads only. Since during this period there was no load applied, it was used as a benchmark for all the data sets. All strain values were compared to this zero-load reading, to show either a positive or negative change in strain values. The bridge elevations taken at this time, through surveying techniques, and will serve as the benchmark for all displacement measurements. A similar method was performed to the model, to have cohesion between measured data and modeled response.

Table F-1 shows the benchmark data set used for the strain values on the Rollins Road Bridge Research Project. Table F-2 shows the benchmark elevation values used for data analysis. All changed in elevation will be a positive or negative displacement.

Benchmark Data Set														
	Channel 32	Channel 27	Channel 3	Channel 28	Channel 5	Channel 6	Channel 30	Channel 1	Channel 21	Channel 23	Channel 22	Channel 2	Channel 25	Channel 24
	3c	8g6	8g1	8g7	8g3	8g4	8g9	T1G3	T1M3B	T1G4B	T1G4T	T5IM4	T1G5B	T1G5T
	1002965	4421663	1003038	4615676	1002992	1003137	4617690	4517683	4498646	4501635	4620728	4458658	4498644	4536689
	Girder 3	Girder 3	Girder 4	Girder 4	Girder 5	Girder 5	Girder 5	Girder 3	Midspan 3	Girder 4	Girder 4	Midspan 4	Girder 5	Girder 5
	Middle/Top	Temp	Top	Temp	Middle	Top	Temp	Bottom	Bottom	Bottom	Top	Top	Bottom	Top
12/11/2000 10:35:10	3792.6	25.15	4273.4	28.6	4674.8	4369.6	451.55	28.95	34.6	38.85	26.85	36.45	26.35	27.95
12/11/2000 10:35:20	3792.2	25.1	4273.2	28.65	4674.4	4369.2	451.4	28.95	34.65	38.9	26.9	36.45	26.3	27.95
12/11/2000 10:35:30	3792.2	25.15	4273.2	28.6	4674.4	4369	451.4	28.95	34.65	38.85	26.9	36.45	26.35	27.95
12/11/2000 10:35:40	3792.6	25.2	4273.4	28.7	4674.8	4368.4	451.4	29	34.6	38.85	26.9	36.45	26.25	27.9
12/11/2000 10:35:50	3792.6	24.95	4273.2	28.65	4674.6	4369.4	451.55	28.95	34.6	38.95	26.9	36.45	26.35	28
12/11/2000 10:36:00	3792.6	25.15	4273	28.65	4674.6	4369.4	451.6	28.95	34.65	38.85	26.9	36.45	26.3	28
12/11/2000 10:36:10	3792.2	25.1	4273.4	28.65	4674.8	4369.6	451.55	29	34.65	39	26.85	36.5	26.25	27.95
12/11/2000 10:36:20	3792.4	25.2	4273.2	28.65	4675	4369.6	451.5	28.95	34.65	38.95	26.9	36.5	26.3	28
12/11/2000 10:36:30	3792.2	25.05	4273.4	28.65	4674.8	4370	451.4	29	34.65	38.85	26.95	36.45	26.4	27.85
12/11/2000 10:36:40	3792.6	25	4273.2	28.7	4674.6	4369.2	451.5	29	34.65	38.85	26.9	36.45	26.3	28.05
12/11/2000 10:36:50	3792.6	25.2	4273.4	28.65	4674.6	4369.2	451.55	29	34.7	38.85	26.9	36.55	26.3	27.95
Average	3792.44	25.11	4273.27	28.65	4674.67	4369.33	451.49	28.97	34.64	38.93	26.90	36.47	26.31	27.96
Standard Deviation	0.20	0.08	0.13	0.03	0.18	0.41	0.08	0.03	0.03	0.05	0.03	0.03	0.05	0.05
95% Confidence	0.12	0.05	0.08	0.02	0.11	0.24	0.05	0.02	0.02	0.03	0.02	0.02	0.03	0.03
CI Low	3792.32	25.06	4273.19	28.63	4674.56	4369.08	451.45	28.96	34.62	38.90	26.88	36.45	26.29	27.93
CI High	3792.55	25.16	4273.35	28.67	4674.78	4369.57	451.54	28.99	34.66	38.96	26.91	36.49	26.34	27.99

Table F-1: Benchmark Data Set

Table F-2: Benchmark Elevations

Benchmark Elevations (ft.)		
December 2000 No Load	Girder 3	151.7338
	Bay 3	156.6243
	Girder 4	151.6632
	Bay 4	156.4805
	Girder 5	151.5077

Again, 95% confidence intervals on the mean were used and examined to determine if the values were within acceptable limits for this project. The data did not follow a normal distribution, so standard deviation techniques were not used even though they are still displayed on the table. All 95% CIs were less than 0.25-microstrain which was deemed an acceptable CI for the measured strain values.

Establishing Benchmark SAP2000 Model

From this data, the material temperatures for the SAP2000 benchmark model were established. The material temperatures, as recorded during the December 2000 zero-load reading were applied as material temperatures for the bridge model. This allows for the thermal load derived from the benchmark data set to be accurately applied to the model. Table F-3 and Table F-4 show the temperature values used for initial material temperatures for the SAP2000 benchmark model. Since the bridge is only instrumented on one side, symmetry was used and assumed acceptable to get material temperatures for the entire bridge.

Table F-3: Deck Temperatures used for SAP2000 Benchmark Model

Deck Temperature (°F)								
Girder 1	Bay 1	Girder 2	Bay 2	Girder 3	Midspan 3	Girder 4	Midspan 4	Girder 5
27.14	36	32.91	35	29	35	32.91	36	27.14

Table F-4: Girder Temperature used for SAP2000 Benchmark Model

Girder Temperature (°F)				
Girder 1	Girder 2	Girder 3	Girder 4	Girder 5
23.06	28.65	25.11	28.65	23.06

An analysis performed having the applied loads being self weight, material temperature, and prestressing loads. The properties for that benchmark model are as close to the initial design conditions as possible. The optimal condition would be to know the initial zero-set values for the strain gauges and then run a calibration on the model to get it to match those initial zero-set values; however that was not the case with RRB. The strain values at girder locations were calculated, and will be used as benchmark strain values. Displacements were also calculated and will be used as benchmark displacement values. The benchmark model strain and displacement values can be seen in Table F-5 and Table F-6. All changes in strain or displacement will be referenced to these benchmark values.

Table F-5: SAP2000 Benchmark Model Strain Values

SAP Benchmark Strains		
Middle	Top	
X	-48.471	Girder 3
	-47.792	Girder 4
-16.019	-46.389	Girder 5

Table F-6: SAP2000 Benchmark Model Displacements

SAP Benchmark Displacements		
		Displacement
Benchmark	Girder 3	-0.4055
	Girder 4	-0.4060
	Girder 5	-0.4084

SAP2000 Output

In SAP2000, load cases were created for each applied vehicle load and corresponding thermal load cases. These results in a total of 24 load cases, four per year for vehicle load and four per year for thermal loading. A load combination is created for each load case in order to include dead, prestress, applied vehicle load,

and applied thermal loading. As a result, there are 12 load combinations, four per year. The load combinations are titled 2000LC1ALL, 2001LC2ALL, 2008LC4ALL and so on. Those titles specify the year which the data is being analyzed, the load case, and that it includes all loads. Once the analysis cases are successfully run, the output data from SAP2000 needs to be post-processed. SAP2000, as most structural analysis packages, only exports forces and moments for beam elements. From axial force and moment, stresses and resulting strains in the member at the location of the strain gauge is calculated. Figure 84 shows the process used to calculate strain at gauge locations from the SAP2000 output tables. Further calculations for each load case can be seen in Figure F-1.

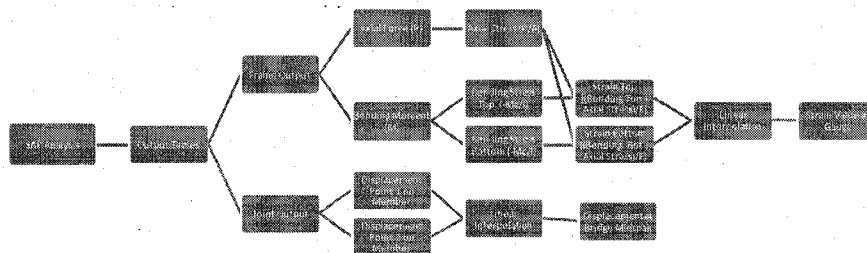


Figure F-1: SAP Output to Bending Strain at Gauge Location Flowchart

In summary, axial forces are used to calculate axial stresses, while bending moments are used to calculate bending stress in the top and bottom of the beam section. These stresses are combined to form strain throughout the depth of the beam. Using linear interpolation, the strain value at the depth of gauge is calculated. For displacement measurements, the displacements at the end nodes of the element are output from

SAP2000, and then linear interpolation is used to get the displacement at the location where the surveyors took the measurement.

Load Test Data to SAP2000 Comparison

There is post-processed data from the field measurements, post-processed data from the SAP2000 model, benchmark readings from the field measurements, and a benchmark SAP2000 model. To get the comparison used in this research, the delta comparisons, several simple steps must be done once the data is post-processed and the benchmarks are determined. The delta comparison is done for both the recorded data and model response data. It is achieved by comparing measured data versus benchmark data. Once the delta is established for recorded and model response data, conclusions may be made. The theory behind this process is a change in the behavior of the bridge will be accurately captured and shown as a similar change in behavior in the SAP2000 model, if all conditions are properly modeled since all behavior is still well within the linear elastic range.

The purpose of comparing measured structural response data to an analytical model is for the purpose of parameter estimation and model updating. MUSTANG is currently in the design phase by other researchers at UNH. Upon completion, manual parameter estimation and model updating will be done to observe the response when structural parameters were changed in an attempt to update the bridge model to the 2008 status of the bridge. The response of the model as compared to the bridge and draw conclusions.

Levels of Different Models

In order to simplifying comparing the three different load tests, three separate models were created. All models were originally based on the initial benchmark model, only differing in the load cases that were applied to the model. Using the load test data, the structural properties of these models are updated to track the progress of the bridge.

For the 2000 model, the bearing pad stiffness was left as calculated because the benchmark model was also created using the first recorded 2000 load test data. The selected structural properties that were changed in the 2000 model were removing specific components included when modeling the bridge. These elements include the CFRP reinforcement, prestressing, and thermal loads. By removing these elements from the model, the difference between design and monitoring based models can be seen.

For the 2001 and 2008 models all structural components were kept in the models. The parameter that was changed during manual parameter estimation was the stiffness of the elastomeric bearing pads. This will be also the focus of the runs in MUSTANG as part of future work. Also, looking at the most recent bridge inspection report, there are no noted changes from opening in 2000 to the deck, girder, or abutments. The rotational and axial stiffness values of the elastomeric bearing pad will be altered independently to see how each effects the performance of the bridge. When the models are run through MUSTANG, aspects such as modulus of elasticity and moment of inertia for specific elements will also be included in the parameter

estimation, however for the scope of this research project those properties will not be examined in the manual parameter estimation.

Discussion of Manual Parameter Estimation Results

To reiterate, the only gauges used in the SHM program for RRB were the gauges embedded in the HPC girders. These gauges are oriented in the longitudinal direction and capture the global structural response of the bridge given the loadings. Using only the girder gauges also limits the computations to a reasonable limit for the scope of the Rollins Road Bridge Research Project. A variety of results were seen after running the manual parameter estimation, which was expected, and will prove to be a good base when it comes time to run the bridge model in MUSTANG. For the results, the tables entitled "SAP Relative Strain" and "Measured Relative Strain" are the two values that are compared when the table "2000 Runs" is created and follows the same method for all three years.

Table F-8 shows the results from the 2000 bridge model run through manual parameter estimating techniques. The first run shows the differences between the benchmark model and this model, the only thing changing between those two is temperature and load application location. In the two contributing tables, the changes in trends can be easily seen. These results are fairly promising, showing only slight changes in the data. There is noted to be a larger difference in values as the test progresses, suggesting temperature might have an even greater effect on the bridge than originally thought.

The abutments could also be affected by the change in temperature, therefore changing the global response. Not including thermal loads in the model does not have much effect in the beginning, since that is very close to the time of the benchmark model. As time progresses the difference grows because thermal loads start to have a large effect. When the prestressing is removed from the analysis, there is a strong difference in the beginning of the analysis but yet again as time goes on that effect becomes less. Not including the CFRP follows a similar trend with the initial model; however the differences are a little larger. The deflection measurements, when temperature is not included are very similar to the initial model, only slight variations. The deflection measurements when there is no prestress have a larger difference overall as when compared to the first model. Deflection measurements when CFRP is not included also are similar to the initial model, however have slightly larger differences. When temperature is modeled as a gradient there is the slight difference seen as well.

SAP Relative Strain				
	<i>Girder 3 Top</i>	<i>Girder 4 Top</i>	<i>Girder 5 Middle</i>	<i>Girder 5 Top</i>
u3 46833		u2 224651.5		
2000LC1ALL	-5.14	-3.54	8.68	-3.56
2000LC2ALL	-4.05	-3.06	9.65	-3.97
2000LC3ALL	-2.42	-3.31	8.32	-1.60
2000LC4ALL	-1.50	-3.39	6.78	0.77
u3 46833		u2 224651.5 No Temperature		
2000LC1ALL	-4.97	-3.66	8.49	-3.83
2000LC2ALL	-4.30	-3.41	8.19	-6.11
2000LC3ALL	-3.26	-3.72	5.28	-6.06
2000LC4ALL	-2.64	-3.73	2.73	-5.19
u3 46833		u2 224651.5 No prestress		
2000LC1ALL	8.19	10.23	40.87	10.37
2000LC2ALL	9.28	10.71	41.84	9.96
2000LC3ALL	10.91	10.46	40.51	12.33
2000LC4ALL	11.83	10.38	38.97	14.70
u3 46833		u2 224651.5 No FRP		
2000LC1ALL	-7.54	-5.83	6.51	-5.75
2000LC2ALL	-6.48	-5.44	7.30	-6.40
2000LC3ALL	-4.85	-5.77	5.90	-4.01
2000LC4ALL	-3.83	-5.81	4.40	-1.55
u3 46833		u2 224651.5 Temp as gradient		
2000LC1ALL	-5.29	-3.73	8.60	-3.44
2000LC2ALL	-5.47	-4.41	9.08	-3.08
2000LC3ALL	-5.03	-6.21	7.11	0.18
2000LC4ALL	-4.69	-7.32	5.16	3.08

Measured Relative Strain				
	<i>Channel 32 3gc 1002965 Girder 3 Top</i>	<i>Channel 3 gg1 1003038 Girder 4 Top</i>	<i>Channel 5 gg3 1002992 Girder 5 Middle</i>	<i>Channel 6 gg4 1003137 Girder 5 Top</i>
2000LC1ALL	-5.44	-7.07	17.38	-9.16
2000LC2ALL	-1.09	-3.64	18.13	-6.10
2000LC3ALL	4.74	3.27	20.27	1.47
2000LC4ALL	7.85	7.84	22.58	7.67

2000 Runs									
Stiffness Value	u3	46833	0						
	r2	224651.5							
			Strain				Deflection		
			Girder 3	Girder 4	Girder 5	Girder 5			
			Top	Top	Middle	Top	Girder 3	Girder 4	Girder 5
	2000LC1ALL		-0.30	-3.53	8.71	-5.60	-0.17	-0.23	-0.37
2000LC2ALL		2.95	-0.58	8.48	-2.13	-0.20	-0.31	-0.28	
2000LC3ALL		7.16	6.58	11.95	3.07	-0.14	-0.31	-0.31	
2000LC4ALL		9.34	11.23	15.81	6.90	-0.15	-0.02	-0.05	
Stiffness Value	u3	46833	No Temperature						
	r2	224651.5							
			Strain				Deflection		
			Girder 3	Girder 4	Girder 5	Girder 5			
			Top	Top	Middle	Top	Girder 3	Girder 4	Girder 5
	2000LC1ALL		-0.46	-3.41	8.89	-5.33	-0.17	-0.23	-0.37
2000LC2ALL		3.20	-0.24	9.94	0.01	-0.21	-0.33	-0.30	
2000LC3ALL		7.99	6.99	14.99	7.54	-0.17	-0.34	-0.35	
2000LC4ALL		10.49	11.57	19.86	12.86	-0.19	-0.06	-0.09	
Stiffness Value	u3	46833	No prestress						
	r2	224651.5							
			Strain				Deflection		
			Girder 3	Girder 4	Girder 5	Girder 5			
			Top	Top	Middle	Top	Girder 3	Girder 4	Girder 5
	2000LC1ALL		-13.63	-17.30	-23.49	-19.53	-0.37	-0.43	-0.56
2000LC2ALL		-10.38	-14.35	-23.72	-16.05	-0.39	-0.51	-0.47	
2000LC3ALL		-6.17	-7.19	-20.24	-10.86	-0.33	-0.51	-0.50	
2000LC4ALL		-3.98	-2.54	-16.39	-7.03	-0.35	-0.21	-0.24	
Stiffness Value	u3	46833	No FRP						
	r2	224651.5							
			Strain				Deflection		
			Girder 3	Girder 4	Girder 5	Girder 5			
			Top	Top	Middle	Top	Girder 3	Girder 4	Girder 5
	2000LC1ALL		2.10	-1.24	10.87	-3.41	-0.18	-0.24	-0.38
2000LC2ALL		5.39	1.79	10.83	0.30	-0.20	-0.32	-0.29	
2000LC3ALL		9.58	9.04	14.37	5.49	-0.14	-0.32	-0.32	
2000LC4ALL		11.67	13.66	18.18	9.23	-0.16	-0.02	-0.05	
Stiffness Value	u3	46833	Temp as gradient						
	r2	224651.5							
			Strain				Deflection		
			Girder 3	Girder 4	Girder 5	Girder 5			
			Top	Top	Middle	Top	Girder 3	Girder 4	Girder 5
	2000LC1ALL		-0.14	-3.34	8.78	-5.71	-0.17	-0.23	-0.37
2000LC2ALL		4.37	0.76	9.05	-3.02	-0.19	-0.31	-0.29	
2000LC3ALL		9.76	9.48	13.16	1.30	-0.13	-0.31	-0.33	
2000LC4ALL		12.54	15.17	17.43	4.59	-0.14	-0.01	-0.06	

Table F-8: 2000 Manual Parameter Estimation Results

Table F-9 shows the results from the August 2001 bridge model run through manual parameter estimation. The first run uses the load cases from the August 2001

load test while keeping the same model used in the beginning of the 2000 analysis. This shows that there is a definite difference in the behavior between 2000 and 2001. An initial thought was that this could be due to stiffening of the bearing pads, so that was modeled as fixed in the axial direction and allowing complete rotation. The results from that change were a little better than the first results, however something is still not accurately captured. Increasing rotational stiffness and axial stiffness was tried, leading to the third run which did not differ much from the first run. As seen in the two contributing tables, there is a large difference in girder 3 gauges, being in the entirely wrong direction. Girders 4 and 5 are in the right area, however values measured in the model are much less than recorded in the field. For completeness, both the axial and rotation degrees of freedom were modeled as fixed, resulting in values worse off than the first run. Deflection differences do not seem to have changed that much, only when both degrees are changed to fixed.

SAP Relative Strain				
	<i>Girder 3</i>	<i>Girder 4</i>	<i>Girder 5</i>	<i>Girder 5</i>
	<i>Top</i>	<i>Top</i>	<i>Middle</i>	<i>Top</i>
<i>u3 46833</i>		<i>u2 224651.5</i>		
2001LC1ALL	-107.87	86.14	67.05	86.45
2001LC2ALL	-106.87	87.48	67.97	84.49
2001LC3ALL	-103.93	88.09	64.55	86.26
2001LC4ALL	-101.85	89.06	63.42	88.13
<i>u3 1000000</i>		<i>u2 0.0000001</i>		
2001LC1ALL	-105.13	88.88	74.04	89.23
2001LC2ALL	-104.16	90.19	74.87	87.24
2001LC3ALL	-101.18	90.84	71.54	89.04
2001LC4ALL	-99.09	91.83	70.42	90.93
<i>u3 70000</i>		<i>u2 500000</i>		
2001LC1ALL	-107.59	86.42	68.97	86.73
2001LC2ALL	-106.60	87.75	69.86	84.77
2001LC3ALL	-103.66	88.35	66.46	86.53
2001LC4ALL	-101.60	89.31	65.32	88.38
<i>u3 fixed</i>		<i>u2 fixed</i>		
2001LC1ALL	-154.05	39.94	44.29	40.00
2001LC2ALL	-152.87	41.47	45.26	38.26
2001LC3ALL	-151.44	40.57	40.98	38.48
2001LC4ALL	-151.14	39.76	38.77	38.57
<i>u3 fixed</i>		<i>u2 free</i>		
2001LC1ALL	-105.12	88.89	74.08	89.24
2001LC2ALL	-104.15	90.20	74.90	87.25
2001LC3ALL	-101.17	90.85	71.58	89.06
2001LC4ALL	-99.08	91.84	70.45	90.94

Measured Relative Strain				
	<i>Channel 32</i>	<i>Channel 3</i>	<i>Channel 5</i>	<i>Channel 6</i>
	<i>3gc</i>	<i>gg1</i>	<i>gg3</i>	<i>gg4</i>
	<i>1002965</i>	<i>1003038</i>	<i>1002992</i>	<i>1003137</i>
	<i>Girder 3</i>	<i>Girder 4</i>	<i>Girder 5</i>	<i>Girder 5</i>
	<i>Top</i>	<i>Top</i>	<i>Middle</i>	<i>Top</i>
2001LC1ALL	206.73	287.82	302.55	268.29
2001LC2ALL	208.36	290.30	300.04	270.47
2001LC3ALL	211.96	293.58	297.87	274.42
2001LC4ALL	216.54	296.87	297.24	278.93

2001 Runs								
Stiffness Value	u3	46833						
	r2	224651.5						
		Strain				Deflection		
		Girder 3 Top	Girder 4 Top	Girder 5 Middle	Girder 5 Top	Girder 3	Girder 4	Girder 5
	2001LC1ALL	314.60	201.68	235.49	181.85	-0.19	-0.32	-0.36
	2001LC2ALL	315.23	202.82	232.07	185.98	-0.22	-0.35	-0.34
2001LC3ALL	315.89	205.50	233.32	188.16	-0.17	-0.28	-0.23	
2001LC4ALL	318.39	207.81	233.82	190.80	-0.16	-0.11	-0.16	
Stiffness Value	u3	10000000						
	r2	0.0000001						
		Strain				Deflection		
		Girder 3 Top	Girder 4 Top	Girder 5 Middle	Girder 5 Top	Girder 3	Girder 4	Girder 5
	2001LC1ALL	311.86	198.94	228.51	179.07	-0.23	-0.35	-0.39
	2001LC2ALL	312.52	200.11	225.17	183.24	-0.26	-0.38	-0.37
2001LC3ALL	313.14	202.74	226.33	185.37	-0.21	-0.31	-0.26	
2001LC4ALL	315.63	205.04	226.82	188.00	-0.19	-0.15	-0.19	
Stiffness Value	u3	70000						
	r2	500000						
		Strain				Deflection		
		Girder 3 Top	Girder 4 Top	Girder 5 Middle	Girder 5 Top	Girder 3	Girder 4	Girder 5
	2001LC1ALL	314.32	201.41	233.58	181.56	-0.23	-0.35	-0.39
	2001LC2ALL	314.96	202.55	230.18	185.71	-0.26	-0.38	-0.37
2001LC3ALL	315.63	205.23	231.41	187.89	-0.21	-0.31	-0.26	
2001LC4ALL	318.14	207.56	231.92	190.55	-0.19	-0.15	-0.19	
Stiffness Value	u3	fixed						
	r2	fixed						
		Strain				Deflection		
		Girder 3 Top	Girder 4 Top	Girder 5 Middle	Girder 5 Top	Girder 3	Girder 4	Girder 5
	2001LC1ALL	360.79	247.88	258.26	228.29	-0.64	-0.77	-0.82
	2001LC2ALL	361.23	248.83	254.78	232.21	-0.67	-0.80	-0.79
2001LC3ALL	363.40	253.02	256.89	235.93	-0.63	-0.74	-0.70	
2001LC4ALL	367.67	257.11	258.47	240.36	-0.64	-0.59	-0.64	
Stiffness Value	u3	fixed						
	r2	free						
		Strain				Deflection		
		Girder 3 Top	Girder 4 Top	Girder 5 Middle	Girder 5 Top	Girder 3	Girder 4	Girder 5
	2001LC1ALL	311.85	198.93	228.47	179.05	-0.28	-0.40	-0.44
	2001LC2ALL	312.51	200.10	225.14	183.23	-0.31	-0.43	-0.42
2001LC3ALL	313.13	202.73	226.30	185.36	-0.26	-0.36	-0.31	
2001LC4ALL	315.62	205.03	226.79	187.99	-0.24	-0.20	-0.24	

Table F-9: 2001 Manual Parameter Estimation Results

Table F-10 shows the results from the 2008 manual parameter estimating runs.

As was done in the 2001 data, the first run kept bridge conditions the same as initially modeled, only changing the load. This follows a similar trend to the 2001 data where

girder 3 modeled and measured response were in different directions, and in this load test girder 4 also had the different directions. Girder 5 strain values are in the correct direction, however are significantly less in the modeled data when compared to the measured response. For the 2008 runs, they were done similar to the methods performed in the 2001 runs. The best run seemed to be the fixed axial and free rotation condition. This is what would be expected as the elastomeric bearings begin to experience hardening after eight years of service. However, the best fit in deflection was when the axial and rotational stiffness was reduced to 5,000.

SAP Relative Strain				
	<i>Girder 3</i>	<i>Girder 4</i>	<i>Girder 5</i>	<i>Girder 5</i>
	<i>Top</i>	<i>Top</i>	<i>Middle</i>	<i>Top</i>
<i>u3 46833</i>		<i>u2 224651.5</i>		
2008LC1ALL	-40.12	-23.28	36.50	43.76
2008LC2ALL	-38.53	-21.94	36.99	46.07
2008LC3ALL	-37.11	-21.71	37.25	46.18
2008LC4ALL	-33.33	-19.35	40.35	51.71
<i>u3 5000</i>		<i>u2 5000</i>		
2008LC1ALL	-54.39	-37.54	-5.50	29.35
2008LC2ALL	-52.76	-36.16	-4.95	31.70
2008LC3ALL	-51.32	-35.90	-4.63	31.83
2008LC4ALL	-47.41	-33.42	-1.24	37.49
<i>u3 1000000</i>		<i>u2 1000000</i>		
2008LC1ALL	-38.00	-21.15	42.98	45.91
2008LC2ALL	-36.46	-19.86	43.43	48.18
2008LC3ALL	-35.07	-19.66	43.67	48.25
2008LC4ALL	-31.43	-17.44	46.64	53.64
<i>u3 fixed</i>		<i>u2 fixed</i>		
2008LC1ALL	-44.83	-27.98	39.09	39.04
2008LC2ALL	-44.95	-28.35	38.52	39.63
2008LC3ALL	-44.72	-29.31	38.06	38.55
2008LC4ALL	-45.96	-31.98	38.06	39.04
<i>u3 fixed</i>		<i>u2 free</i>		
2008LC1ALL	-37.64	-20.79	43.47	46.28
2008LC2ALL	-36.04	-19.44	43.95	48.61
2008LC3ALL	-34.62	-19.20	44.21	48.71
2008LC4ALL	-30.81	-16.82	47.28	54.27

Measured Relative Strain				
	Channel 32	Channel 3	Channel 5	Channel 6
	3gc	gg1	gg3	gg4
	1002965	1003038	1002992	1003137
	Girder 3	Girder 4	Girder 5	Girder 5
	Top	Top	Middle	Top
2008LC1ALL	-104.11	123.41	171.79	70.03
2008LC2ALL	-100.22	127.55	176.26	74.74
2008LC3ALL	-97.61	129.98	175.18	78.42
2008LC4ALL	-85.22	142.08	188.29	90.21

2008 Runs										
Stiffness Value	u3	46833								
	r2	224651.5								
		Strain				Deflection				
		Girder 3	Girder 4	Girder 5	Girder 5	Girder 3	Girder 4	Girder 5		
		Top	Top	Middle	Top					
	2008LC1ALL	-63.99	146.69	135.29	26.27	-0.67	-0.69	-0.81		
	2008LC2ALL	-61.69	149.49	139.26	28.67	-0.72	-0.63	-0.79		
	2008LC3ALL	-60.50	151.68	137.93	32.25	-0.44	-0.66	-0.74		
	2008LC4ALL	-51.89	161.43	147.94	38.50	-0.61	-0.71	-0.69		
Stiffness Value	u3	5000								
	r2	5000								
		Strain				Deflection				
		Girder 3	Girder 4	Girder 5	Girder 5	Girder 3	Girder 4	Girder 5		
		Top	Top	Middle	Top					
	2008LC1ALL	-49.73	160.94	177.29	40.68	-0.13	-0.15	-0.27		
	2008LC2ALL	-47.46	163.71	181.20	43.05	-0.18	-0.09	-0.25		
	2008LC3ALL	-46.29	165.88	179.81	46.59	0.10	-0.12	-0.20		
	2008LC4ALL	-37.81	175.50	189.53	52.72	-0.08	-0.17	-0.15		
Stiffness Value	u3	1000000								
	r2	1000000								
		Strain				Deflection				
		Girder 3	Girder 4	Girder 5	Girder 5	Girder 3	Girder 4	Girder 5		
		Top	Top	Middle	Top					
	2008LC1ALL	-66.11	144.56	128.81	24.12	-0.76	-0.78	-0.90		
	2008LC2ALL	-63.77	147.41	132.82	26.56	-0.80	-0.71	-0.87		
	2008LC3ALL	-62.54	149.64	131.52	30.17	-0.53	-0.74	-0.82		
	2008LC4ALL	-53.79	159.53	141.65	36.56	-0.70	-0.79	-0.77		
Stiffness Value	u3	fixed								
	r2	fixed								
		Strain				Deflection				
		Girder 3	Girder 4	Girder 5	Girder 5	Girder 3	Girder 4	Girder 5		
		Top	Top	Middle	Top					
	2008LC1ALL	-59.29	151.39	132.70	30.99	-0.81	-0.83	-0.95		
	2008LC2ALL	-55.28	155.90	137.73	35.11	-0.87	-0.78	-0.94		
	2008LC3ALL	-52.89	159.29	137.13	39.88	-0.61	-0.82	-0.90		
	2008LC4ALL	-39.26	174.06	150.23	51.17	-0.81	-0.91	-0.89		
Stiffness Value	u3	fixed								
	r2	free								
		Strain				Deflection				
		Girder 3	Girder 4	Girder 5	Girder 5	Girder 3	Girder 4	Girder 5		
		Top	Top	Middle	Top					
	2008LC1ALL	-66.48	144.20	128.33	23.75	-0.76	-0.78	-0.90		
	2008LC2ALL	-64.19	146.99	132.31	26.14	-0.80	-0.72	-0.88		
	2008LC3ALL	-63.00	149.18	130.98	29.71	-0.53	-0.75	-0.83		
	2008LC4ALL	-54.41	158.91	141.02	35.94	-0.70	-0.79	-0.77		

Table F-10: 2008 Manual Parameter Estimation Results

Conclusions on Manual Parameter Estimating Results

The results from the manual parameter estimation offer a variety of different contributions. For one, they show that changing attributes in the model does have an effect on the behavior of the bridge model. This can be seen in the 2000 runs and throughout the process as bearing pad stiffness is altered. The 2001 data shows that something is not being accurately captured by the model when compared to the bridge response since there is such a huge difference in the numbers. Reasons for this could be change in material properties due to the temperature or an effect caused by the abutments and ground conditions changing due to thermal and seasonal effects. The 2008 runs were closer, still not great, when compared to the 2000 runs. This could be because the temperature during the April 2008 load test was closer to the December 2000 load test than the August 2001 load test. This again shows how much of an effect environmental factors have when conducting bridge tests.

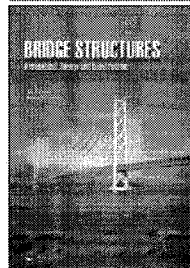
When the model is run through MUSTANG, things such as moment of inertia and modulus of elasticity will be easily modified to see if those parameters have a larger effect on the response of the model. Including the abutment and ground conditions into the model and then running parameter estimation could also give great insight into the structural response exhibited by the bridge in the field. A good way to see if the abutments are affecting the structural response would be to take survey measurements during the load test and throughout the year to see how the abutments are moving. This can then be correlated to change in structural response of the bridge.

Optimal Conditions

As with most research projects, conditions are not always ideal and therefore the desired results are not achieved. If there was enough data to do an empirical correction for all recorded structural response data, it would be interesting to see the results of the manual parameter estimation. Also, if the initial strain readings were recorded and a better benchmark model was able to be calibrated using that initial data, it is possible that better results would have been seen. The parameter estimation using MUSTANG will put a lot of work into getting the 2000 load test model accurately capturing the structural response for all load cases, and once that model is calibrated to that data it will continue on to the following two years.

**APPENDIX G – NONDESTRUCTIVE TESTING FOR DESIGN VERIFICATION OF
BOSTON'S CENTRAL ARTERY UNDERPINNING FRAMES AND
CONNECTIONS (Santini-Bell, Sanayei, Brenner, Sipple, & Blanchard,
2008)**

This article was downloaded by [Santini-Bell, Erin]
On: 22 July 2008
Access Details: [subscription number 794993282]
Publisher: Taylor & Francis
Informa Ltd Registered in England and Wales Registered Number: 1072954
Registered office: Mortimer House, 37-41 Mortimer Street, London W1T 3JH, UK



Bridge Structures
Assessment, Design and Construction

Publication details, including instructions for authors and subscription information:
<http://www.informaworld.com/SANPUB/bridge-connections/1773653301>

**Nondestructive testing for design verification of Boston's
Central Artery underpinning frames and connections**

Erin Santini-Bell^a, Masoud Sanayei^b, Brian Brenner^c, Jesse Sipple^a, Adam
Blanchard^d

^a Department of Civil Engineering, University of New Hampshire, Durham, NH, USA
^b Department of Civil and Environmental Engineering, Tufts University, Medford, MA,
USA

^c Fay, Spofford & Thordike, Burlington, MA, USA

^d LeMessurier Consultants, Cambridge, MA, USA

Online Publication Date: 01 June 2008

To cite this Article: Santini-Bell, Erin, Sanayei, Masoud, Brenner, Brian, Sipple, Jesse and Blanchard, Adam (2008)
Nondestructive testing for design verification of Boston's Central Artery underpinning frames and connections', Bridge
Structures, 4:2, 87 – 98

To link to this article: DOI: 10.1080/15732480802246337
URL: <http://dx.doi.org/10.1080/15732480802246337>

PLEASE SCROLL DOWN FOR ARTICLE

Full terms and conditions of use: <http://www.informaworld.com/terms-and-conditions-of-access.pdf>

This article may be used for research, teaching and private study purposes. Any substantial or systematic reproduction,
re-distribution, re-selling, loan or sub-licensing, systematic supply or distribution in any form to anyone is expressly
forbidden.

The publisher does not give any warranty express or implied or make any representation that the contents will be
complete or accurate or up to date. The accuracy of any instructions, formulae and drug doses should be
independently verified with primary sources. The publisher shall not be liable for any loss, actions, claims, proceedings,
demand or costs or damages whatsoever or howsoever caused arising directly or indirectly in connection with or
arising out of the use of this material.

Nondestructive testing for design verification of Boston's Central Artery underpinning frames and connections

Erin Santini-Bell^{a*}, Masoud Sanayei^b, Brian Brenner^c, Jesse Sipple^a and Adam Blanchard^d

^aDepartment of Civil Engineering, University of New Hampshire, Durham, NH 03824, USA; ^bDepartment of Civil and Environmental Engineering, Tufts University, Medford, MA 02155, USA; ^cFay, Spofford & Thorndike, Burlington, MA 01803, USA; ^dLeMessurier Consultants, Cambridge, MA 02139, USA

Prior to the demolition of the Boston Central Artery viaduct in March 2004, a research team implemented a programme of nondestructive testing for design verification of two structural steel highway bents. The tested support bents were used to underpin the original Interstate-93 Central Artery viaduct during construction of the new cut-and-cover tunnel below it. Upon opening of the tunnel, traffic was rerouted from the elevated viaduct to the new tunnel, and the demolition process of the viaduct structure began. Two of the remaining support bents of the underpinning structure were fitted with sensors (strain gages, hiltometers, slide wire potentiometers, and a 50 kip (222.4 kN) load cell) and loaded by a 50-ton (444.8 kN) crane. The measured structural response was compared to the expected response from finite element structural models, and the structural models were updated using parameter estimation techniques for design verification. Using as-built information, considering original design assumptions, and parameter estimation simulation results, the researchers selected a set of sensor types and locations for the nondestructive field test. Key design parameters of the underpinning finite element model such as connection stiffness values were successfully estimated using structural parameter estimation. As a result, the updated structural response correlated well with the collected nondestructive test data.

Keywords: nondestructive testing; model updating; structural parameter estimation; design verification

Introduction

As part of the Central Artery/Tunnel project in Boston, the existing six lane steel framed Central Artery viaduct was replaced by an 8–10 lane cut-and-cover tunnel. The viaduct remained in service during tunnel construction. To allow for excavation below the viaduct, the existing foundations were underpinned by a series of steel frame bents (Harrington 1998). The new highway tunnel was opened in stages: northbound lanes in March 2003 and southbound lanes in December 2003. With traffic rerouted to the new tunnels, demolition proceeded on the existing viaduct structure. The procedure for demolition was to remove the existing highway superstructure, temporarily exposing the steel underpinning frames before these were also demolished, as shown in Figure 1. Prior to the final demolition, two underpinning frames were the subjects of a series of nondestructive tests (NDTs) to collect measurements for structural design verification and finite element model (FEM) updating. Loading and measuring the performance of the steel bents, Bent 56 (shown in Figure 2) and Bent 57 (shown in Figure 3)

provided a unique opportunity for structural *in situ* testing and response measurements.

The goals of the NDTs were to perform design verification and to perform structural parameter estimation. The process of design verification involved revisiting the original design assumptions and comparing the *in situ* performance of the structure to the predicted response. Structural parameter estimation involved adjustment of stiffness parameters of the analytical model at the element level to match measured performance. Structural parameter estimation can be used to determine the stiffness-related parameters of a structural member, such as axial rigidity, bending rigidity, and torsional rigidity using applied loads and measured responses. The estimated parameter values are then compared to the design values of the parameters for design verification and model updating.

Structural parameter estimation is the process of reconciling an *a priori* FEM of the structure with NDT data from the structure. It has great potential for the purpose of damage identification and structural condition assessment of in-service structures, as well as

*Corresponding author. Email: Erin.Bell@UNH.edu



Figure 1. Aerial view of the Central Artery underpinning system during dock demolition.

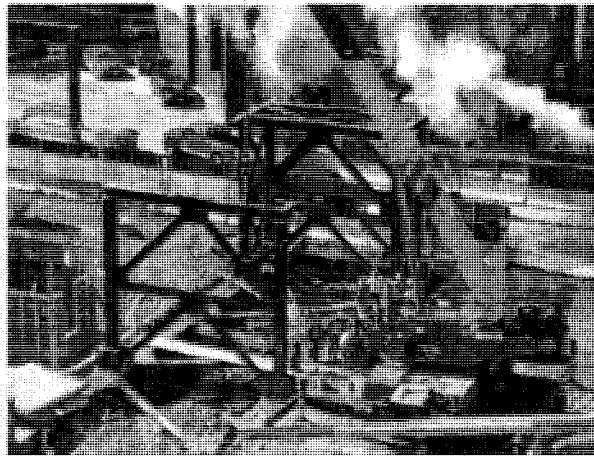


Figure 2. Crane loading for Bent 56.

design verification and model updating (Santini-Bell *et al.* 2007). Farrar *et al.* (2003) and Farrar and Jauregui (1998) summarise the current state of the art, damage identification methods. In general, structural parameter estimation techniques compare the actual measured response of a structure with the analytical

expected response. Both Aktan *et al.* (1997) and Jang *et al.* (2002) offer a comprehensive study of the integration of the analytical and the experimental sides of parameter estimation. Multi-response parameter estimation allows the user to combine different types of NDT data collected for a given structure

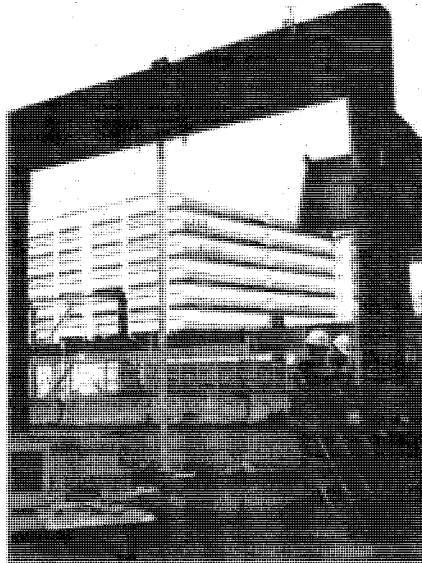


Figure 3. Bent 57 with PVC pipe protection for the slide wire potentiometer to measure displacements.

(Santini-Bell 2003). During this NDT of the underpinning frame, static displacement using a slide wire potentiometer, rotations using Geomechanic Model 900 high gain tiltmeters and strains using $\frac{1}{4}$ -inch strain gages from Vishay measurements were collected (see Figure 4). Multi-response structural parameter estimation combines algorithms for strains (Sanayei *et al.* 1997) and displacements and rotations (Sanayei and Nelson 1986).

Design verification involves using nondestructive testing methods on an existing structure to verify assumptions made during the original design phase. Several researchers have investigated issues relating to monitoring and design verification. Xu and Zhu (2000) collected field measurements from the Tsing Ma suspension bridge during Typhoon Victor. The objective of the research was to measure wind behaviour but design verification was not specifically included in the presented research. McElwain and Laman (2000) investigated in-service bridge behaviour in comparison to AASHTO code estimates without performing design verification. Myrvoll *et al.* (2000) performed a full-scale test for design verification of bridge structures. Tang *et al.* (2005) used finite element analysis for

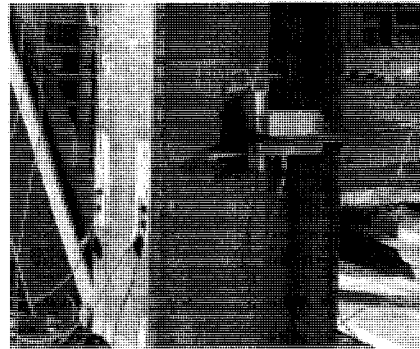


Figure 4. Detail of strain gauge and filmeter connections.

damage analysis for reinforced concrete arch structures. In Nowak *et al.* (2000), several bridges were proof-loaded with tanks in order to calculate actual stress response levels. Feng *et al.* (2004) introduced the idea of a baseline model for structural health monitoring of in-service bridges but does not carry the concept into the initial design of the structure. Shiu *et al.* (1990) discussed the idea of design verification for a cable-stayed bridge but did not address application to medium-span service bridges.

The research presented is part of a comprehensive research effort, funded by the National Science Foundation, to shift the bridge design paradigm to include instrumentation, testing, design verification and structural modelling (Santini-Bell *et al.* 2007). Any differences between the assumed design parameters and the estimated parameters can help to reveal the current condition of the structure. Using a discrete mathematical model, such as a FEM, the stiffness parameter estimates reveal not only damage location but also damage severity. Parameter estimation can also determine the current load rating of an in-service bridge accounting for any loss in stiffness during the life of the bridge. It can also be used to predict the remaining life of in-service structures given current loading conditions.

Nondestructive testing

Two steel underpinning frames were selected for nondestructive testing. Figure 2 shows the east high pick up frame at Central Artery Bent 56 and Figure 3 shows the west frame at Bent 57 (numbering refers to the original bent designation from the 1950s highway construction, where Bent 1 was the support frame

farthest to the north at the Charles River). At the time of testing, the I-93 viaduct had been demolished, temporarily leaving the steel support frames in place. This paper will focus on instrumentation, testing and analysis of Bent 57, a moment frame with no cross-bracing. These frames were located at the end of Broad Street in downtown Boston. They were tested after the bridge deck and connecting girders were removed as part of the demolition of the entire elevated viaduct (Figure 1).

Bent 57 consisted of moment-resistant welded connections between steel rolled W-shapes (Figure 5). The columns were W14 × 145 sections oriented in the weak direction (i.e. the flanges are in the same plane as the opening of the frame). The top framing beam was a W36 × 300 section oriented in the strong direction (i.e. the web is in the same plane as the opening of the frame). The columns were connected to the top of the tunnel slurry walls by a bolted moment connection at the base. This connection was assumed to act as fixed for the purpose of structural parameter estimation. Only the upper connections were considered unknown for parameter estimation. The foundation connections were not included in the parameter estimation scenarios because the base condition for Bent 57 was fixed to the ground by a moment connection. The original designers and researchers had great confidence in this connection.

During the underpinning operation, loads from the existing viaduct were jacked into the steel frame structures (Harrington 1998). After the jacking operation, load transfer was accomplished by torch cutting existing steel columns below the new connection points. Underpinning support of the expressway viaduct was in place for approximately 5 years during construction of the cut-and-cover tunnel below. The underpinning frame was fitted with 12 strain gages, three tiltmeters, and a slide wire potentiometer to measure displacement at the mid-span of the frame. Parameter estimation simulations were performed to select strategic sensor locations on the frame (Figure 5) so that the target unknown parameters would be observable during testing (Sanayei and Javdekar 2002). Each sensor location has four strain gages and one tiltmeter so that the bending moment and displacement can be calculated for each location, as shown in Figure 4. Engineering judgement and physical restrictions on the location options were a large part of the measurement selection process (Blanchard 2004).

A field data acquisition system, provided by Geocomp, Inc., was connected to the load cells and all of the sensors on the bent, as shown in Figure 4. Bent 57 was loaded by crane via a system of pulleys and cables. The maximum loads were determined by finite element analysis to ensure that there would be no

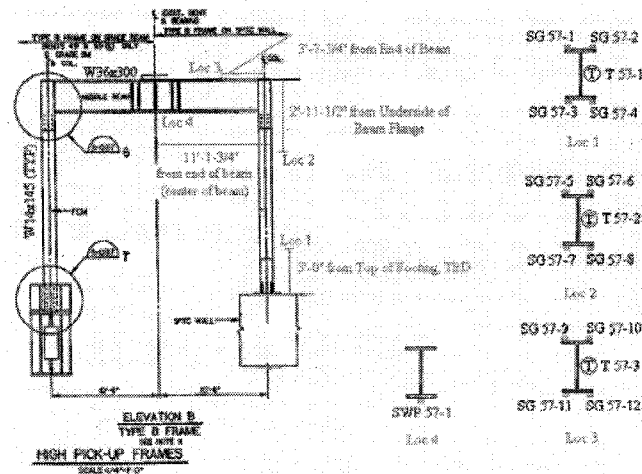


Figure 5. Strain gage locations for Bent 57.

out-of-plane displacement. A maximum vertical load of up to 50 kips (222.4 kN) was measured at the contact point on the structure through a load cell (Figure 6a). Physical restrictions of the crane required that a grounded pulley be used to apply lateral loads (Figure 6b). For lateral loading of Bent 57, brackets were welded to the Bent 58 across Broad Street immediately to the south. A maximum horizontal load of up to 25 kips (111.2 kN) was measured at the contact point on the structure through a load cell (Figure 6b). The load was measured using a load cell attached directly to the loading frame. During the NDT of the frame, applied loads, strains, fits, and displacements were measured at predetermined loading and unloading intervals of 10 kip each (44 kN). Each loading and unloading cycle was repeated three times. Figure 7 shows the load-displacement curve for the top beam of Bent 57 for load case 1. Note that only one displacement measurement was collected during the load test using the slide wire potentiometer.

Both measurements for strain and rotation were reference-independent, so there was no need to measure against a datum. The slide wire potentiometer (SWP) for displacement was not a reference-independent instrument, so it needed to be connected to a datum point. The SWP was secured to the ground and a steel wire was extended and connected to the centre of the W36 \times 300 needle beam. A PVC conduit was used to shield the wire from wind-induced vibrations (Figure 3). The strain gages were spot welded onto the frame at

specified locations shown in Figure 4. The tiltmeters were clamped onto the structure so that they could be reused. The temperature was not considered in the post-processing of the data given that the actual test for each frame occurred within a 1 h window and the temperature differential was negligible.

Structural model

Figure 8 shows the deformed shape of the structural model for Bent 57 with pinned connections. The model was prepared using GT Strudl[®], 29.1 (GT Strudl 2006). Member properties were calculated using as-built shop drawings, noting that the structure was in place for less than 10 years and visual inspection indicated no signs of corrosion or structural damage. Two FEMs were created assuming both pinned and full fixity at column base supports. Table 1 shows the results from both connections types. Initially, the shear deformation of the beam was ignored, assuming that it was negligible. However, given the depth-to-length ratio of the beam, shear deformation was considered as part of the design verification process. The only unknown parameters considered in the structure were the rotational stiffness values of the two connections between the columns and the beam at the top of the frame.

The structural model of Bent 57 was analysed to produce baseline responses for correlation with the field measurement. The strains, rotations, and

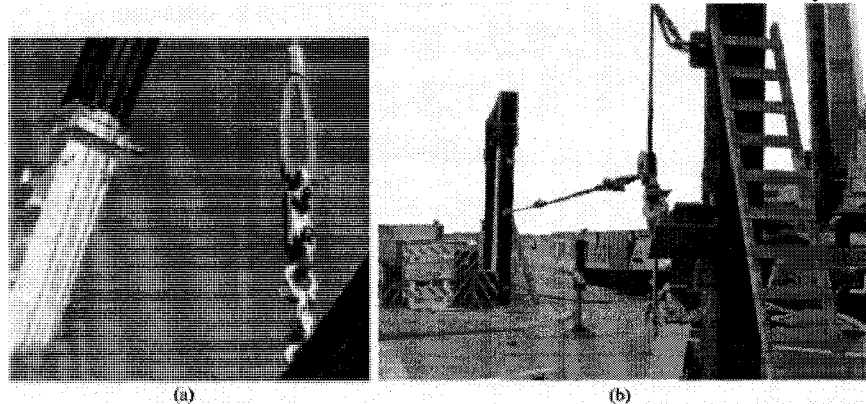


Figure 6. (a) Load cell on Bent 57 measuring load transferred directly to the steel frame. (b) Lateral load applied to Bent 57 using a bracket, load cell, and cable connected to adjacent bent (modified for clarity).

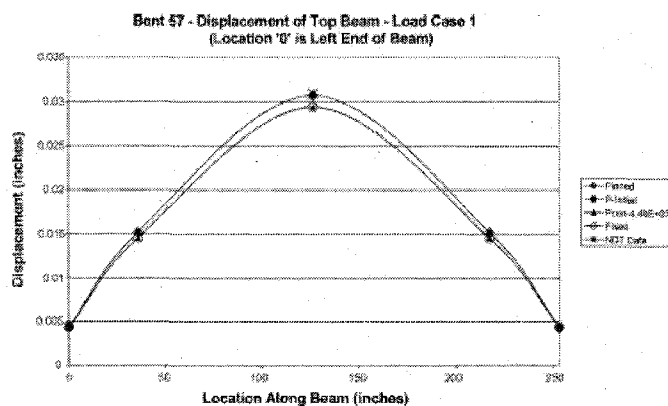


Figure 7. Deflected shape of Bent 57 top beam due to load case 1.

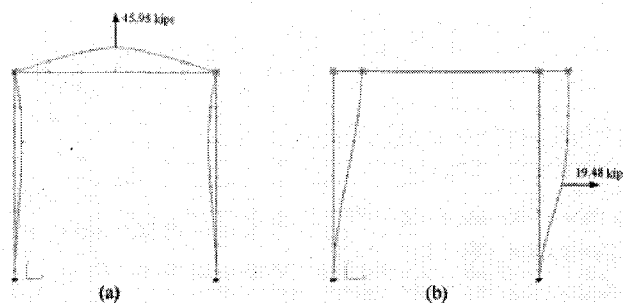


Figure 8. Deformed shape of the finite element model of Bent 57. (a) Vertical loading and (b) horizontal loading.

Table 1. Summary of simulated results for varying upper connection stiffness values for Bent 57.

Connection stiffness	Connection stiffness value in.-kip/radian (m-kN/radian)	Connection moment	Mid-span deflection, in. (cm)
'Pinned'	10^4 (11.3×10^3)	no moment	0.03822 (0.976)
'Fixed'	10^7 (11.3×10^6)	large moment	0.03692 (0.9194)

displacements measured from the NDT were charted along with the strains, rotations, and displacements from the FEM for comparison.

Data quality analysis was performed (Blanchard 2004) on the raw data to select the measurement set for parameter estimation and design verification. The data quality analysis was based on the comparison of the measured response with the expected response as well as repeatability patterns within the measured data sets.

Parameter estimation

The Matlab[®]-based parameter estimation program, PARIS[®] (PARAMeter Identification System, Sanayei 1997), developed at Tufts University, estimates the parameters of the elements and connections of a structure's FEM (Figure 9). The structure can be excited either statically with applied loads, F ,

Downloaded By: [Santini-Bell, Erin] At: 16:03 22 July 2008

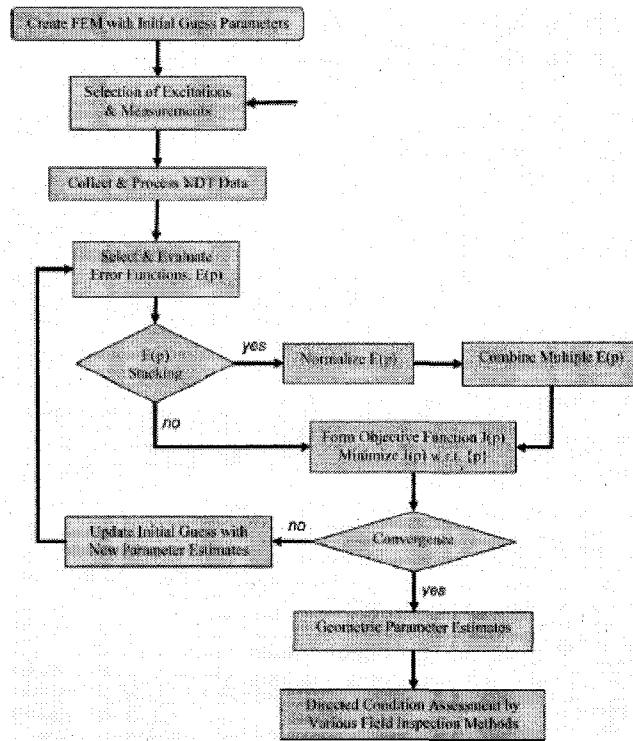


Figure 9. Flowchart for parameter estimation in PARIS©.

measuring displacements and rotations, U , and static strains or dynamically measuring frequency response function and extracting natural resonance frequencies, ω , and associated mode shapes, Φ , for stiffness and mass parameter estimation. A selected number of measurements gathered sparsely at certain strategically selected degrees of freedom (DOF) were used for parameter estimation.

For this research, only the static stiffness displacement and rotation-based and strain error function was used for parameter estimation. A full explanation of other error functions that are used for multi-response parameter estimation available in PARIS© is given in Santini-Bell *et al.* (2007). Although this multi-response parameter estimation protocol provides the user with an additional opportunity for data use, the user must also use engineering judgement to ensure

that only compatible measurement sets are combined, for example all selected measurement sets must capture the linear-elastic response of the structure. A brief overview of both error functions is presented here.

Static stiffness-based error function

The static stiffness based error function, $\{E_s(p)\}$ (Sanayei and Nelson 1986, Sanayei *et al.* 1992) is developed using the finite element equilibrium, equation (1), for linear elastic structures. Using partitioning and static condensation, the unmeasured data points are removed resulting in an algebraically non-linear error function

$$[F] = [K][U] \quad (1)$$

$\{U_a\}$, $\{F_a\}$ and $\{F_b\}$ are considered as known measured data. Essentially $\{E_{res}(p)\}$ is residual forces at the measured DOF (2). $\{F_{predicted}\}$ is based on the measurements, $\{U_a\}$, and submatrices of the analytical $\{K\}$. $\{F_{measured}\}$ is the applied set of forces

$$\{E_{res}(p)\} = \{F_{predicted}\} - \{F_{measured}\} \quad (2)$$

The resulting matrix, $\{E_{res}(p)\}$ is NMDOF \times NSF, where NMDOF is the number of DOF measured per load case (LC) and NSF is the number of applied force sets or load cases.

Static strain error function

Displacements and rotations are not the only type of measurements that can be collected during a NDT. A NDT can be designed to collect strain data. Strains are typically much smaller in magnitude than displacements and easier to collect in the field. Many researchers believe that strain gauges record more robust measurements and are reference independent. Due to this fact, the static strain error function, $\{E_{str}(p)\}$, was developed using strain data in the parameter estimation procedure (Sanayei and Saletnik 1996a,b). In equation (3), $\{B\}$ is a mapping or compatibility matrix that is created using the user-input data regarding the location of the strain measurements along the element in the x - and y -direction for a two-dimensional frame element and in the x -, y - and z -direction for a three-dimensional frame element

$$\{e\} = \{B\}\{U\} \quad (3)$$

The analytical strains, $\{e\}$ are predicted using applied forces and analytical stiffness matrix, $\{K\}$. The measured strains, $\{e_{measured}\}$, are measured during an NDT. $\{E_{str}(p)\}$ is based on residual strain measurements

$$\{E_{str}(p)\} = \{e_{predicted}\} - \{e_{measured}\} \quad (4)$$

Parameter estimation trials using NDT data

The assumption of a fixed base connection was confirmed using simulated parameter estimation runs in an attempt to find more appropriate connection stiffness values. For each parameter estimation simulation, a different base condition was used included full, partial, and no fixity. The final base connection stiffness estimated was approximately 10^{10} in.-kip/radian (11.3×10^9 m-kN/radian), which closely approximates a fixed connection, as assumed by the original design. The rotational stiffness of the two

upper connections, designed as 'fixed' or infinitely stiff, were the main focus of the parameter estimation. By definition, all of the beam-to-column connections of Bent 57, a moment frame, are full penetration welded moment connections. Several iterations of structural analysis were conducted using the FEM of Bent 57 with differing connection stiffness values. Resulting responses with respect to connection stiffnesses are shown in Table 1.

Figures 10 and 11 present the effect of estimated connections stiffness values on the resulting mid-span deflection and connection moments, respectively. These figures indicate that there is a significant change in both deflection and moment when a stiffness of approximately 10^4 in.-kip/radian (11.3×10^6 m-kN/radian SI units) is used and then the rate of change slows down again at 10^8 in.-kip/radian (11.3×10^7 m-kN/radian). Bent 57 was designed as a 'moment frame' with the assumption of a stiff connection. The parameter estimates values for Bent 57 using the NDT data are shown in Table 2.

The converged parameter estimates for the connection stiffness values were then used to update the FEM. The structural responses of the three different connection conditions were then compared: pinned, fixed, and the converged condition (F_{con}). F_{con} was calculated by PARIS© using the collected measured response. As expected, the deflected shape shown in Figure 12 demonstrates that the converged condition (2) is a very close approximation of the fixed condition (3).

Beam deflection

In order to more completely evaluate the NDT data, the effects of shear deflection must be considered in the FEM. Unlike most beams where shear deformation is negligible (Timoshenko and Young 1935), the needle beam for Bent 57 had a depth to length ratio of 3/21, requiring shear deflection consideration. For the deflection of the centre span of the beam due to the vertical centre load, the shear deflection accounts for 22.2% of the total deflection. For the deflection of the centre span of the beam due to the induced shear of horizontal load case 2, the shear deflection is 6.7% of the total deflection.

The FEM did not account for the shear deflection in the frame. Therefore, the NDT data for these deflections was reduced by 22.2% and 6.7%, respectively, for accurate comparison between the NDT data and the FEM. The FEM results were generated by plotting the displacements of points along the beam under different connection stiffness values, resulting in four curves representing the four stiffness conditions (pinned, initial guess, converged, and fixed).

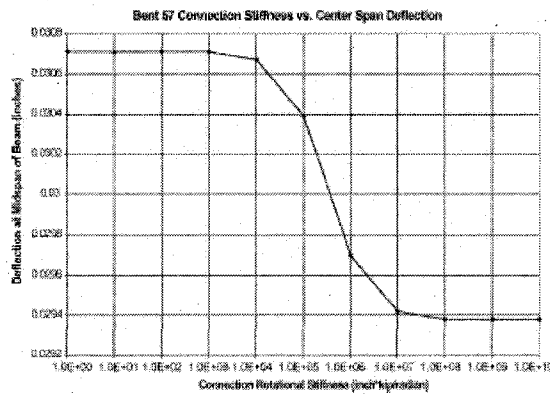


Figure 10. Variation of mid-span deflections due to differing connection stiffness values.

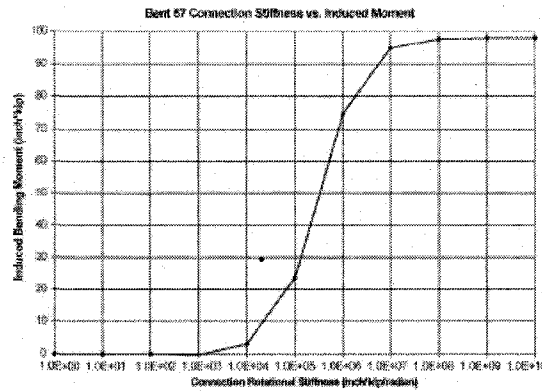


Figure 11. Variation of induced moment at connection due to differing connection.

Table 2. Summary of parameter estimates using NDT data for the connection stiffness values for Bent 57.

Connection	Initial stiffness value, in.-kip/radian (m.-kN/radian)	Final parameter estimate, in.-kip/radian (m.-kN/radian)
Beam-to-column	10^5 (11.3×10^3)	9.58×10^7 (10.8×10^6)
Column-to-footing	10^{10} (11.3×10^8)	10^{10} (11.3×10^8)

Ideally, the NDT data should fall between the two extreme connection stiffness conditions – pinned and fixed. As a verification of the NDT data points, the FEM curves were re-calculated including shear deflection and were compared to the unmodified NDT data. The simulated mid-span deflection values are shown in Table 2 and compared with the raw NDT deflection, 0.03842 inches (0.0976 m). The large shear area of the W36 x 300 allows the NDT data to be evaluated with respect to the shear displacement with confidence, and the plots with the post-processed

NDT data and FEM-generated curves can be used with confidence as well.

Connection moments

Strain data from the NDT was transformed into moment values at the locations where the strains were measured. The calculations for this transformation excludes the strain due to member elongation (from axial force) to determine the induced moment at that point. The calculated moments were compared with the FEM moment curves to determine how close the FEM approximated the NDT data. FEM moment

diagrams were generated by determining the moment at several points along the member for the four connection stiffness cases: pinned, initial, converged and fixed. Figure 13 shows the moment diagram of the beam due to load case 1; the envelope between the extreme conditions (pinned and fixed) is very small. Thus, any measurement error in the NDT strain data would have a significant effect on the moment value calculated for the NDT data. This NDT data point is a relatively good match for the model that had been updated with the converged stiffness case.

Parameter estimation results

Overall, the updated model indicates a general trend that the converged connection stiffness was a very close approximation to the fixed condition in all load cases and members. Also, the initial condition was a very close approximation to the pinned condition, illustrating that the initial guess at the stiffness of the beam-column connections was not close to the value it finally converged upon, and that the value the parameter estimation runs returned was a very close approximation of the design assumptions made by the engineers that designed the bent.

The FEM stiffness-curvature curves were generated by calculating deflection (or moment) at several locations along a structural member with four beam-column connection stiffness values (pinned, initial, converged, and fixed). The NDT data was plotted on the same axes as the FEM curves for a direct visual comparison to the FEM curves. In the beam portion of the frame due to load case 1, the envelope between the

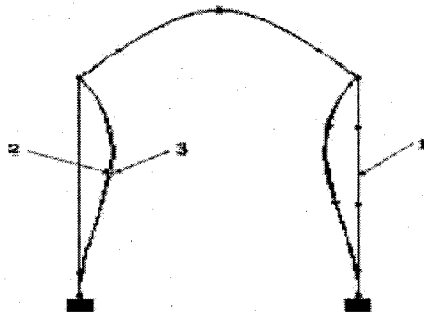


Figure 12. Deformed shapes of (1) pinned condition, (2) converged condition and (3) fixed condition due to load case 1.

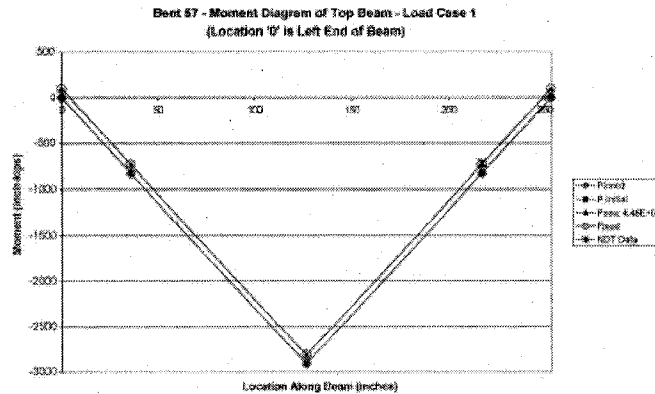


Figure 13. Moment diagram for Bent 57 top beam due to load case 1.

extreme connection stiffness conditions (pinned and fixed conditions) was very small, but the NDT data still fit very closely to the FEM stiffness-curvature curves.

In general, the trends shown in Figures 12 and 13 are consistent with the design assumptions. The NDT data typically reflects the fixed condition curves. The FEM updated with the parameter estimation results was a vast improvement over the initial guess at the unknown parameter values, which was the goal of this analysis. The parameter estimation value returned for the stiffness of the upper connections closely mimics the behaviour of the structure as if these connections had infinite stiffness (fixity). The real stiffness of the upper connections is likely very close to the converged value of 9.58×10^7 in.-kips/radian (10.8×10^6 m-kN/radian) because when the FEM model was updated with the converged parameter values, the FEM curve moved away from the pinned condition curve and very close to the fixed condition curve. An improvement of this magnitude between initial and converged FEM curves shows the parameter estimates reflect the field conditions.

Conclusions

NDT data obtained from the Central Artery was used for parameter estimation and model updating. Using Parameter Identification System (PARIS®), the static stiffness-based error function with the NDT data from the underpinning bents of Boston's Central Artery proved successful. The rotational stiffness values of the connections between columns and beam were successfully estimated. The success of the parameter estimation is verified in that a similar value was converged upon from several different initial parameter values (showing that starting at any point, the minimum residual between NDT data response and simulated response could be found). Also, the estimated parameter values verified the connection stiffness simple design assumptions made by structural engineers.

Bent 57 was considered to be a fixed connection (high rotational stiffness), so the initial parameter 'best-guess' was a low rotational stiffness (to prove the high value could still be converged upon). The value that was converged upon was input into a FEM that showed a structural response close to that of a fixed connection. The FEMs of Bent 57 were then compared to the NDT strain data that was considered to be accurate data. Generally, the NDT data agreed with the updated FEM model. There were a few cases that the inherent measurement error in the NDT data exceeded the difference between the predicted FEM results and the collected NDT data.

This research illustrates that, via parameter estimation and model updating, the final parameter estimates were able to more closely approximate the design assumptions made by design engineers, as reflection through NDT data. This paper presents a small-scale proof-of-concept example of structural parameter estimation for design verification. The authors plan to take the lessons learned through this example, including sensors placement, data quality, and realistic expectations from parameter estimation to design verification for a full bridge structures using NDT data and structural parameter estimation.

The lessons learned from this research, NDT, and parameter estimation and model updating will be used for future projects such as a load test that took place in April 2008 at the Rollins Road Bridge in Rollinsford, NH. This test was conducted by the University of New Hampshire in conjunction with the New Hampshire Department of Transportation (NHDOT). The Rollins Road Bridge Project will be used as a benchmark for the structural health monitoring and asset management programme at the NHDOT.

Acknowledgements

For the NDTs, Modern Continental Corporation provided a 50-ton crane, two man-lifts, one excavator, a surveying crew, steel connections, welding, field support, and other assistance. The research team expresses gratitude to Vice President, Paul Pedini, and his talented, energetic group for their exceptional contributions. Instrumentation was provided by Geocomp Corporation, headed by Dr Allen Marr. His talented field staff was led by Dr Robert Nyren. The group installed all strain gages and tiltmeters, and the whole assembly including the load cell and slide wire potentiometer was hooked up to the firm's data acquisition system in the field. Assistance was also provided by the Massachusetts Highway Department, the Federal Highway Administration, the management consultant Bechtel/Parsons Brinckerhoff, and the section designer Fay Spofford & Thorndike/HNTB.

References

- Aktan, A.E., et al., 1997. Structural identification for condition assessment: experimental arts. *Journal of Structural Engineering, ASCE*, 123 (12), 1674-1684.
- Blanchard, A.P., 2004. *Objective function investigation and load case selection for parameter estimation with non-destructive test data from Boston's central artery*. MS Thesis No. 6532, Tufts University, Medford, MA.
- Farrar, C.R. and Jauregui, D.A., 1998. Comparative study of damage identification algorithms applied to a bridge: I. Experiment. *Smart Materials and Structures*, 7 (5), 704-719.
- Farrar, C.R., et al., 2003. *Damage prognosis: current status and future needs*. Los Alamos National Laboratory Report LA-14051-MS.
- Feng, M.Q., Kim, D.K., Yi, J.H., and Chen, Y.B., 2004. Baseline models for bridge performance monitoring. *Journal of Engineering Mechanics*, 130 (5), 562-569.
- GT Strudl®, 2006. *GT Strudl®* (29.1). Georgia Institute of Technology, CASE Center, Atlanta, GA.

- Harrington, P.F., 1998. The challenges of underpinning the central artery. *Civil Engineering Practice*, Fall/Winter, 65-76.
- Jang, J.H., et al., 2002. Experimental investigation of system-identification-based damage assessment on structures. *Journal of Structural Engineering, ASCE*, 128 (5), 673-682.
- McElwain, B.A., and Laman, J.A., 2000. Experimental verification of horizontally curved I-girder bridge behavior. *Journal of Bridge Engineering*, 5 (4), 284-292.
- Myrvoll, F., et al., 2000. Full scale measurements for design verification of bridges. In: *Proceedings of SPIE - The International Society for Optical Engineering*, 4062, 1, 827-835.
- Nowak, A.S., Kim, S., and Stankiewicz, P.R., 2000. Analysis and diagnostic testing of a bridge. *Computers and Structures*, 77 (1), 91-100.
- Sanayei, M., 1997. *PARIS - PARAmeter Identification System*. Medford, MA: Tufts University.
- Sanayei, M., et al., 1997. Structural model updating using experimental static measurements. *Journal of Structural Engineering, ASCE*, 123 (6), 792-798.
- Sanayei, M. and Javdekar, C.N., 2002. Sensor placement for parameter estimation of structures using Fisher information matrix. In: *Proceedings of 7th International Conference on Applications of Advanced Technology in Transportation (AATT 2002)*. Wang, K.C.P., editor. 5-7 August 2002, Cambridge, MA, 386-393.
- Sanayei, M. and Nelson, R.B., 1986. Identification of structural element stiffnesses from incomplete static test data. In: *Proceedings of SAE Aerospace Technology Conference and Exposition*, SAE, Long Beach, CA, 1 October, Paper no. 861793.
- Sanayei, M., Onipede, O., and Babu, S.R., 1992. Selection of noisy measurement locations for error reduction in static parameter identification. *AIJA Journal*, 30 (9), 2299-2309.
- Sanayei, M. and Saletnik, M.J., 1996a. Parameter estimation of structures from static strain measurements; I: Formulation. *Journal of Structural Engineering, ASCE*, 122 (5), 555-562.
- Sanayei, M. and Saletnik, M.J., 1996b. Parameter estimation of structures from static strain measurements; II: Error sensitivity analysis. *Journal of Structural Engineering, ASCE*, 122 (5), 563-572.
- Santini-Bell, E., 2001. *Using multiple non-destructive test data types and data sets for condition assessment of bridge decks*. Doctoral Dissertation, Tufts University, Medford, Massachusetts.
- Santini-Bell, E., Sanayei, M., Javdekar, C.N., and Slavsky, E., 2007. Multi-response parameter estimation for finite element model updating using non-destructive test data. *Journal of Structural Engineering, ASCE*, 133 (4), 1068-1079.
- Shiu, K.N., et al., 1990. Verification of cable-stayed bridge design with field measurements. 7th Annual International Bridge Conference, The Engineer's Society of Western Pennsylvania, Pittsburgh, PA, June 18-20, p. 113.
- Tang, X.S., Zhang, J.R., Li, C.X., Xu, F.H., and Pan, J., 2005. Damage analysis and numerical simulation for failure process of a reinforced concrete arch structure. *Computers and Structures*, 83 (31-32), 2609-2631.
- Timoshenko, S. and Young, D.H., 1935. *Elements of strength of materials*, 4th edn. New York: D. Van Nostrand.
- Xu, Y.L., Zhu, L.D., Wong, K.Y., and Chan, K.W.Y., 2000. Field measurement results of Tsing Ma suspension bridge during typhoon Victor. *Structural Engineering and Mechanics*, 10 (6), 545-559.